Open access • Journal Article • DOI:10.1021/ACS.CHEMREV.9B00402

Cyclotides: From Structure to Function — Source link

Simon J. de Veer, Meng-Wei Kan, David J. Craik

Institutions: University of Queensland

Published on: 12 Dec 2019 - Chemical Reviews (American Chemical Society)

Topics: Cyclotides

Cyclotides: From Structure to Function

Simon J. de Veer, Meng-Wei Kan and David J. Craik*

Institute for Molecular Bioscience, The University of Queensland, Brisbane, QLD 4072, Australia

*Corresponding Author: David J Craik

Email: d.craik@imb.uq.edu.au

ABSTRACT

This article reviews the class of plant-derived macrocyclic peptides called cyclotides. We include an account of their discovery, characterization and distribution in the plant kingdom, as well as a detailed analysis of their sequences and structures, biosynthesis and chemical synthesis, biological functions and their applications. These macrocyclic peptides are around 30 amino acids in size and are characterized by their head-to-tail cyclic backbone and cystine knot motif, which render them to be exceptionally stable, with resistance to thermal or enzymatic degradation. Routes to their chemical synthesis have been developed over the past two decades and this capability has facilitated a wide range of mutagenesis and structure–activity relationship studies. In turn, these studies have led both to an increased understanding of their mechanisms of action as well as facilitating a range of applications in agriculture and medicine, as eco-friendly crop protection agents and as drug leads or scaffolds for pharmaceutical design. Our overall objective in this review is to provide readers with a comprehensive overview of cyclotides that we hope will stimulate further work on this fascinating family of peptides.

CONTENTS

1. INTRODUCTION

Cyclotides are naturally occurring macrocyclic peptides found in plants[1-8] that are defined by their unique cyclic cystine knot (CCK) structural motif, illustrated in Figure 1 for the prototypic cyclotide kalata B1.[9] The CCK motif comprises a head-to-tail cyclic backbone that is cross-braced with a cystine knot formed by six conserved Cys residues. Naturally occurring cyclotides discovered so far range in size from 28 to 37 amino acid residues but this range has been extended at the upper end to around 45 amino acids by examples of chemically synthesized cyclotides into which extra amino acids have been inserted into one or more of the six backbone loops between the conserved Cys residues.

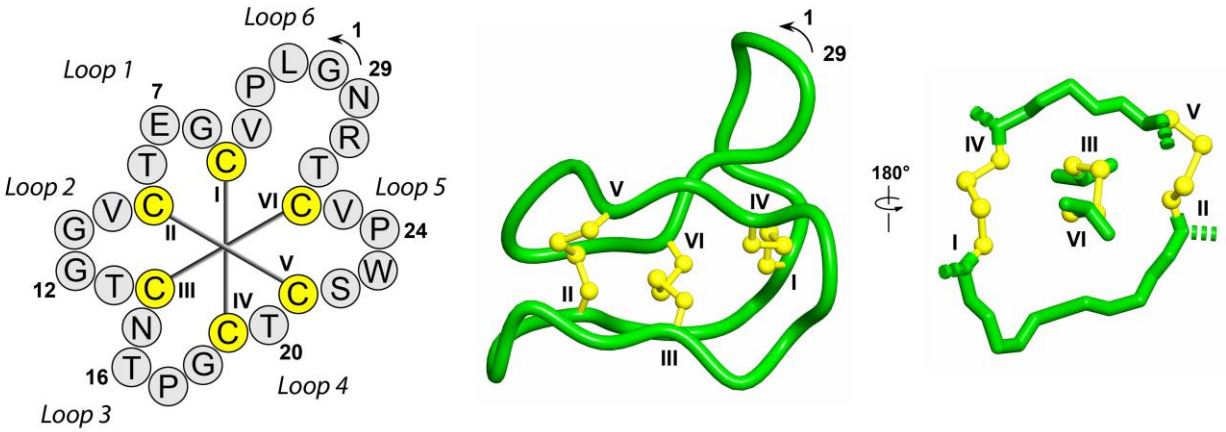

Figure 1. **Sequence and 3D structure of the prototypic cyclotide kalata B1.** The sequence features six Cys residues (conserved in all cyclotides and numbered here I-VI) linked in a I–IV, II–V and III–VI connectivity that forms a cystine knot. In this motif, two disulfide bonds and their connecting backbone segments form a ring that is threaded by the third disulfide bond. The backbone segments between the Cys residues are referred to as 'loops' and are numbered 1–6. A linear representation of the sequence of kalata B1, together with cyclotides from other plant families, can be found in Figure 5. The 3D structure of kalata B1 (PDB 1NB1) determined by NMR spectroscopy[9] shows that the sequence folds into a compact structure with the cystine knot at its core. The residue numbering starts at Gly1 and finishes at Asn29 (sequence direction indicated by the arrow), which reflects the sequence arrangement of the linear precursor protein from which kalata B1 is processed.

Cyclotides are of interest because of their unique structure that engenders them with exceptional stability, their natural functions as plant defense peptides, and their wide range of applications as bioactive molecules in agriculture and medicine. Our aim in this article is to provide a comprehensive description of the chemistry and biology of cyclotides, spanning studies from structure to function. We focus mainly on studies reported over the last five years but include discussion of earlier background studies relating to the discovery and characterization of cyclotides. A search of the Web of Science database in September 2019 returned 617 articles retrieved with the topic (title/keywords/abstract) "cyclotide(s)." After removing 241

articles in this set that made only peripheral mention of cyclotides and the manual selection of another 65 articles that refer to peptides that are cyclotides but were not explicitly named as such in the articles, we derived a set of 441 papers[1-441] to form the primary reference list for this article. These papers are listed chronologically in the References section of this article. Arranging the references in this way provides readers with a bibliographic timeline of the development of the field, which we believe has not been done in any previous review. Additional background references 442–452 that are relevant for this review, but are not considered to be cyclotide-focused articles, are numbered by order of citation in the text.

The term 'cyclotide' was introduced into the literature in 1999,[14] but several discoveries underpinning the field can be traced back to the early 1970s when kalata B1 and related peptides were discovered based on their reported uterotonic activity in a medicinal tea used in Africa.[1-5] At that time, neither the sequence nor the cyclic nature of kalata B1 was known but its approximate amino acid content and size of around 30 amino acids had been determined by 1973.[2-5] The cyclic nature of kalata B1 was revealed when its three-dimensional structure was reported in 1995[9] and the CCK motif was formally defined in 1999.[14] Independent discoveries of several macrocyclic peptides of similar size with homologous sequences in the period 1993-1999[6-8,13-15] led to the recognition that these peptides belong to the cyclotide family as they contained the characteristic CCK.

Figure 2 highlights key milestones in the history of the cyclotide field. Over the last 20 years the field has developed from being primarily focused on the discovery[7-9,13,21-34,37] and structural characterization[14,19,20] of these macrocyclic peptides to the development of methods for their chemical synthesis and folding,[11,12,16-18,38-40,45] the delineation of their ribosomal biosynthetic pathways[29] and modes of action,[29,35,37] through to applications of these molecules in agriculture and medicine.[199] Notably, a cyclotide-containing product (Sero-X) reached the market as a commercial eco-friendly insecticide in 2017 and a range of natural and synthetically engineered cyclotides is currently being evaluated as drug leads for a variety of diseases.[108,117,145,176,179,188,217,218,238,254,261,266,277,301,311-313,318,325-328,347,348]

CyBase (www.cybase.org.au)[87,127] is a database dedicated to the curation and cataloguing of cyclotide data and contains a wealth of information on cyclotide sequences, structures and biological activities, as well as incorporating several useful tools for the analysis of cyclotide data.[171] Additional background reading may be found in a book[298] and selected key reviews from the last five years (2014-

2019)[273,353-355,384,417] covering broad aspects of cyclotide chemistry and biology as well as in specialized reviews on their discovery,[354] structures,[274] bioactivities[303,354-356,366,383] and applications.[95,272,275,276,299,354-356,359,363,366,415] Earlier reviews[56-60,72-78,93-97,129-136,159-168,191-199,220-230,243-250] provide valuable insights as to how the cyclotide field developed in the preceding decade (2004–2013).

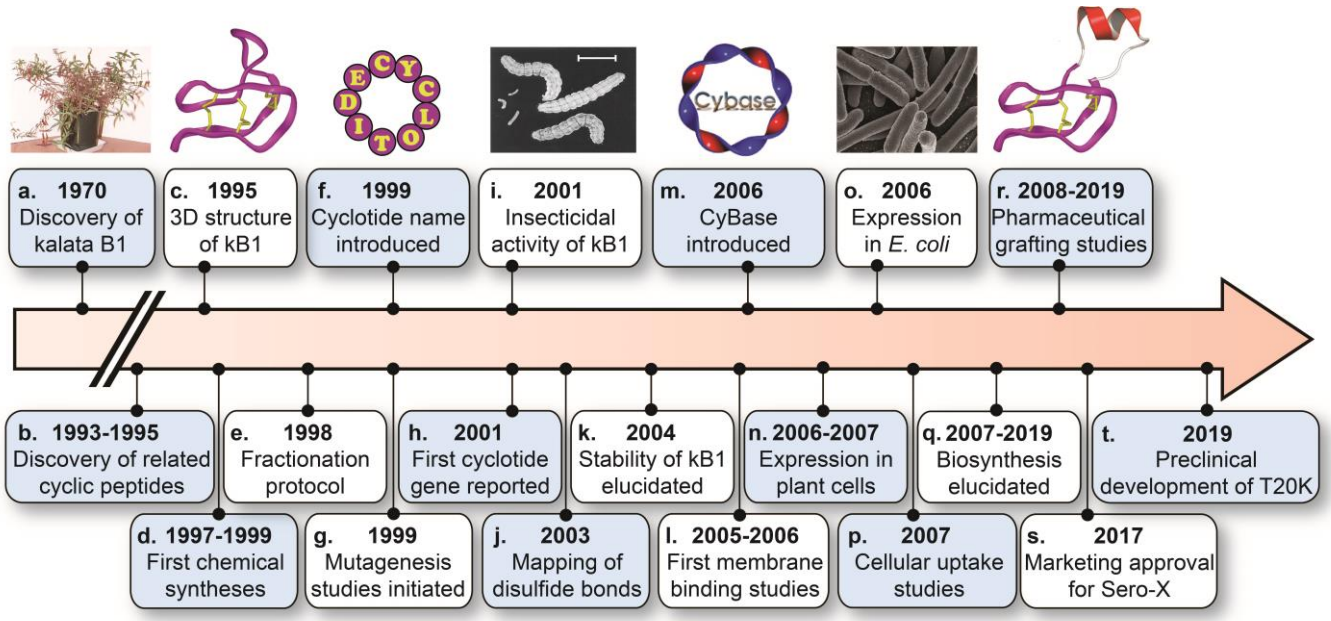

Figure 2. **Timeline of key milestones in the cyclotide field.** Reference citations are provided in the list at the end this article. **a.** Kalata B1 was originally discovered in a uterotonic medicine derived from an African plant from the Rubiaceae family, *Oldenlandia affinis*;[1] **b.** Other related macrocyclic peptides were discovered in the period 1993 to 1995 from Violaceae and Rubiaceae plants;[6-8] **c.** The 3D structure of kalata B1, determined by NMR, was first reported in 1995 (PDB 1KAL)[9] and updated in 2003 (PDB 1NB1);[41] **d.** A series of papers from 1997 to 1999 reported solid-phase peptide synthesis methods for producing cyclotides;[11,12,16,18] **e.** A general fractionation process for the extraction of bioactive peptides was reported in 1998.[13] **f.** The name cyclotide (cyclo-peptide) was introduced in 1999[14] in a paper that reported the sequences of 12 macrocyclic peptides and defined the 'cyclic cystine knot', i.e., a cystine knot motif embedded within a head-to-tail cyclic backbone; **g.** With the development of synthesis methods, it became possible to undertake mutagenesis studies, starting with open-chain analogs[20] and later including an Ala scan[125] and a Lys scan;[170] **h.** Evidence that cyclotides are ribosomally synthesized was first reported in 2001[29] following the isolation of RNA from *O. affinis* leaf corresponding to several cyclotide precursor proteins encoding kalata B1, B2, B6, and B7; **i.** Evidence that kalata B1 had insecticidal activity against *Helicoverpa punctigera* (cotton budworm) was reported in the same paper; **j.** A chemical method for mapping the disulfide bonds of kalata B1 was reported in 2003;[40] **k.** The factors that determine the exceptional stability of kalata B1, including the relative contributions of the cystine knot and the cyclic backbone were elucidated in 2004;[47] **l.** The first studies of cyclotides binding to membranes were reported in 2005 and 2006, focusing on binding to micelles as mimics of membranes;[66,67] **m.** The database CyBase which curates and analyzes cyclotide sequences was introduced in 2006[87] and subsequently updated;[127,171] **n.** Initial attempts to culture cyclotide-bearing plant cells were reported in 2006,[90] demonstrating that *O. affinis* cells could be cultured and a range of cyclotides could be detected in the cell cultures;[113] **o.** The use of *E. coli* and intein-based constructs to express kalata B1 was first reported in 2006;[70] **p.** The idea that some subclasses of cyclotides could penetrate cell membranes and target intracellular spaces was first reported in 2007;[98] **q.** A wide range of studies reported aspects of cyclotide biosynthesis in the period 2007–2019, including mutagenesis studies on asparaginyl endopeptidases and various knock-down studies *in vivo* along with *in vitro* experiments;[101,115,205,206] **r.** In 2008–2019, more than 20 studies in which cyclotides were used for pharmaceutical applications were reported,[251,363] including testing *in vitro* or in animal models of grafted cyclotides for a range of diseases including cancer, pain, obesity, wound healing and cardiovascular disease. The concept of grafting cyclotides was earlier introduced in 2006;[85] **s.** Cyclotide-containing extracts of *Clitorea ternetea* (butterfly pea) were approved for application to cotton and macadamia nut crops in Australia as a commercial insecticide in May 2017; **t.** The preclinical development of [T20K]kalata B1 is scheduled to commence in 2019 for applications in multiple sclerosis.[426] Figure adapted and updated from a recent book on cyclotides.[298]

2. DISCOVERY

2.1 Peptide-based discovery

Early studies of cyclotides[7-9,13-15] were based on discovery and characterization efforts at the peptide level. The general approach for these studies involved either bioassay-guided or mass-guided fractionation of plant extracts, followed by peptide isolation and purification, amino acid analysis, Edman sequencing and chemical, NMR[9] or mass spectrometry-based[10] approaches to deduce disulfide connectivity. The first step in many of the early discovery programs was a pre-screening procedure to determine if a given plant tissue might contain cyclotides (Figure 3). Various protocols[13,15,57,69,116,123] have been reported for quickly screening if a plant might be cyclotide-positive, with the simplest based on extraction (using dichloromethane/methanol, aqueous acetonitrile, or aqueous buffer) and purification on a C18 reverse phase column followed by a main-screen. The latter typically involves (A) examination of a reversed phase HPLC-MS profile for late-eluting peaks that are (B) in the mass range 2800-4000 Da and (C) contain six Cys residues as judged by a mass shift of 348 Da after reduction and S-alkylation, as shown in Figure 3.[116]

The rationale for the target HPLC elution range was that all of the cyclotides discovered in early studies were somewhat hydrophobic and eluted relatively late on HPLC. Similarly, many of the initial cyclotides were in the mass range 2500–4000 Da and it was assumed that new cyclotides would fall within a similar range. Finally, by definition, a cyclotide must contain six Cys residues so the mass shift test in step C of the screen provided a simple way of testing for that criterion. An example of the 348 Da mass shift after reduction and alkylation is illustrated for the identification of the cyclotide Cter A from *Clitoria ternatea* (butterfly pea) seeds in Figure 3.

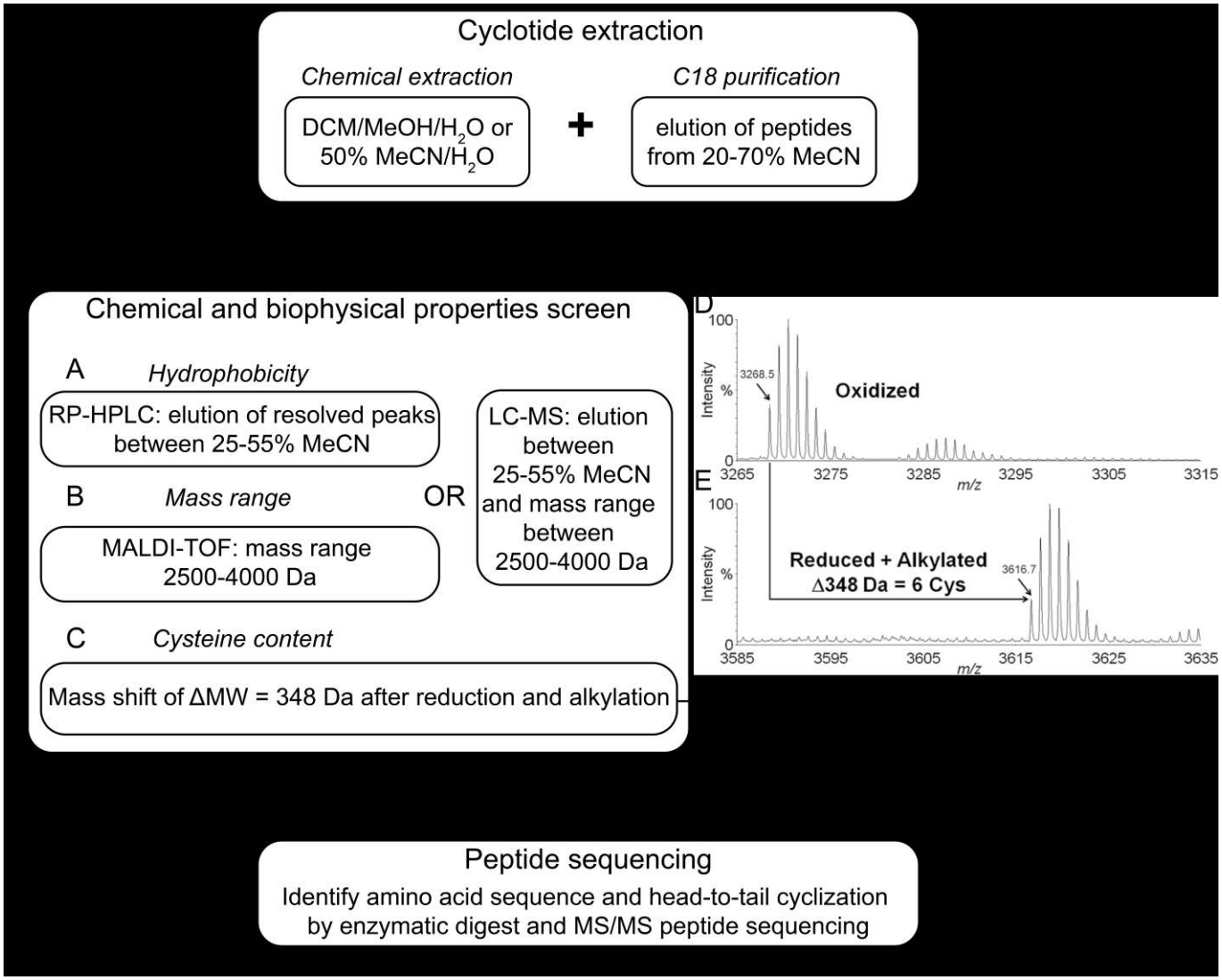

Figure 3. **Schematic overview of the procedure for extracting, isolating and characterizing cyclotides.** After isolation from a plant extract and purification of a putative cyclotide peak by reverse-phase HPLC in a pre-screen, examining the (A) HPLC retention time, (B) mass range, and (C) mass shift after reduction and S-alkylation allows a peak to be classified as a probable cyclotide, ready for sequencing in a post-screen. Scheme adapted from Gruber et al.[116] The right panels show the offset-aligned MALDI-TOF spectra of the (D) "native" and (E) "reduced and carbamidomethylated" cyclotide, Cter A (reproduced with permission from Poth et al.[204])

Once a putative cyclotide has been discovered, it can be further characterized by enzymatic cleavage and sequencing. Figure 4 shows the output from a typical sequencing protocol. A critical aspect of cyclotide analysis is that they are impervious to enzymatic digestion in their cystine knotted state, so that reduction of the disulfide bonds is crucial before the cyclic backbone can be linearized for sequencing. Often Cys residues are also alkylated after reduction to eliminate the possibility of disulfide reformation. Conveniently, the vast majority of cyclotides contain a conserved Glu residue in loop 1, which makes endoproteinase Glu-C a convenient enzyme for linearizing full-length cyclotides after reduction. Trypsin digestion is also often used as a complementary approach to produce shorter fragments for either Edman or MS/MS sequencing, as illustrated in Figure 4 for the MS/MS sequencing of the cyclotide Cter B from *C. ternatea* seeds.[204]

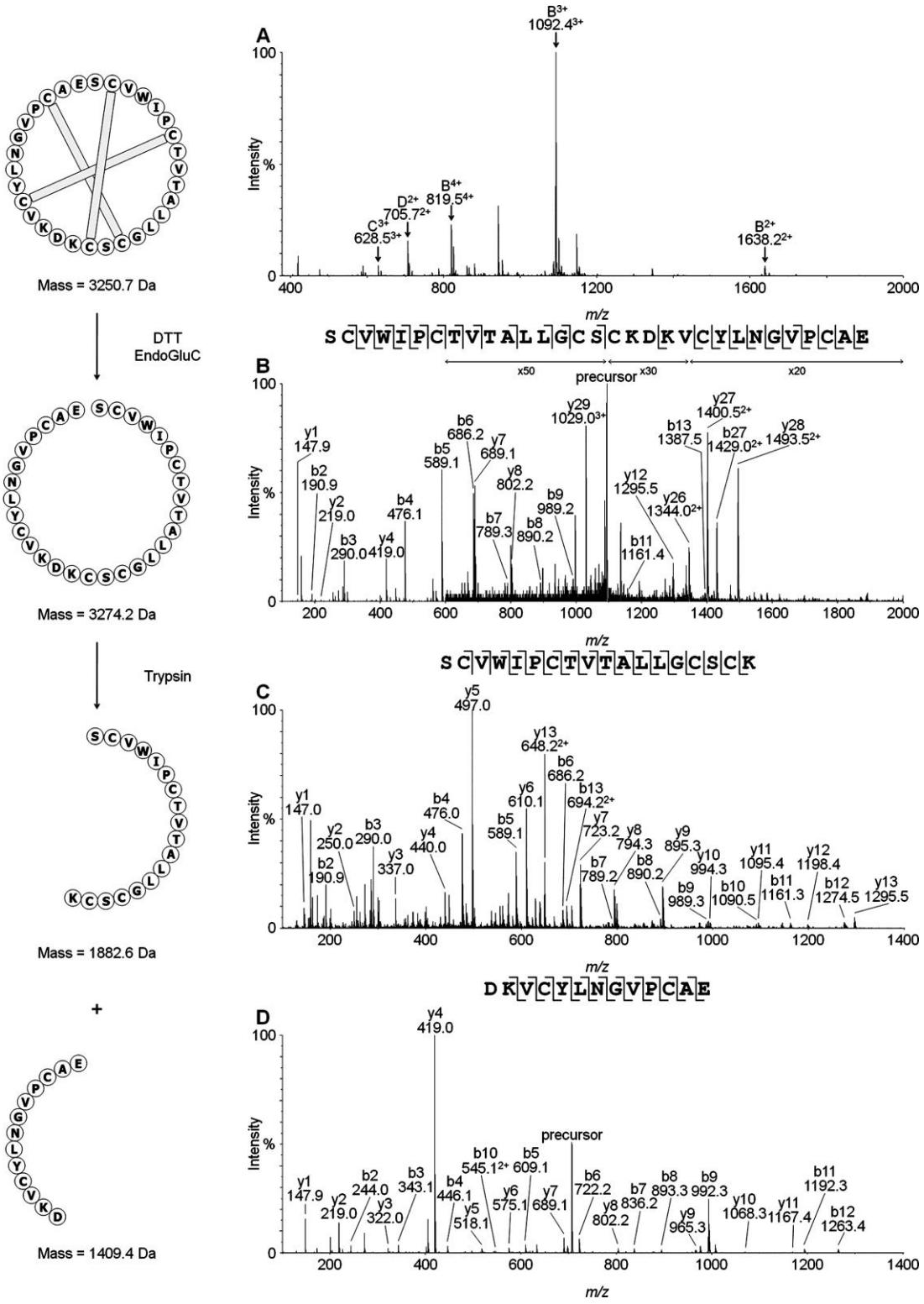

Figure 4. **Example of MS/MS sequencing of a cyclotide (Cter B).** Left panels show the digestion scheme and masses of cyclotide digest fragments. (A) MALDI-TOF/MS spectrum of a combined trypsin and endoproteinase Glu-C digest. The peaks are labeled according to their charge state, where B^{2+}, B^{3+}, and B^{4+} correspond to the full-length linearized Cter B, and C^{3+} and D^{2+} signify smaller fragments produced by cleavage of the cyclic precursor at two points along the peptide backbone. (B) MS/MS of precursor 1092.4^{3+} (3274.2 Da). (C) MS/MS of precursor 628.5^{3+} (1882.6 Da). (D) MS/MS of precursor 705.7^{2+} (1409.4 Da). Figure reproduced with permission from Poth et al.[204]

Since the original isolation and sequencing procedures described above were developed, there have been a number of variations and improvements in approaches for detecting cyclotide peptides and sequencing them using mass spectrometry.[160,239,307,337,372,377] Some of these improvements relate to the increasing knowledgebase on cyclotides. For example, it is now apparent that not all cyclotides elute late on HPLC, a property that should be taken into account in future cyclotide screens, as exemplified by the recent discovery of Lys-rich cyclotides from Pacific Island plants.[317] Other improvements have involved new methods for analyzing MS data and new ways for generating fragment masses. For example, the recently described PepSAVI-MS approach[373] uses statistical methods to help identify bioactive peptide targets from complex biological samples. It was originally used to identify bioactive cyclotides from *Viola odorata*[373] and more recently was used to discover novel anti-cancer cyclotides from the same plant.[410] In the later study, the value of ultraviolet photodissociation mass spectrometry for sequencing cyclotides without the need for extensive enzymatic digestion was demonstrated for cycloviolacin O8.[410] In this approach, the fact that the cyclic backbone is linearized as part of the MS analysis, rather than through cleavage by a specific enzyme, leads to complex overlapping spectra. Accordingly, data analysis can be challenging but, as the cyclotide knowledgebase expands, the approach has great promise.

Although the cyclic backbone presents challenges in cyclotide sequencing, the exceptional stability of cyclotides that derives from it also presents novel opportunities for cyclotide discovery, particularly by expanding the types of sample that can be analyzed. For example, cyclotide sequences have been successfully identified in dried herbarium samples that were up to 200 years old,[307] indicating that a cyclic backbone and cystine knot provide stability that enables analysis of stored samples. In that study, the herbarium specimens examined covered 17 of the 23–31 genera in the Violaceae. Cyclotides were positively identified in 150 species, with each species containing a unique set of between one and 25 cyclotides, many of which were exclusive to a given plant species.

As a result of the multitude of sequencing efforts over the last two decades, the sequences of more than 372 cyclotides are now available in CyBase, with tens of thousands more predicted to exist.[116,155] The sequences of a small selection of some of the more widely studied cyclotides are listed in Figure 5, including representatives from the three main sub-groups of cyclotides referred to as the bracelet, Möbius and trypsin inhibitor cyclotides. Bracelet cyclotides are so named because their circular topology mimics an amino acid

bracelet. Möbius cyclotides are similar but have a twist in their circular backbone due to a *cis*-Pro peptide bond in their backbone, forming a conceptual Möbius strip.[14] The trypsin inhibitor cyclotides are named based on their potent inhibitory activity against the serine protease trypsin. The sequences of trypsin inhibitor cyclotides are quite different to those of the other two sub-groups and are highly homologous to a family of linear peptides called knottins and, thus, are also referred to as cyclic knottins.[24,27,28,45,59,119,196] We include them in the cyclotide family as they contain a CCK motif and their biosynthetic pathway shares common features with cyclotides from the Möbius and bracelet sub-groups. Recently, another grouping of cyclotides that comprised members of the Möbius and bracelet sub-groups was reported, namely the Lys-rich cyclotides,[317] but it is too early to decide how big this grouping might be.

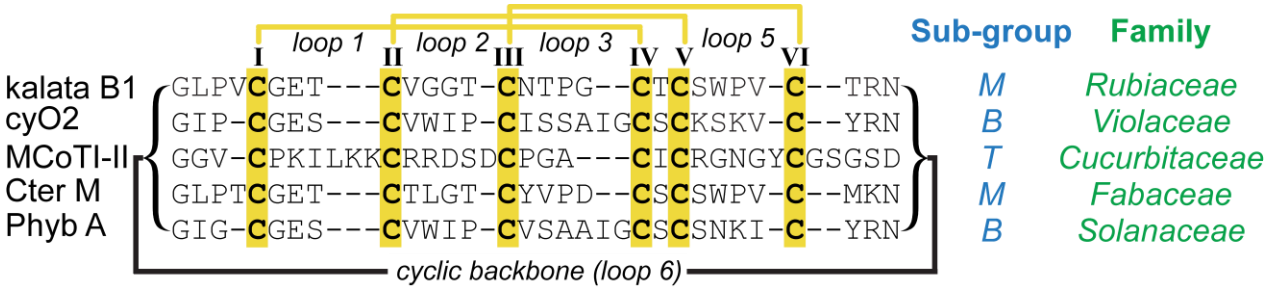

Figure 5. **Sequences of selected cyclotides.** Examples include kalata B1, cycloviolacin O2 (cyO2) and *Momordica cochinchinensis* trypsin inhibitor-II (MCoTI-II) as representatives of the Möbius (M), bracelet (B) and trypsin inhibitor (T) sub-groups, respectively. These are the most studied prototypic sequences from these sub-groups, as well as being representative examples from the Rubiaceae, Violaceae and Cucurbitaceae plant families, respectively. Also shown are the sequences of Cter M and Phyb A, as examples of cyclotides from the Fabaceae and Solanaceae plant families. Key features of the sequences include the six conserved Cys residues (numbered I–VI) and the six backbone loops (loops 1–6). A conserved Asn or Asp residue in loop 6 corresponds to the C-terminal residue of the cyclotide domain in the precursor protein and is essential for biosynthetic cyclization of the peptide backbone.

Cyclotides do not occur in all plants, but so far they have been found in plants from five major plant families: the Rubiaceae, Violaceae, Solanaceae, Cucurbitaceae and Fabaceae. Table 1 lists the currently known cyclotide-bearing species within these families, and illustrates that the total number of cyclotide-bearing plant species varies widely amongst these five families. None of the families has been exhaustively screened but it is currently thought that cyclotides are ubiquitous in the Violaceae family, being detected in every species so far screened from that family. By contrast, cyclotides are rather sparse in the other families, occurring in fewer than 5% of Rubiaceae plants screened so far and occurring in just a handful of species from the other three plant families. Thus, there are many remaining questions about the evolution and distribution of cyclotides across plant families and many more discovery efforts are required.

Table 1. Plant species in which cyclotides have been reported[a]

Plant family and species	*Example cyclotides*[b]	*Comments*
Violaceae		
Viola abyssinica	vaby peptides[215]	Cyclotides have been found in every member of the Violaceae family examined so far and it is hypothesized that they are ubiquitous in this family. The Violaceae comprises more than 900 species across 23–31 genera. Cyclotides typically occur in all tissues of these plants, including roots, stems, leaves and flowers.
V. adunca	Vaf-1[c]	
V. arvensis	violapeptides[15]	
V. baoshanensis	viba peptides[151]	
V. biflora	vibi peptides[42,120]	
V. cotyledon	vico peptides[42]	
V. decumbens	vide A[226]	
V. hederacea	cycloviolacins;[63] vhl peptides	
V. ignobilis	vigno peptides[332]	
V. labridorica	vila A-D[181]	
V. nivalis	vini A[226]	
V. odorata L	cycloviolacin O1-O25;[14,156] vodo M, N, O;[43] violacin A;[83]	
V. philippica	viphi peptides;[203] kalata B1	
V. pinetorum	vpl and vpf peptides	
V. tianshanica	cycloviolacin T1[182]	
V. tricolor	vitri peptides[180]	
V. yedoensis	cycloviolacins[126]	
Gloeospermum blakeanum	globa peptides[155]	
G. pauciflorum	glopa peptides[155]	
Hybanthus denticulatus	hyde A[d]	
H. floribundus	hyfl peptides	
H. parviflorus	hypa A[26]	
Hymanthera obovata	hobo A[d]	
Leonia cymosa	cylcoviolins[23]	
Melicytus chathamicus	mech peptides[317]	
M. latifolius	mela peptides[317]	
M. macrophyllis	mema A and B[d]	
M. ramiflorus	mra peptides[139]	
Noisettia orchidiflora	NorA[403]	
Orthion oblanceolatum	orto A[d]	
Pombalia calceolaria	poca peptides[411]	
Rinorea bengalensis	cT10[409]	
R. dentate	riden A[323]	
R. gracilipes	rigra A[d]	
R. lindeniana	rili A; rili B[d]	
R. sumatrana	visu 1 and 2[344]	
R. virgate	rivi 1–7[409]	
Rubiaceae		
Carapichea ipecacuanha	caripe peptides[262,367]	The Rubiaceae is one of the largest plant families known. Many other species in the Rubiaceae have been screened, but so far only these species have been reported as cyclotide-positive. Cyclotides typically occur in all tissues of these plants, including roots, stems, leaves and flowers.
Chassalia chartacea	chassatides[235]	
Chassalia curviflora	chacur[c]	
Chassalia discolor	CD-1[c]	
Chassalia parvifolia	circulins[7,22,406]	
Hedyotis biflora	hedyotides[207,213,280,350]	
H. centranthoides	hcf-1[c]	
H. terminalis	htf-1[c]	
Oldenlandia affinis	kalata peptides[1-5,9]	
Palicourea condensata	palicoureins[25]	
P. rigida	parigidin-br1[236,329,345]	
P. tetragona	paltet 1[c]	
Psychotria brachiata	psybra 1[c]	

Psychotria brachyceras	Psyleio and psybry peptides[c]	
Psychotria leiocarpa	Psyleio peptides[338]	
Psychotria leptothyrsa	psyle peptides[157,158]	
Psychotria longipes	cyclopsychotride A[8]	
Psychotria poeppigiana	psypoe 1	
Psychotria solitudinum	psysol 2[305]	
Psychotria suterella	PS-1[c]	
Cucurbitaceae		
Momordica clarkeana	TI peptides[315]	These trypsin inhibitor cyclotides are also referred to as cyclic knottins; typically, these peptides are found only in seeds.
M. cochinchinensis	MCoTI peptides[24]	
M. denticulate	TI peptides[315]	
M. diocia	Modi peptides[424]	
M. gilgiana	TI peptides[315]	
M. macrophylla	TI peptides[315]	
M. subangulata	TI peptides[315]	
Fabaceae		
Clitoria ternatea	Cter peptides;[204] cliotides[206]	These cyclotides are biosynthetically processed from 'hijacked' genes (i.e. from albumin genes in which an ancestral albumin subunit is replaced by a cyclotide domain)
Solanaceae		
Petunia axillaris	Phyb peptides[237]	So far only one genus (Petunia) from the Solanaceae family has been found to be cyclotide-positive.
Petunia integrifolia	Phyb peptides[237]	
Petunia x hybrida	Phyb peptides[237]	

[a]Data derived from CyBase (www.cybase.org.au)[87,127,171] and a separate report;[252]

[b]The selected examples of peptides from these plants are not exhaustive and many of these plants also contain other cyclotides;

[c]Partial peptide sequence or precursor sequence reported in CyBase with no primary literature citation;

[d]Reported in Gerlach et al.[252]

Aside from documenting the currently known distribution of cyclotides in the plant kingdom, Table 1 is useful for highlighting the various nomenclature schemes that have been used for cyclotides. In early studies, some of these macrocyclic peptides were named based on the names of the plants from which they were derived; for example, kalata B1 refers to peak B1 identified in a chromatographic trace of an extract from the African plant (*O. affinis*) known locally as kalata-kalata.[1] A variety of other nomenclatures were introduced in the early 1990s. For example, macrocyclic peptides from *Chassalia parvifolia* were referred to as circulins based on their head-to-tail cyclic backbone,[7] those from *Leonia cymosa* were referred to as cycloviolins,[23] and those from the native Australian violets (*Viola hederaceae*) as cycloviolacins.[63,81] A standardized nomenclature scheme was suggested in 2001,[26] based on the proposal that a systematic name be based on a pronounceable version of the first two letters of the genus name and first two letters of the species name followed by a capital letter. For example, according to this scheme the first cyclotide from *Hybanthus parviflorus* was named hypa A.[26] This nomenclature has been widely, but not universally, adopted with some adaptations in various studies since then and is the one that we recommend for naming of cyclotides. Two recent articles provide a broader discussion of nomenclature for ribosomally synthesized peptides in general[271] and cyclic peptides[351] in particular.

In general, cyclotides do not occur as singletons and cyclotide-bearing plants typically contain several to many dozens of cyclotides. For example, *Viola hederaceae* contains at least 57 cyclotide-like masses in its proteome,[52] and *C. ternatea* expresses more than 79 cyclotide peptides.[204,206,333,440] It is currently not known why a single plant might produce so many subtle variations, i.e. many of the cyclotide variants in a single plant contain just one or two residue changes, and these are often conservative changes. For example, kalata B1 and B2 are the two major components of *O. affinis* and differ at five residues, most of which are highly conservative substitutions, such as Ser to Thr, or Leu to Ile, with the most prominent change being an Asn to Asp mutation. The reason for the diversity of cyclotides in a single plant is not known but may reflect a strategy of plants to overcome the potential development of resistance by pests or pathogens to the protective cyclotide armory.

It generally seems to be the case that most plants have their own individual suite of cyclotides, and it is uncommon for one cyclotide to occur in multiple plant species. For example, an extensive screen of plants from the Violaceae family indicated that fewer than one-third of the cyclotides discovered were

present in more than one plant species,[307] meaning that more than two-thirds of cyclotides are unique to a particular plant. Exceptions do occur; for example, kalata B1 has been identified in six separate plants to date, including *O. affinis*, *Viola odorata*, *V. tricolor*, *V. baoshanensis*, *V. yedoensis* and *V. philippica*. Similarly, cycloviolacin O12 occurs in seven different species (*Viola tricolor*, *V. arvensis*, *V. baoshanensis*, *V. yedoensis*, *V. tianshanica*, *V. abyssinica* and *V. philippica*). Aside from these relatively uncommon occurrences of one cyclotide appearing in multiple plants, each plant seems to have its own suite of cyclotides and indeed, within each plant, the suite of cyclotides in different tissues varies. For example, analyzing *Viola hederacea* extracts prepared from different tissues revealed that certain cyclotides were enriched in aerial tissues (leaves and flowers), whereas others were more abundant in the roots and tended to be more hydrophobic.[52] More recently, tissue-specific expression studies in *C. ternatea* also identified separate suites of cyclotides in aerial and belowground tissues, with the two clusters of cyclotides having different biophysical properties and activity profiles.[333]

Aside from the variation in cyclotide content between separate tissues in a single plant, there have also been reports of variation in the cyclotide content of a plant species over different seasons or in different geographic locations. For example, studies on *Viola odorata* identified seasonal variation in cyclotide content by comparing plant samples collected in summer and winter[53] and recent studies examining *Viola odorata* samples collected from different parts of India revealed that expression levels of many cyclotides varied according to geographic location.[377] Such variations are probably more widespread than is currently recognized and the topic represents an important future area of study in cyclotide ecology, as are studies on the potential up- or down-regulation of cyclotides in response to specific biotic or abiotic treatments, a notion that has been only briefly addressed so far.[173,390]

There have been numerous studies of plant-derived cystine knot molecules that have sequences similar to cyclotides but do not have a cyclic backbone.[83,99,138,139,157,172,207,235,237,265,306,333,337,343,424] The first such example was violacin A.[83] We refer to these molecules as acyclotides[237] although others have alternatively suggested the name uncyclotides.[207,235] Our preference is for the term ‘acyclotide’ because it does not imply a temporal or mechanistic link between cyclotides and these linear analogs, whereas ‘uncyclotides’ could give the impression that an uncyclotide is molecule that was once cyclic and no longer is. As discussed in Section 4, acyclotides mainly arise because of mutations in their precursor proteins that

do not allow the cyclization to proceed in the first place. On this point, we note that since the focus of this review is on cyclotides, we will not further discuss the growing the range of acyclotides being reported.

Returning to the sequencing methodologies, we note that although MS/MS based sequencing is now faster and more cost-effective than Edman sequencing, it has a shortcoming in that Ile and Leu are isobaric and are not readily distinguished using standard MS/MS sequencing approaches. As a result of this limitation, some authors have presented newly discovered cyclotide sequences via homology, with Ile and Leu designations in the reported sequences based on related cyclotides rather than having been experimentally verified. For this reason, it is recommended that peptide-based discovery should be complemented by data at the nucleic acid level, where the Ile and Leu ambiguity can be readily resolved, as described in Section 2.2.

2.2 Nucleic acid-based discovery

The fact that cyclotides are genetically encoded and then transcribed and translated into precursor proteins that are post-translationally processed allows their sequence information to be determined from cDNA libraries or deduced from genome or transcriptome data. Following the first report of a cyclotide precursor protein sequence in 2001 that was identified from a cDNA library produced using RNA isolated from *O. affinis* leaf tissue,[29] many other cyclotide precursor sequences have been reported. Typically, the cyclotide precursors comprise an endoplasmic reticulum (ER) signal sequence followed by one or more cyclotide-encoding domains that are flanked N- and C-terminally with leader sequences implicated in biosynthesis. As described in Section 4, mature cyclotides are processed from these precursor proteins principally by asparaginyl endopeptidases.

Figure 6 shows a schematic representation of the various precursor protein architectures for cyclotides deriving from the Violaceae, Rubiaceae, Cucurbitaceae, Fabaceae and Solanaceae plant families, along with a pie chart showing the number of cyclotide peptides currently known in each of these families. Two points should be noted from this figure. The first is that most cyclotides are encoded by dedicated genes, i.e., genes whose sole function appears to be encoding cyclotide precursors. An exception is that cyclotides from the Fabaceae family are encoded by co-opted or ‘hijacked’ genes in which a cyclotide domain appears to have usurped part of an albumin gene, i.e. one of the two albumin subunits (PA1b) is

replaced by the cyclotide domain Cter M in the example shown in Figure 6. This phenomenon suggests that multiple independent evolutionary pathways have led to cyclotide production by plants.

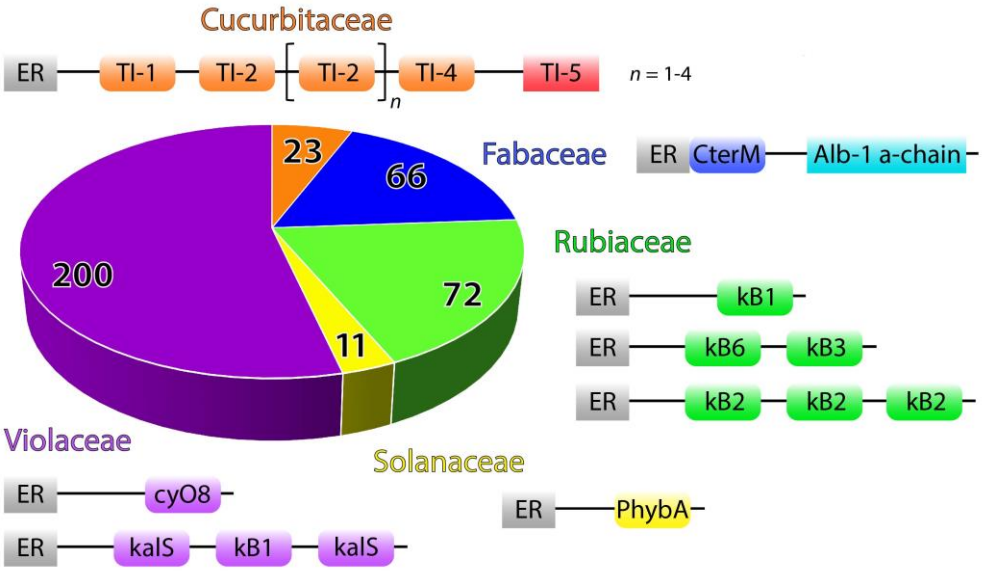

Figure 6. **Schematic illustration of precursor protein architectures for selected cyclotides within the five cyclotide-producing plant families.** Cyclotide domains are represented as rounded rectangles labelled with the name of the mature cyclotide, e.g. kB1 = kalata B1, kB2 = kalata B2, kalS = kalata S, etc; cyO8 = cycloviolacin O8; TI-2 = MCoTI-II. ER refers to the endoplasmic reticulum signal sequence and TI-5 is colored differently to TI-1, TI-2, and TI-4 to indicate that it is an acyclic knottin. The pie chart shows the number of mature cyclotide peptide sequences that have been experimentally verified within each of the five plant families to date.

The second point to make from Figure 6 is that many cyclotide precursors encode multiple copies of the same cyclotide (e.g. the *Oak4* gene has three copies of the sequence encoding kalata B2), or copies of several different cyclotides (e.g. *Oak2* encodes kalata B6 and kalata B3). This multiplicity leads to some challenges in the bioinformatic analysis of cyclotide-encoding nucleic acid sequences, but overall a combination of discovery at the nucleic acid and peptide level is a powerful approach to the identification of new cyclotide sequences. Before discussing an example of this approach for cyclotide sequencing, we first describe a historical timeline of nucleic acid-based studies of cyclotides, not only in terms of sequencing but more broadly on the role that nucleic acid-based studies have contributed the development of the cyclotide field.

The discovery that cyclotides were genetically encoded and expressed as precursor proteins was first reported for the Rubiaceae plant *O. affinis* in 2001,[29] and expanded to the Violaceae in 2004[49] and later to other families in the dicot lineage of flowering plants. In 2005, genetic studies established a link between

defense-related and developmental transcriptional responses of cyclotide-like precursors in maize.[62] This was the first time that cyclotide-like nucleic acid sequences were reported in a monocot plant, an observation that was subsequently confirmed in a range of other monocots, albeit with the nucleic acid sequences presumed to encode acyclic versions of cyclotides.[86] Concurrently, in 2006, the first paper to report the genetic basis of an acyclotide in a dicot plant was published.[83] In 2007 and 2008, the roles of asparaginyl endoproteinase enzymes in cyclotide biosynthesis were elucidated via the expression of cyclotide precursors in transgenic plants.[101,115] An extensive study in 2010 of cyclotide proteins and precursors from the genus *Gloeospermum* filled in a gap in the cyclotide map of Violaceae-related plants and included a discussion of not only the cyclotide precursors but also their processing proteins.[155] In 2011, the first report of an unusual biosynthetic origin for cyclotides in legumes (Fabaceae family) was published,[205] and this was followed soon after by a paper reporting additional cyclotides from 'hijacked' or chimeric albumin precursors.[206] The deciphering of the genes for a plant from the Cucurbitaceae family, *M. cochinchinensis* in 2012 demonstrated the multidomain nature of the trypsin inhibitor cyclotide precursor and suggested that the genes expanded by parallelism involving biosynthesis using asparaginyl endoproteinase enzymes.[234] The first report of cyclotides in a Solanaceae plant also occurred in 2012,[237] aided by transcript data. The combined approach involving proteomics, transcriptomics and genomics for cyclotide sequencing was broadly applied to many species in 2013.[252] In 2015, the discovery of genes for a new series of linear derivatives of cyclotides in monocot plants (Poaceae family) provided new insights into the evolution of cyclotides.[265] In 2016, a link between cyclotide localization *in planta* and function in the Fabaceae plant *C. ternatea* was reported, drawing heavily on data at both the peptide and transcript levels.[333] Cyclotides expressed in above-ground tissues had activities directed towards insect pests while those in tissues in contact with soil tended to have bioactivity consistent with a role against nematode pests. Most recently, a breakthrough in our understanding of cyclotide biosynthesis occurred in 2019 with the discovery of the enzyme, kalatase, that is involved in the N-terminal processing of cyclotide precursors.[434] All of these studies and a range of others cited in the references highlight that central role that molecular biology has played in cyclotide discovery via nucleic acid information, which nicely complements the vital role that chemistry has played for discovery and characterization at the peptide level.

A recent paper by Du et al.[424] provides a good illustration of how nucleic acid based sequencing can go hand-in-hand with peptide-based discovery and sequencing. In that report, a cDNA library generated using RNA isolated from *Momordica dioica* seeds was used to characterize the precursor protein and corresponding gene that encodes the Modi 1–6 peptides, all of which were subsequently identified in the plant extract. Figure 7 illustrates the structure of the *M. dioica* TIPTOP (Two Inhibitor Peptide TOPologies) precursor protein encoding six cyclotide domains, each with 34 amino acids, including two copies of Modi 2. The corresponding peptides were all isolated by HPLC and sequenced using MS/MS. The final cyclotide-like domain, Modi 6 is an acyclotide that lacks the C-terminal SGSD sequence. The observation that a single gene encodes multiple cyclotides and a single C-terminal acyclotide was reported earlier for other *Momordica* precursors.[234,315] As noted earlier, an important factor to note when combining peptide-based and nucleic acid-based discovery approaches is that the combined approach removes the ambiguity associated with isobaric Ile and Leu residues.

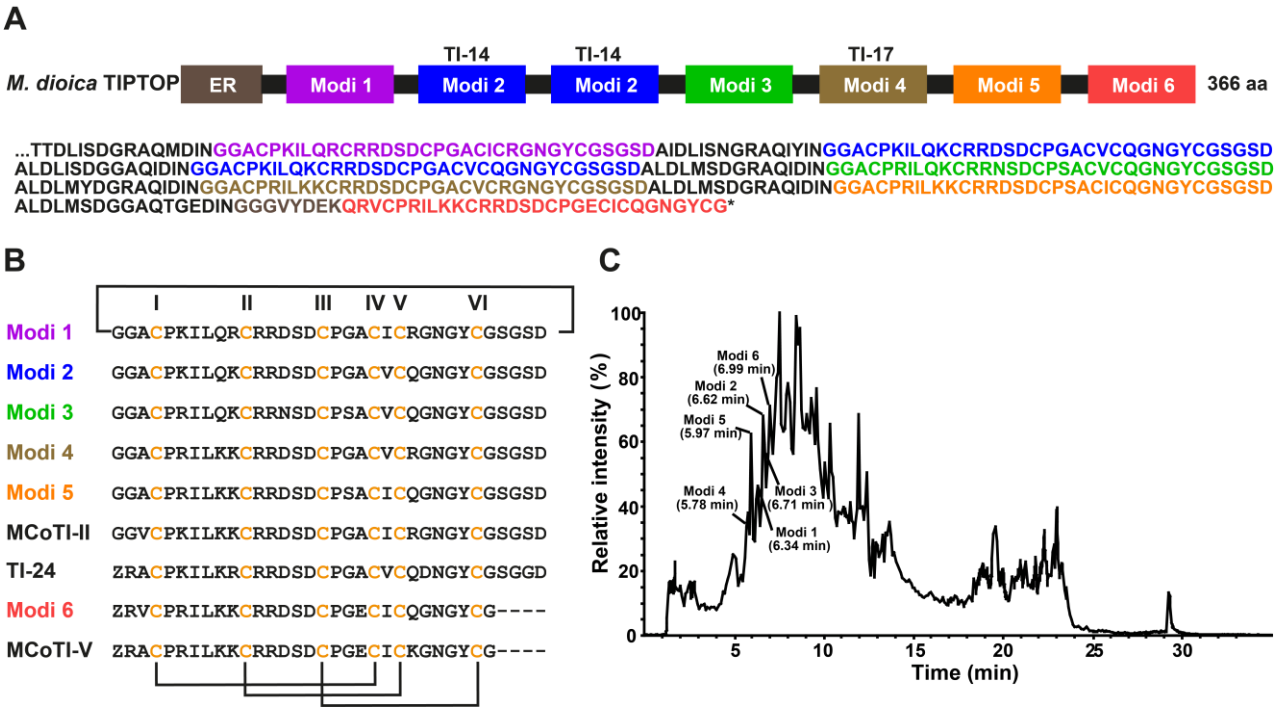

Figure 7. **Gene precursor sequence and derived peptides from *Momordica dioica*.** (A) Schematic diagram of the *M. dioica* TIPTOP precursor and the sequence of encoded peptides. Sequences colored blue (Modi 2) and brown (Modi 4) correspond to the previously reported peptides TI-14 and TI-17, respectively. The novel sequences are colored in purple (Modi 1), green (Modi 3), orange (Modi 5), and red (Modi 6). (B) Sequence alignment of known MCoTI-II, TI-24, and MCoTI-V and novel Modi peptide sequences (cyclic: Modi 1–5; acyclic: Modi 6). Cys residues (numbered I–VI) are highlighted in orange. The N-terminal residue of the acyclic peptides (Modi 6, TI-24 and MCoTI-V) is a pyroglutamic acid (Z) residue. (C) LC-MS trace of the crude peptide extract from *M. dioica* seeds and their corresponding retention time. Adapted with permission from Du et al.[424] with a typographical error in the sequence of TI-24 in that paper corrected above.

With the increasing availability of plant genomes and transcriptomes, access to the required nucleic acid data for cyclotide discovery is becoming more convenient, less expensive and, accordingly, more widely used. Recent examples of transcriptome or genome-based approaches to cyclotide discovery include the discovery of a suite of Lys-rich peptides from *Melicytus* plants,[389] as well as from *V. odorata* and a variety of traditional Chinese medicinal plants.[389,412,416]

2.3 Quantification

As is apparent from Figure 7, cyclotides are readily detected using LC-MS and may be quantified using standard curves in extracts or in prepared solutions of purified cyclotides.[219] Because of their wide range of potential applications in agriculture and medicine there has been much interest in quantifying cyclotides in biological solutions,[64] cells[91,152,153,341,342] as well as *in vivo*[121,122,201,202,339,340,436] and in environmental samples.[208-210] A range of MS-based approaches have been used in these studies and the challenges of dealing with identification and quantification of cyclotides in complex mixtures are starting to be addressed.[259]

3. STRUCTURE

3.1 Primary structure and amino acid composition

Cyclotides have the generic sequence cyclo-[C^{I}–X_a–C^{II}–X_b–C^{III}–X_c–C^{IV}–X_d– C^{v}–X_e–C^{VI}–X_f], where a = 3–6 residues, b = 4–5 residues, c = 3–7 residues, d = 1 residue; e = 4–6 residues and f = 5–8 residues for the currently known naturally occurring cyclotides. Sequences of the full range of known cyclotides are listed within CyBase (www.cybase.org.au),[87,127,171] so we do not reproduce all sequences here (Figure 5 shows a few key examples).

As far as their amino acid content is concerned, cyclotides are composed entirely of proteinogenic amino acids but have markedly different compositions to typical peptide and protein sequences. For example, Figure 8 shows that Cys is the most abundant amino acid in cyclotides, despite being the least abundant amino acid across all peptide and protein sequences listed in UniProt. This observation illustrates

the importance of the cystine knot as the key characteristic feature of cyclotides, and this property has been harnessed in various discovery efforts (Section 2). Other notable differences include the fact that Pro is highly represented in cyclotides relative to most proteins, and Ala is underrepresented. In contrast with these differences between cyclotides and other proteins, the relatively low abundance of His and Met in cyclotides mirrors that trend in other (non-cyclotide) proteins, as does the high natural abundance of Gly and Ser (Figure 8).

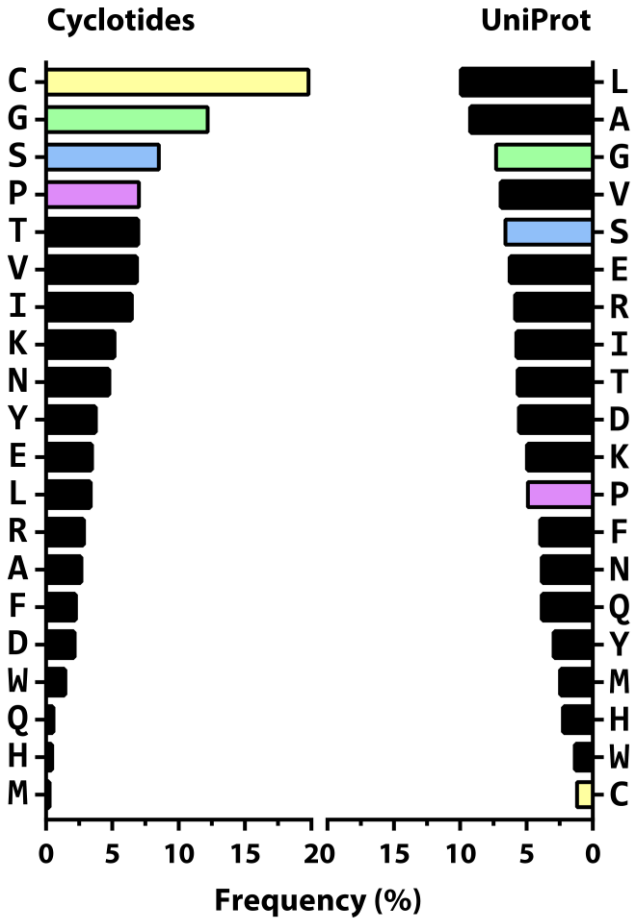

Figure 8. **Relative abundance of proteinogenic amino acids in cyclotides compared to all proteins.** Data generated from an analysis of sequences in CyBase and UniProt. Color coding is used to highlight the four most-abundant amino acids in cyclotides, two of which are different compared to other proteins (Cys and Pro), whereas Gly and Ser are relatively similar in order of abundance.

Unlike many other classes of peptides and proteins, cyclotides are notably free of post-translational modifications, apart from their head-to-tail cyclization and disulfide bonds. The first report[307] of an additional post-translational modification is for putatively glycosylated Lys residues detected by shifts in units of 162 Da corresponding to hexose sugars in several cyclotides from Violaceae plants. Extensive analysis by MS/MS identified cyclotides that were glycosylated variants of cycloviolacin O2, including mema A and mram 1 (from *Melicytus macrophyllus* and *M. ramiflorus* respectively). In both instances, the

additional hexose moieties were associated with loop 5, which contained the peptide sequences KSKV and KDKV respectively. Using a combination of chemical methods and NMR spectroscopy, it was confirmed that the Lys residues were the sites of glycosylation. Another study[337] reported a range of post translational modifications in cyclotides from *C. ternatea*, including deamidation, oxidation, hydroxylation, dehydration, glycosylation, methylation and truncation, suggesting that post-translational modifications might be more common that originally thought.

3.2 Secondary and tertiary (3D) structure

NMR has been the main structural tool used to determine the secondary and tertiary structures of cyclotides, principally because cyclotides have well dispersed and easily assignable NMR spectra. Additionally, like other small disulfide-rich peptides, cyclotides are typically recalcitrant to crystallization, and so X-ray methods are generally not suitable. The major element of secondary structure in most cyclotides is a small β-sheet, which is typically detected via a characteristic pattern of NOEs across two or three β-strands, as illustrated in Figure 9 for kalata B1.[9] Cyclotides also contain multiple turns and some cyclotides, such as cycloviolacin O1,[14] contain a small helix. The β-sheet is conserved in most cyclotides and is intimately connected with the cystine knot at the core of cyclotide structures (Figure 9).

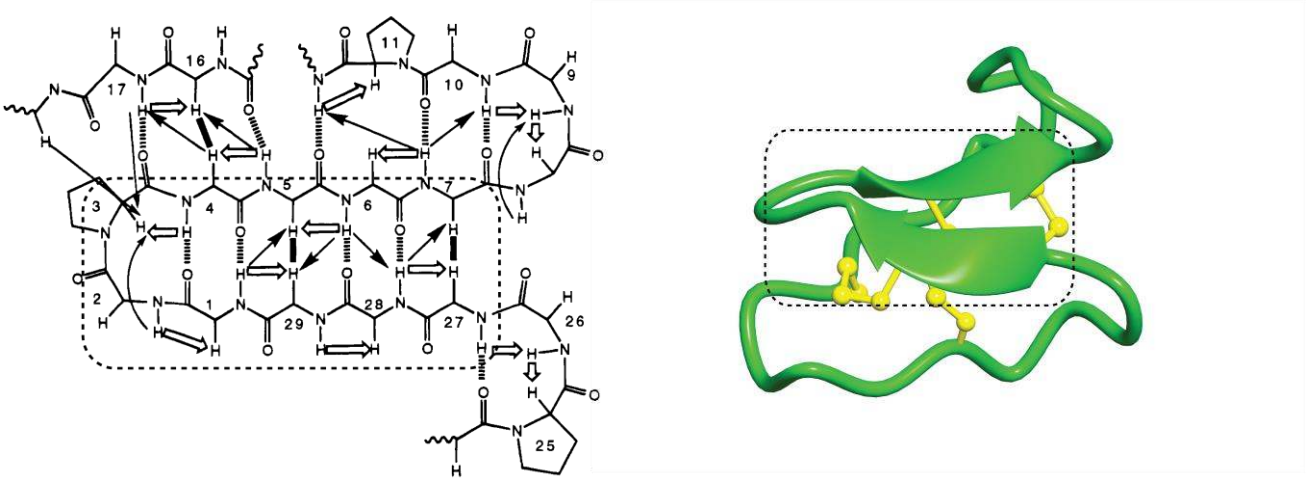

Figure 9. **Secondary and tertiary structural elements within cyclotides.** The left panel shows the NOE pattern defining a small triple-stranded β-sheet in kalata B1, as reported by Saether et al.[9] The right panel shows the 3D NMR structure of kalata B1 (PDB 1NB1), highlighting the cyclic backbone and cystine knot. The dashed boxes highlight the location of the β-sheet on the tertiary structure. Whereas the secondary structure diagram based on NOEs indicates the presence of a putative triple-stranded β-sheet, the third strand is typically somewhat distorted and not always recognized by molecular rendering software, for example, it is illustrated as a β-hairpin denoted by two arrows in (B). Note that the numbering scheme in the schematic diagram is from the original paper[9] as opposed to numbering based on cyclotide precursor genes shown in Figures 1 and 5 (residue 1 in Figure 9 corresponds to Ser22 in Figure 1).

As the placement of Cys residues shows strong conservation among cyclotides and the cystine knot has a dominant effect on structure, other cyclotide structures are very similar to that of kalata B1, with just minor variations in the sizes and conformations of the backbone loops between Cys residues. Table 2 lists the PDB ID codes for cyclotide structures reported to date. Most were determined by NMR spectroscopy, but in a few incidences, X-ray crystallography has been used to determine cyclotide structures. A breakthrough in the ability to obtain crystals of cyclotides occurred in 2014 when racemic crystallography was applied to cyclotide structure determination.[295] In that study, an all-D enantiomer of kalata B1 was synthesized and mixed with synthetic L-kalata B1 to generate a racemic mixture that readily formed crystals suitable for diffraction. Both NMR and X-ray structures gave consistent results in terms of the geometry of the cystine knot motif.

The relatively high structural conservation of cyclotides makes them suitable candidates for predicting the 3D structures of new sequences by modelling, as applied in an early study of vodo M and vodo N from *Viola odorata*.[43] Very recently, the potential to fast-track the structure determination of cyclotides and other cyclic peptides based on just chemical shift information, which avoids the need for time-consuming assignment of NOEs, was demonstrated for kalata B1.[439] Given the extensive set of experimental structures available (Table 2), approaches based on modelling or structure prediction based on chemical shift data are likely to become more common in the future, except in cases where a high resolution experimental structure is required.

Table 2. PDB entries for cyclotide-related three-dimensional structures[a]

Name of peptide	*Organism*	*PDB ID*	*Comment*	*Ref*
Plant-derived native cyclotides				
Kalata B1 (kB1)	*O. affinis*	1KAL[b]	First structure of a cyclotide	9
"	"	1K48	Disulfide pairing is incorrect, not recommended for use[c]	36
"	"	1JJZ	Un-optimized coordinates for 1K48	36
"	"	1NB1	Best high resolution structure, the preferred kB1 structure for analysis[d]	41
"	"	1ZNU	In DPC micelle solution	89
Kalata B2	"	1PT4	In aqueous solution	65
"	"	2KCH	Micelle bound structure	147
"	"	N/A	Solution structure not deposited	88
Kalata B5	"	2KUX	In aqueous solution, pH study	177
Kalata B7	"	2JWM	Mn^{2+} binding in DPC micelle	124
"	"	2M9O	Solution state structure	263
Kalata B8	"	2B38	Solution state structure	79
Kalata B12	"	2KVX	pH study to probe conserved Glu	212
Circulin A	*C. parvifolia*	1BH4	Solution structure by NMR	19
Circulin B	"	2ERI	Solution structure by NMR	67
Varv F	*V. arvensis*	3E4H	First crystal structure of a cyclotide	149
"	"	2K7G	Solution state structure	149
Vhr-1	*V. hederacea*	1VB8	In aqueous solution	52
Vhl-1	"	1ZA8	In aqueous solution	63
Vhl-2	"	2KUK	In aqueous solution	175
Cycloviolacin O1	*V. odorata*	1NBJ	High resolution structure	41
"	"	1DF6	^{1}H NMR solution structure	14
Cycloviolacin O2	"	2KNM	In aqueous solution	146
"	"	2KCG	Solution structure by NMR	147
[E6E^{OMe}]CyO2[e]	"	2KNN	pH study to probe conserved Glu	146
Cycloviolacin O14	"	2GJ0	In aqueous solution	82
Violacin A	"	2FQA	First reported 'acyclotide' structure	83
Tricyclon A	*V. tricolor*	1YP8	Extra-long loop 6 cyclotide	68
Cter M	*C. ternatea*	2LAM	First structure of a Fabaceae cyclotide	205
Palicourein	*P. condensata*	1R1F	Extra-long loop 6 cyclotide	46
MCoTI-I	*M. cochinchinensis*	5WOV	In aqueous solution	407
MCoTI-HA	"	5WOW	Grafted analog of MCoTI-I	407
MCoTI-II	"	1IB9	First structure of a TI cyclotide	27
"	"	1HA9	Comparison with acyclic analogues	28
MCoTI-V	"	2LJS	Acyclic MCoTI peptide	234
Rivi3	*R. virgata*	6DHR	Solution structure by NMR	409
Synthetic cyclotides				
[Ala 1,15]kB1	Disulfide mutant	1N1U	Missing one disulfide bond	38
[Δ23-28]kB1	Acyclic permutant	1ORX	Backbone opened in loop 6	44
[P20D,V21K]kB1	Grafted cyclotide	2F2I	Grafted kB1 analogue to test folding	85
[W19K, P20D,V21K]kB1	Grafted cyclotide	2F2J	Grafted kB1 analogue to test folding	85
All-D kalata B1	Synthetic cyclotide	2JUE	Mirror image synthetic form of kB1	211
Linear kalata B1	Acyclic mutant	2KHB	Backbone opened in loop 6	233
[W23WW]kB1	Synthetic mutant	2MN1	Extra Trp residue in loop 5	284
[GGG]kB1[GGT]	Synthetic mutant	2MH1	kB1 cyclized using sortase A	287
D/L Kalata B1	Racemic mixture	4TTM	Racemic kalata B1	295

[G6A]kalata B1	Synthetic mutant	4TTN	Quasi-racemic mixture	295
[V25A]kalata B1	Synthetic mutant	4TTO	Quasi-racemic mixture	295
[Y15S]kalata B7	Synthetic mutant	2MW0	Used to probe cation binding	346
[ΔSS]MCoTI-II	Folding intermediate	2PO8	Two-disulfide intermediate	106
Linear MCoTI-II	Acyclic mutant	2IT8	Backbone opened in loop 6	119
MTabl13	Grafted cyclotide	2MT8	Grafted MCoTI-II analogue designed as a drug lead for CML	311
kB1[ghrw;23-28]	Grafted cyclotide	2LUR	Grafted kB1 analogue designed as a drug lead for obesity	218
Cyclotide precursor fragments				
OaNTR	*O. affinis*	1WN8	NTR fragment of kalata B3 precursor	49
VoNTR	*V. odorata*	1WN4	NTR fragment of kalata S precursor	49
Cyclotide complexes				
Trypsin:MCoTI-II	*M. cochinchinensis*	4GUX	Crystal structure of complex	255
Hdm2:MCoTI-I	Synthetic cyclotide	2M86	Hdm2 with anti-tumor cyclotide	261
Kalata B7[f]	*O. affinis*	2JWM	In complex with Mn^{2+}	124

[a]Table includes entries found in the PDB (www.rcsb.org) using the search terms "cyclotide" or "kalata" or "knottin" or "MCoTI";
[b]1KAL, the prototypical structure of a cyclotide was determined before the term 'cyclotide' was introduced, so does not appear using the above search strings in the PDB, but is deposited there;
[c]A later study[41] showed that the 1K48 structure has incorrect disulfide connectivity;
[d]We recommend this PDB file (1NB1) as the preferred structure of kalata B1;
[e]Cycloviolacin O2 with Glu6 O-methylated;
[f]The entry for kalata B7 is duplicated on this line (from earlier in the Table) to reflect that it can be considered as a complex (with manganese ions); Table adapted and updated from Kan and Craik.[417]

In describing the features of cyclotide 3D structures, it is useful to remember that cyclotides are categorized into three sub-groups: the bracelet, Möbius and trypsin inhibitor sub-groups. Approximately one-third of natural cyclotides have the Möbius configuration, two-thirds are bracelets, and there are only a relatively small number of trypsin inhibitor cyclotides. Structures have been determined for at least several representatives from each of the three sub-groups. The term Möbius was introduced to reflect the fact that peptides in this sub-group typically have a Trp–Pro (or Tyr–Pro) dipeptide pair in loop 5 (see sequences in Figure 5, as well as Figure 10) that promotes a *cis* conformation of the intervening amide bond, producing a 180° twist in the cyclic backbone, forming a conceptual Möbius strip. This was first noted for kalata B1[9] and has since been experimentally verified in the structures of kalata B2[65] and kalata B5.[263] This nomenclature has been generalized and applies even in cases where structures have not yet been experimentally determined where it is assumed that if there is a Xaa-Pro dipeptide pair in loop 5 then it will probably be of the *cis* conformation.

The *cis*-proline peptide bond is not the only differentiating feature between Möbius and bracelet cyclotides. Sequence analyses of cyclotides from these sub-groups reveal some correlated effects within the various loops, as illustrated in Figure 10. For example, loop 3 typically contains six residues in bracelet cyclotides compared with four residues in Möbius cyclotides and this facilitates the formation of a short helix in loop 3 for bracelets that is not seen in Möbius cyclotides. Despite this difference, Gly is strongly conserved as the final residue in loop 3 for both sub-groups. Minor differences include the prevailing GET sequence in loop 1 of Möbius cyclotides compared with GES in bracelets and, similarly, the preference for Ser as the single residue in loop 4 of bracelets, whereas loop 4 is either Ser or Thr in Möbius cyclotides. Loop 2 also has a higher content of hydrophobic residues in bracelets. A detailed examination of the roles of various residues in the 3D structures of cyclotides was provided by Rosengren et al.[41] and by Burman et al.[186]

Figure 10. **Sequence diversity across individual loops of bracelet and Möbius cyclotides.** The CCK schematic in the center illustrates the disulfide connectivity between the six Cys residues (I–IV, II–V, III–VI) that defines the loop numbering. Logo diagrams display the amino acid frequency at each position in the various loops for the bracelet and Möbius sub-groups. Analysis was performed using 347 cyclotide sequences acquired from CyBase, which included 234 bracelet cyclotides and 113 Möbius cyclotides.

A common feature of Möbius and bracelet cyclotides is a cluster of hydrophobic residues on the surface of their structures, referred to as the hydrophobic patch. This feature is responsible for the characteristic late elution of many cyclotides on HPLC and, in part, for their ability to bind to membranes. For kalata B1, the patch comprises Pro3 and Val4 from loop 6, Val10 from loop 2, and Trp23, Pro24 and Val25 from loop 5. Cycloviolacin O2 also has a patch of hydrophobic residues, but it comprises residues 9–12 from loop 2, and Ile14, Ala17, and Ile18 from loop 3 (Figure 11). In both sub-groups of cyclotides the hydrophobic patch is located adjacent to a conserved Glu residue in loop 1 that is also implicated in membrane binding, as determined via a range of solution state[89,124,147,149] and solid state NMR studies.[370] Neutron reflectometry has also been used to assess the depth of penetration of cyclotides into a membrane monolayer.[233] These studies have been important in defining the modes of action of cyclotides, as described in Section 6.

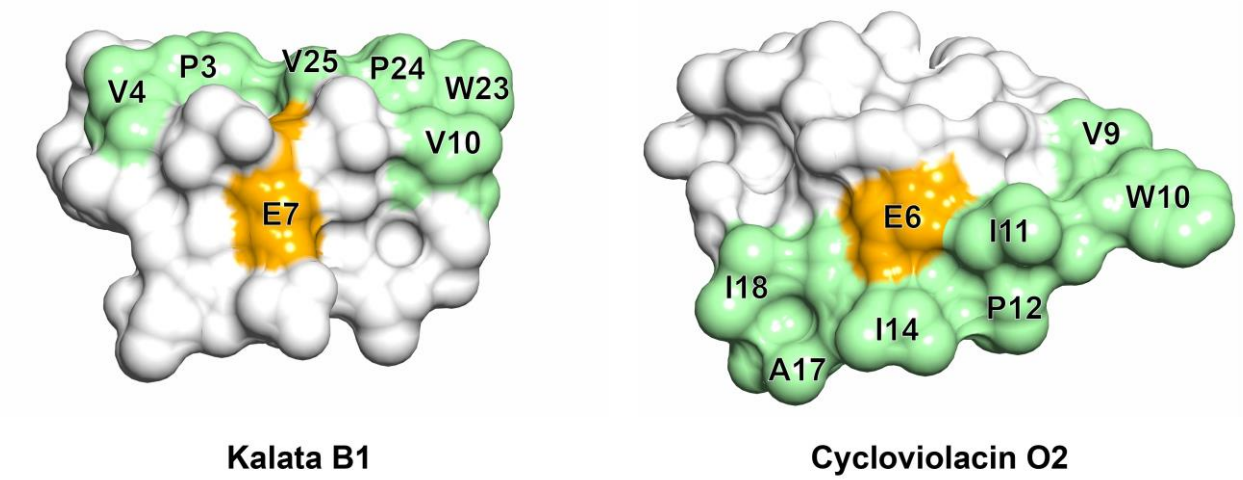

Figure 11. **Location of the hydrophobic patch on the surface of kalata B1 and cycloviolacin O2.** Residues forming the hydrophobic face were identified in mutagenesis studies or by examining peptide interactions with DPC micelles using NMR spectroscopy. These residues are colored green on a surface representation of the 3D structure of kalata B1 (PDB 1NB1) or cycloviolacin O2 (PDB 2KNM), shown in the same orientation. In kalata B1, the hydrophobic face comprises residues from loops 2, 5, and 6, whereas in cycloviolacin O2, loops 2 and 3 primarily form the hydrophobic face. The conserved Glu residue (loop 1) is colored orange.

In addition to the more than 20 structures of Möbius and bracelet cyclotides, there are several structures of trypsin inhibitor cyclotides available, both in the solution state and bound to trypsin, with the best characterized example being MCoTI-II. As shown in Figure 12, the structure of MCoTI-II in solution is very similar to the X-ray structure of MCoTI-II bound to trypsin, reflecting the exceptional rigidity

brought about by the highly cross-braced CCK motif. This rigidity is one of the key features of cyclotides that makes them favorable peptide scaffolds for drug design applications in which bioactive epitopes can be grafted into their sequence.

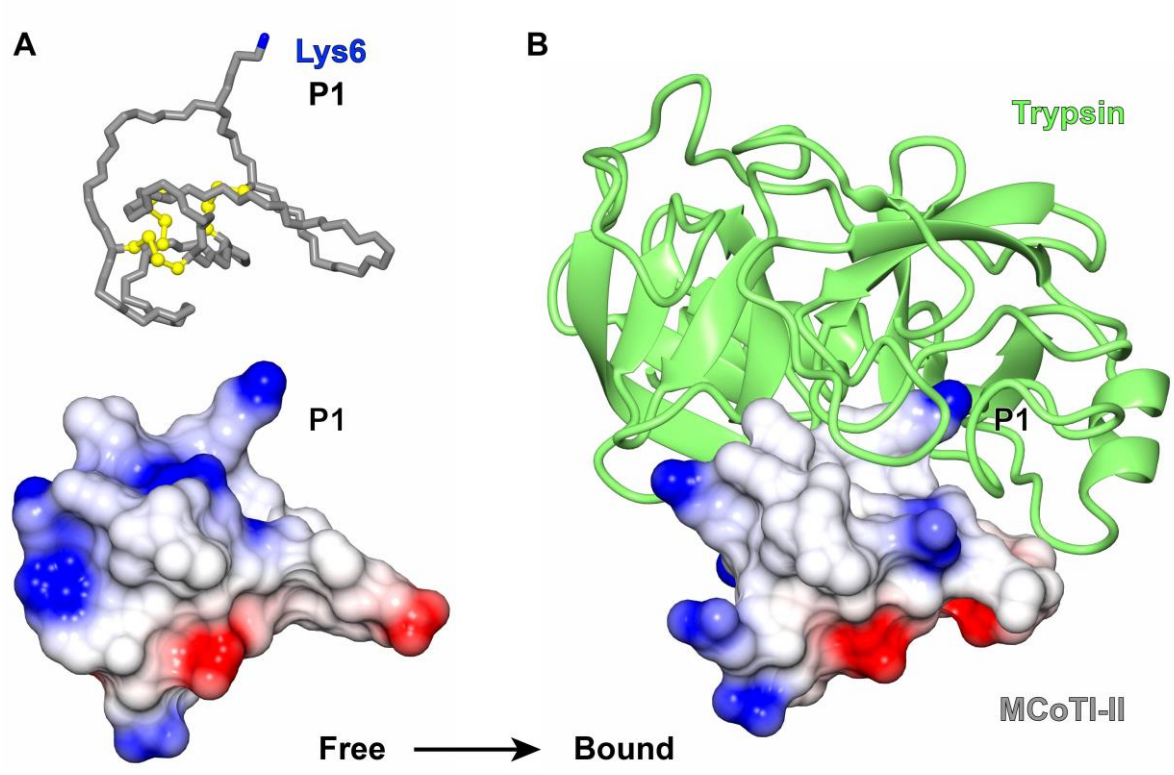

Figure 12. **Structure of MCoTI-II in solution and bound to trypsin.** (A) The solution structure of MCoTI-II (PDB 1IB9) shown as a backbone trace and surface representation (colored by electrostatic potential). The key residue that conveys trypsin specificity is the P1 Lys residue (labeled). (B) Structure of MCoTI-II bound to trypsin determined by X-ray crystallography (PDB 4GUX). The trypsin-bound structure of MCoTI-II is very similar to the solution structure, indicating that MCoTI-II is largely pre-organized into a favorable conformation for binding to trypsin (area of the binding interface is 968 $Å^2$).

3.3 Disulfide connectivity and oxidative folding

For NMR structure determination, it is usual to have first independently determined the disulfide connectivity of a peptide before embarking on NOE-based structure determination. This is often a challenging task to accomplish using chemical methods, especially when multiple disulfide bonds are close to one another, as is the case for a cystine knot. For the original structure determination of kalata B1, the NMR data itself was used to deduce the disulfide connectivity.[9] It is important to stress that the simple observation of an NOE between two Cys residues is not sufficient to establish that the two residues are connected in a disulfide bond. Indeed, in the case of kalata B1 and other cyclotides, it is often the case that Cys residues that are not bonded to one another often have stronger NOEs than those that are connected in

a disulfide bond. Thus, a rigorous analysis of NOE patterns for all possible disulfide pairs and energies of calculated structures is required to properly deduce disulfide connectivity from NMR data.

Aside from interest in defining the thermodynamically preferred equilibrium disulfide connectivity, the kinetics that underpin cystine knot formation in cyclotides is a subject that has fascinated researchers both from a theoretical[141,365] and experimental[142-144] perspective. *In vitro* studies involving reductive unfolding and oxidative refolding have been carried out for the prototypic cyclotides kalata B1, cycloviolacin O2 and MCoTI-II[38,106,214] as representatives of the Möbius, bracelet and trypsin inhibitor sub-groups, respectively. The rate of folding or unfolding can be heavily influenced by the conditions used, but a common feature that has emerged from folding studies is that a stable two-disulfide intermediate is often detectable during the folding and unfolding process. Interestingly, this intermediate appears to be "on pathway" for trypsin inhibitor cyclotides[106] but not for Möbius cyclotides. Figure 13 highlights that the long-lived two-disulfide intermediate, II_a, observed in the oxidative folding of Möbius cyclotide kalata B1 appears to shuffle back to a one-disulfide intermediate and then via an alternative two-disulfide intermediate to produce the final product. Interestingly, bracelet cyclotides appear to be more challenging to fold than cyclotides from the Möbius or trypsin inhibitor sub-groups, and although several approaches have been developed to facilitate the correct folding of these cyclotides.[11,12,104] this sub-class of cyclotides remains to be relatively inaccessible using synthetic chemistry approaches.

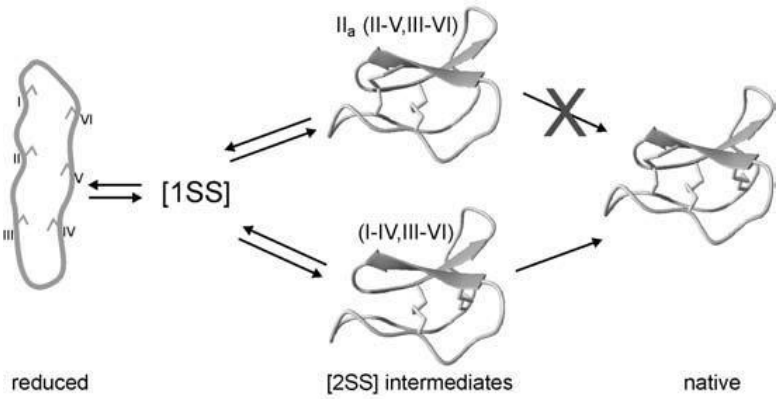

Figure 13. **Oxidative folding of kalata B1.** Simplified schematic illustrating the oxidative folding process for the representative Möbius cyclotide, kalata B1. From the fully reduced peptide on the left-hand side, several one and two-disulfide species are formed, including a major species that can be isolated corresponding to a native two-disulfide intermediate (II_a) with the disulfide bonds II–V and III–VI. This intermediate is not the direct precursor of the native state and has to be partially or completely reduced to convert to another species, which is the direct precursor of the native species, i.e., the two disulfide species (I–IV, III–VI). Figure reproduced with permission from Čemažar et al.[105]

Most experimental work on cyclotide folding kinetics was done in early studies,[38-40,60,84,103-106] and it is only recently that theoretical methods have been applied to cyclotide folding.[365] That study used thermodynamic integration simulations to examine different cystine knot connectivities of cycloviolacin O4 and identified three disulfide pairings with the lowest energy (in order of formation): (1) III–IV, II–V, I–VI; (2) III–V, II–VI, I-IV; and (3) I–IV, II–III, V–VI.[365] However, none of these disulfide pairings correspond to the native form (in no implied order of formation): I–IV, II–V, III–VI.[9] Separate analyses focused on the native disulfide connectivity indicated two possible orders of formation: I–IV, II–V, III–VI and II–V, I–IV, III–VI, suggesting that cycloviolacin O4 could fold via one or both of these paths. It is interesting to note that several theoretical structures of cycloviolacin O4 with non-native connectivity had lower free energies than the native form, which might reflect the challenges encountered when folding bracelet cyclotides *in vitro*, particularly the accumulation of misfolded products.[104] We note that he commentary in this section relates to *in vitro* folding of cyclotides. The situation *in vivo* is likely to be different and involve an array of auxiliary proteins, including protein disulfide isomerase[103] as well as probably involving flanking domains in the precursor proteins, as is described in Section 4.

3.4 Quaternary structure

It is not known whether quaternary complexes of cyclotides have a functional role in nature, but early studies using analytical ultracentrifuge measurements established that kalata B1 and kalata B2 can self-associate to form tetramers and octamers at low millimolar concentrations.[55] More recent NMR studies have suggested that self-association might be driven by hydrophobic interactions that facilitate formation of a multimeric core.[267] This model was based on concentration-dependent changes in ^{1}H chemical shifts observed for kalata B2,[267] and is shown in Figure 14. One possible role for such self-association could be to minimize disruption of the membranes of vacuoles in which cyclotides are stored in plant cells, although as yet there is no evidence to support this suggestion. It has also been suggested that the mechanism by which cyclotides form pores in insect membranes might involve self-association. It is challenging to decipher what aggregation-state a cyclotide might adopt in membrane environments but initial studies using electrophysiology[148] and neutron reflectometry[233] have provided initial insights that such aggregation is possible.

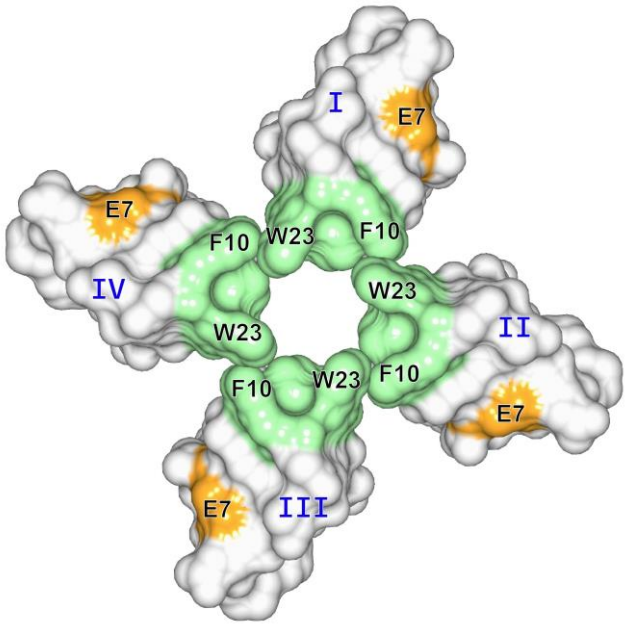

Figure 14. **Model of the proposed kalata B2 tetrameric complex.** NMR experiments using different sample concentrations were performed to identify changes in ^{1}H chemical shifts between monomeric and oligomeric kalata B2. These analyses indicated that self-association was mediated by the hydrophobic face of kalata B2, particularly Trp23 and Phe10, enabling a model of the tetrameric complex to be produced (reported by Rosengren et al.)[267] Dimerization of two tetramers has been proposed to enable formation of an octomeric complex.

3.5 Dynamics

The dynamics of cyclotides, both free in solution[183,296] and when bound to target proteins[183] have been studied by a range of NMR methods, as well as by molecular dynamics simulations.[118,119,285,286,324] The general conclusion to emerge from these studies is that, as expected, the cyclotide framework is rigid and there is not a great deal of flexibility in the backbone loops, with loop 6 being the most flexible, consistent with it generally being the largest of the six loops.

4. BIOSYNTHESIS

4.1 Insights from the arrangement of cyclotide-encoding genes

The first evidence that cyclotides are gene-encoded and ribosomally-synthesized as precursor proteins emerged with the identification of four cDNA clones (*Oak1–Oak4*) from the kalata B1-producing plant *O. affinis*.[29] Prior to this finding, cyclotide biosynthesis was relatively enigmatic as the peptide's original N- and C-termini are masked by the head-to-tail cyclic backbone. With the sequences of several

cyclotide precursors in hand, it was evident that the site for biosynthetic cyclization is located in loop 6, with the cyclotides encoded by *Oak1–Oak4* containing a conserved Gly-Leu-Pro tripeptide motif at the N-terminus and an Asn or Asp residue at the C-terminus.[29] Interestingly, the Oak1–4 proteins are quite different in length (111 to 210 amino acids) as they encode between one and three distinct cyclotide domains. In Oak1, the single kalata B1 domain is preceded by an N-terminal pro-sequence (23-amino acids) and followed by a short pro-sequence at the C-terminus (seven-amino acids). These sequence motifs were named the N-terminal repeat (NTR) and the C-terminal repeat (CTR), respectively, as they are also highly conserved in Oak3 (encoding a single kalata B7 domain), and in multi-domain precursors (Oak2 and Oak4) where they flank each cyclotide sequence. Indeed, the presence of sequence conservation at the expected processing sites suggested that enzymes were probably involved in cyclotide processing and head-to-tail cyclization. Differences in the consensus sequence at each site also suggested that each cleavage step was carried out by separate enzymes, with a conserved Asn or Asp residue just prior to the CTR implicating the involvement of enzymes from the asparaginyl endopeptidase (AEP) family, also named vacuolar processing enzymes, that were known to have key processing roles in plants. Figure 15 shows a schematic representation of the kalata B1-encoding precursor (Oak1), along with precursors from other plant families.

The identification of cyclotide-encoding cDNA clones from plants in the Violaceae family revealed that several aspects of cyclotide biosynthesis inferred from *O. affinis* also occur in other plant families (Figure 15). Four cDNA clones isolated from *Viola odorata*, including the first precursors that encode bracelet cyclotides, were found to display a similar arrangement to either *Oak1* (one cyclotide domain) or *Oak4* (three cyclotide domains).[49] Additional precursor sequences were subsequently identified from *Viola tricolor*[68] and *Hybanthus floribundus*.[69] In each precursor, the cyclotide domain is again flanked by NTR and CTR sequences, with certain residues at the processing sites showing high conservation. At the C-terminus, cleavage again occurs after an Asn or Asp residue, and a conserved Leu residue is present at the P2′ position within the CTR. At the N-terminus, Gly is the first residue of the cyclotide domain and Leu is also present at P2 in most NTR sequences. However, other positions show varying levels of diversity and the NTR and CTR sequences show little overall similarity to Oak1. These differences may reflect subtle specificity differences in the enzymes from Violaceae and Rubiaceae plants.

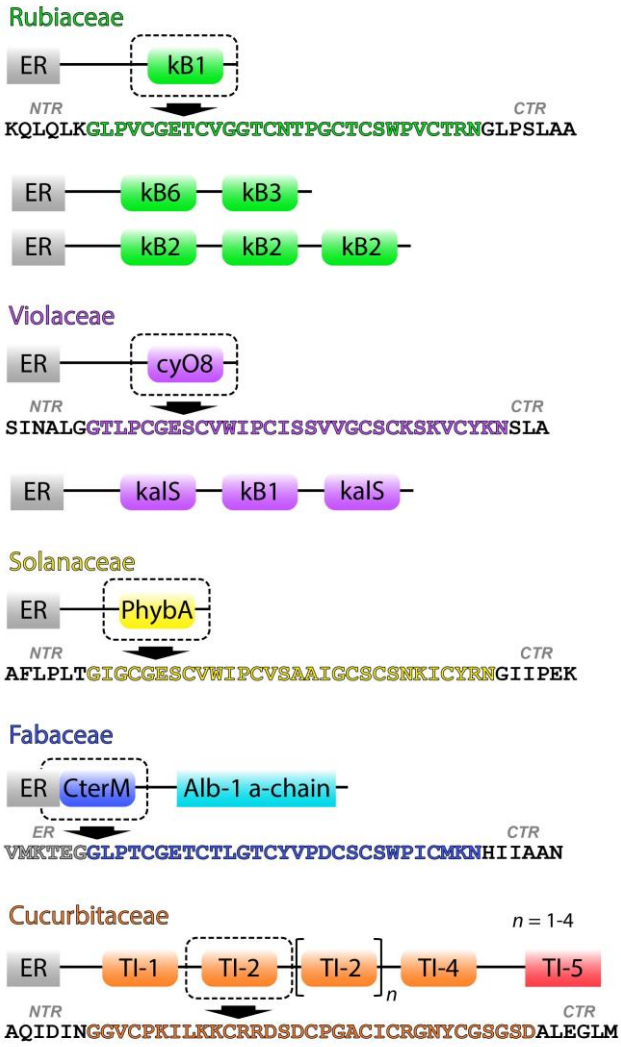

Figure 15. **Arrangement of cyclotide-encoding genes from five plant families.** The domain structure of the various cyclotide-encoding genes is shown in colored schematic diagrams. Dedicated genes expressing a single cyclotide have been identified in the Rubiaceae, Violaceae, and Solanaceae families. Plants in the Rubiaceae, Violaceae, Cucurbitaceae families also express precursors that encode multiple cyclotides. Cyclotides are produced by certain Fabaceae plants via co-opted genes, where the cyclotide domain replaces the albumin b-chain. The sequence of an example cyclotide for each family is shown below to illustrate the N-terminal repeat (NTR) and C-terminal repeat (CTR) sequences that flank each domain. In genes encoding multiple cyclotides, the linker sequence between adjacent cyclotide domains is comprised of the CTR of the preceding domain, followed by the NTR of the subsequent domain. Note that Fabaceae genes do not contain an NTR sequence as cyclotide domain commences immediately after the endoplasmic reticulum (ER) signal sequence.

Another observation to emerge in early studies was that synthetic peptides based on the *O. affinis* NTR and *V. odorata* NTR adopted a helical conformation in solution.[49] At the time, the proposed helical nature of the NTR was suggested to assist with protein folding. However, a recent study has shown that, when conjugated to the cyclotide domain, the NTR is not helical but is structurally disordered and promotes self-association, suggesting that the NTR might function as a vacuolar-targeting motif.[330] Overall, natural variations in precursor sequences from Rubiaceae and Violaceae plants have provided key insights into

cyclotide biosynthesis. For example, the identification of violacin A, an acyclotide found in *V. odorata*, provided strong evidence to support the importance of the C-terminal Asn or Asp residue for cyclization.[83] The gene encoding violacin A carries a point mutation that introduces a premature stop codon just prior to the C-terminal Asn residue and, consequently, the corresponding peptide is not cyclized *in planta* as it lacks an intact AEP recognition site.

Cyclotide-encoding sequences have now been identified in plants from the Fabaceae (*Clitoria ternatea*),[204,206] Curcurbitaceae (*Momordica cochinchinensis*)[234,315] and Solanaceae (*Petunia x hybrida*).[237] Thus, it is possible to survey the various precursor proteins and identify features that are common across the five plant families. At present, sequence data is predominantly focused on the cyclotide domain (Figure 10), which enables analysis of the cyclization site in a diverse range of cyclotides. Here, the C-terminal amino acid is a conserved Asn (78% of cyclotide sequences) or Asp (22%) residue, which is consistent with CTR processing and cyclization being carried out by AEPs in each of the five plant families. In bracelet and Möbius cyclotides, Asn is more prevalent than Asp at this position (88% and 77% of sequences, respectively). By contrast, the C-terminal residue in all known sequences of trypsin inhibitor cyclotides is Asp. At the N-terminus, Gly is found in almost all sequences. However, in bracelet cyclotides, other small residues are occasionally found at the N-terminus, such as Ser, although this variation is rare.

In the corresponding precursor proteins, each cyclotide domain has flanking sequences at the N- and C-terminus, but sequence conservation at each processing site is only modest. At the C-terminal site, a hydrophobic residue (Leu or Ile) is often found at the P2′ position and basic residues tend to occupy P2 in all families except the Cucurbitaceae, where Ser is present at P2.[234,315] As noted earlier, sequence variation at this processing site probably reflects specificity differences for AEPs from each plant family that carry out head-to-tail cyclization. Sequence differences are even more pronounced at the N-terminal processing site (Figure 15). For precursor proteins in the Fabaceae, the cyclotide domain is immediately preceded by the endoplasmic reticulum signal sequence, indicating that N-terminal processing for these cyclotides occurs during transit through the secretory pathway.[204,206] Precursors in each of the remaining plant families feature an NTR sequence, as seen in Rubiaceae and Violaceae precursors. In Cucurbitaceae precursors, cleavage at the N-terminal site occurs after a conserved Asn residue, suggesting that N-terminal processing for these proteins is carried out by AEPs.[234,315] However, there is little similarity with NTR sequences in

Rubiaceae, Violaceae or Solanaceae precursors, apart from a hydrophobic residue (Leu or Ile) at the P2 position, implying that N-terminal processing occurs via different mechanisms in separate plant families.

4.2 Expression in model plants

Several aspects of cyclotide biosynthesis have been examined in transgenic plants to provide complementary functional data. Initially, this work was predominately carried out using model plants that do not naturally produce cyclotides, such as *Arabadopsis thaliana* and *Nicotiana benthamiana*, due to their ease of genetic manipulation and lack of endogenous cyclotides that could potentially confound analysis of plant extracts. The focus of the first study on *in planta* cyclotide production was the kalata B1-encoding precursor, *Oak1*.[101,115] Transgenic *A. thaliana*, *N. benthamiana* and *N. tabacum* plants expressing *Oak1* cDNA were all found to produce cyclic kalata B1 containing three disulfide bonds, although the major products were incompletely processed linear peptides that contained one or more CTR residues (and were gradually converted to linear kalata B1) as well as a truncated peptide that lacked the first residue of the cyclotide domain. Interestingly, none of the processing intermediates contained NTR-derived residues, suggesting that cleavage at the NTR site is the first step in the processing pathway.[115] Access to cyclotide expression in transgenic plants also provided an opportunity to examine the role of AEPs in cyclotide biosynthesis using either chemical tools or site-directed mutagenesis. Initially, the activity of endogenous AEPs was blocked using a peptide aldehyde inhibitor that was infused into the leaves of *N. benthamiana* plants.[101] In leaves treated with an AEP inhibitor, the level of processed linear kalata B1 was markedly decreased and cyclic kalata B1 was not detected, indicating that AEPs are required for proteolytic cleavage at the CTR site and cyclization.

Mutagenesis studies were subsequently performed to further establish the role of AEPs and examine specificity requirements at the NTR and CTR processing sites. Transgenic plants expressing a mutant *Oak1* construct where the C-terminal Asn in kalata B1 was modified to Ala yielded only linear kalata B1 and incompletely processed peptides.[115] A similar result was observed when the C-terminal Asn was mutated to Asp, even though Asp is present at this position in many native cyclotides. A series of additional mutations were examined at sites in the CTR and N-terminal residues of kalata B1. The length of the CTR

could be decreased from seven residues to three residues without affecting production of cyclic kalata B1, but no cyclic peptide was produced when the CTR was absent, suggesting that cyclization is potentially coupled to cleavage of the CTR.[115] At the NTR cleavage site, no cyclic kalata B1 was detected when P2′ Leu (residue 2 in the cyclotide domain) was mutated to Ala and a similar effect was observed when P1′ Gly (residue 1) was replaced with Ala.

These observations were extended in a later mutagenesis study that considered a broader range of substitutions at the NTR and CTR cleavage sites.[221] Within the NTR, mutating P1 Lys to Ala did not affect processing, whereas replacing P2 Leu with Ala led to the production of additional misprocessed peptides without impairing production of cyclic kalata B1. Truncating the CTR established that the previously identified tripeptide Gly-Leu-Pro could be decreased to two residues (Gly-Leu), but further truncation was not compatible with cyclization. Point mutations at the CTR cleavage site also revealed a series of substitutions that had contrasting effects on cyclic kalata B1 production. However, there is an important caveat to several of these findings as they consider production of cyclic kalata B1 in non-specialist plants that do not express ligase-type AEPs. Indeed, a recent study has shown that certain mutations within the CTR are compatible with cyclic kalata B1 production when a ligase-type AEP (OaAEP1b) is co-expressed with the mutant *Oak1* sequence.[399] Overall, studying the effect of targeted mutations on cyclic kalata B1 production *in planta* has significantly contributed to dissecting the mechanisms that drive kalata B1 processing and cyclization, as illustrated in Figure 16. The next steps were to explore whether processing requirements for cyclotide precursors were similar in other plant families and to identify the class of enzymes responsible for processing at the Oak1 NTR site.

The identification of precursor genes in *M. cochinchinensis* that encode trypsin inhibitor cyclotides paved the way to study enzymatic processing in different families of plants and cyclotides. This notion was of particular interest as, in TIPTOP proteins, the NTR and CTR processing sites for each cyclotide domain had different sequences to other plant families, with cleavage after Asn at the NTR site (DIN↓GGV) and after Asp at the CTR site (GSD↓ALE).[234] This observation indicated that AEPs potentially mediated both cleavage events in TIPTOP proteins. To test this hypothesis, the *TIPTOP2* precursor was expressed in *Arabadopsis thaliana* under the control of the *OLEOSIN* promoter to enrich expression in the seeds. Wild-

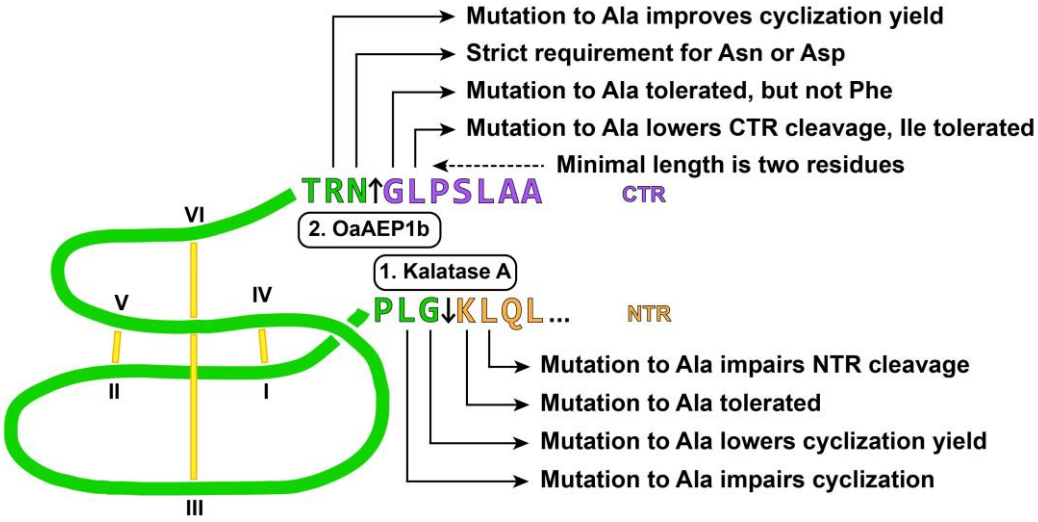

Figure 16. **Overview of key findings from *in planta* mutagenesis experiments studying enzymatic processing of kalata B1.** Kalata B1 is expressed as a precursor protein (the example shown is Oak1) that, after folding to form the cystine knot, undergoes enzymatic processing to remove pro-sequences at the N-terminus (N-terminal repeat, NTR) and C-terminus (C-terminal repeat, CTR) prior to cyclization. First, cleavage at the N-terminal processing site is carried out by the papain-like cysteine protease, kalatase A, with the P2 Leu residue (within the NTR) shown to be important for efficient processing, whereas P1 Lys can be replaced by other amino acids. Second, cleavage at the C-terminal processing site is carried out by an asparaginyl endopeptidase (AEP, such as OaAEP1b), with the P1 (Asn or Asp) and P2′ (Leu or Ile) residues shown to be important. Head-to-tail cyclization is also AEP-mediated and is proposed to be coupled to CTR processing, with residues at the N- and C-terminus of the cyclotide domain found to influence the efficiency of converting the linear substrate to cyclic product. For simplicity, only the final four residues of the NTR are shown.

type plants expressing *TIPTOP2* correctly processed the precursor protein to generate the three encoded cyclotides MCoTI-I, MCoTI-II and MCoTI-IV, although the linear form of each peptide was also detected, as well as the C-terminal acyclic trypsin inhibitor MCoTI-V.[234] *TIPTOP2* was also expressed in mutant plants that lacked all four Arabadopsis AEPs. Seed extracts from these plants did not contain any of the cyclic or linear forms of the three MCoTI cyclotides, supporting the role of AEPs in NTR and CTR cleavage, whereas processing of MCoTI-V was unaffected as processing of this domain did not occur after an Asn or Asp residue and was expected to be AEP-independent.

Very recently, the elusive class of enzymes involved in Oak1 NTR processing was identified by activity-guided fractionation using plant extracts and a synthetic kalata B1 precursor.[434] Initial studies were done using an extract from *N. benthamiana* leaves because transgenic plants expressing *Oak1* had been shown to carry out NTR processing without requiring a co-expressed *O. affinis* enzyme. Incubating plant extracts with a synthetic kalata B1 precursor that contained a four-residue NTR (LQLK) confirmed that *N.*

benthamiana produces one or more endogenous enzymes that can liberate the NTR from LQLK-kalata B1. A candidate enzyme was subsequently isolated and identified as the papain-like cysteine protease NbCysP6. The NTR processing activity of this enzyme was verified by expressing recombinant NbCysP6 in *E. coli* and characterizing its ability to cleave LQLK-kalata B1. To identify homologous enzymes in the native kalata B1 producer *O. affinis*, a transcriptome was assembled from leaf and shoot tissue to search for endogenous papain-like cysteine proteases that were similar to NbCysP6. These analyses revealed three candidates, one of which (*OaRD21*) was expressed in *E. coli* and confirmed to cleave LQLK-kalata B1 at the NTR processing site.[434] Interestingly, the resulting acyclic intermediate was resistant to enzymatic degradation if the cystine knot was present, whereas the reduced acyclic peptide was rapidly digested. *In planta* mutagenesis experiments were subsequently performed in transgenic *N. benthamiana* plants that co-expressed OaAEP1b, which revealed that the hydrophobic residue often present at P2 at the NTR cleavage site is particularly important for correct processing (Figure 16). However, misprocessed peptides containing an N-terminal Ala residue were still cyclized by OaAEP1b and generated mutant cyclotides with two to four additional residues in loop 6.

In parallel to mutagenesis studies on cyclotide biosynthesis, additional work has focused on tracing the localization of the various precursors and auxiliary proteins *in planta*. In one study, transgenic *N. benthamiana* plants were used to track the processing of green fluorescent protein (GFP)-tagged cyclotide precursors.[189] The full length Oak1–GFP precursor was found to be targeted to the vacuole, suggesting that excision and cyclization of the cyclotide domain occurs at the location where cyclotides are subsequently stored. Additionally, the N-terminal flanking region was found to be sufficient to target GFP to the vacuole, but the C-terminal propeptide, which is involved in peptide cyclization, was not a targeting signal.[189]

4.3 Enzyme-guided studies to explore cyclization mechanisms

With the emergence of new findings on cyclotide precursors and their processing, the field is well-placed to further explore cyclization mechanisms and identify the individual enzymes involved. The first AEP ligase to be isolated from a cyclotide producing plant was purified from an extract of *C. ternatea* seed pods.[289] This enzyme was named butelase 1, with searches of an assembled *C. ternatea* transcriptome using

peptide sequences produced by trypsin digestion revealing that butelase 1 was a member of the legumain family of cysteine proteases. With sufficient quantities of purified enzyme in hand, it was possible to characterize the enzyme's activity *in vitro* and study the cyclization of synthetic precursors with various modifications. Butelase 1 was found to efficiently cyclize a synthetic kalata B1 precursor when the CTR was engineered to match the sequence of a Fabaceae cyclotide precursor (HVIA). Truncating the CTR to two residues (HV) led to improved cyclization efficiency, whereas further truncations or mutating the P1 Asn residue to Asp, Ala, Gln or Glu all led to a decrease in cyclization efficiency.[289]

The specificity of butelase 1 was further examined using an intermolecular ligation assay where the sequence of one peptide segment (containing the N↓HV motif) was fixed and the incoming segment (analogous to the cyclotide N-terminus) was varied.[289] In one series of incoming peptides, the P1′ position was varied and Ile was fixed at P2′, with subsequent ligation assays revealing that butelase 1 tolerated a broad range of amino acids at P1′ as only Pro, Asp and Glu were not favored. However, butelase 1 was more selective at P2′ as Ile, Leu and Val were clearly preferred when a second series of peptides was screened that contained diversity at P2′ and Leu was fixed at P1′. Assays were also performed using a kalata B1-HV precursor that had undergone reduction and *S*-alkylation, which revealed that folding was not a prerequisite for cyclization as the reduced precursor was cyclized with 50-fold higher catalytic efficiency than the cystine-knotted precursor.[289]

The identification of an AEP ligase in *O. affinis* marked the discovery of a second cyclizing enzyme from a cyclotide-producing plant. OaAEP1b was identified from analyses of an *O. affinis* cDNA library and genomic DNA, and was subsequently produced by recombinant expression in *E. coli* as a ubiquitin fusion protein that contained a His6 tag.[304] Activation of the OaAEP1b zymogen was achieved by incubation at pH 4.5, which promoted cleavage of the N-terminal propeptide and a 123-amino acid domain at the C-terminus. The cleavage specificity of OaAEP1b was examined using internally quenched fluorescent peptide substrates based on the kalata B1 C-terminal processing site (Abz[STRN↓GLPS]3-NO_2-Tyr). These assays revealed that replacing the P2 Arg residue with Lys or the P1′ Gly residue with Ala or Ser had minimal effects on substrate cleavage. By contrast, OaAEP1b displayed a strong preference for hydrophobic residues at P2′, as observed for butelase 1, as a modified substrate where Leu was replaced by Ala was cleaved at a considerably lower rate that was below the limit of detection.[304]

These findings are consistent with cyclization assays performed using a synthetic kalata B1 precursor, where the P2′ Leu to Ala mutation markedly decreased the rate of CTR cleavage. Cyclization assays were also carried out using precursors that were modified at the N-terminus, including an N-acetylated precursor and a precursor containing a tetrapeptide NTR sequence.[304] Neither of these peptides were correctly processed to generate cyclic kalata B1, indicating that efficient cyclization requires a native N-terminus and is subject to specificity requirements for the incoming N-terminal segment. With respect to the latter, it is interesting to note that, in Oak1, the P1′–P3′ segment in the CTR (GLP) is an exact match for the first three residues of kalata B1. The mechanism for cyclization was also examined by performing assays in the presence of ^{18}O-labelled water to detect whether hydrolysis of the acyl-enzyme complex occurred following CTR cleavage. Whereas an isotopic shift was observed for a modified kalata B1 precursor that was cleaved but did not undergo cyclization, a similar shift was not seen for a separate precursor that was converted to cyclic kalata B1.[304] These findings support a model for AEP-mediated cyclization where cleavage of the CTR proceeds to ligation without an intermediate hydrolysis step. In a subsequent study, the crystal structure of a zymogen form of OaAEP1b was reported, which identified several residues that appeared to be important for function.[394] One of the residues targeted for mutagenesis, Cys247, was shown to influence the efficiency of OaAEP1b-mediated cyclization of a synthetic model peptide, and replacing this residue with Ala generated a mutant ligase that displayed more than two-orders of magnitude improvement in catalytic efficiency.

In recent work, ligase-type AEPs from *Petunia x hybrida* were discovered using an *in planta* cyclization assay to evaluate candidate enzymes identified from RNA-seq data.[397] Four candidate AEPs were tested in transgenic *N. benthamiana* plants by co-expressing *Oak1* with each petunia enzyme and comparing the ratio of cyclic to acyclic kalata B1 in leaf extracts. Remarkably, the most efficient ligase identified in this screen (PxAEP3b) was identical at 275 out of 304 residues to another isoform (PxAEP3a) that showed much weaker ligase activity. These two AEPs offered a unique model system to identify structural features that distinguish a ligase-type AEP from a typical hydrolase, which were investigated by examining the requirements for converting PxAEP3a into an improved ligase with equivalent activity to PxAEP3b.[397] A key difference between the two enzymes was located at residues 294–301 in the protease domain, which included a six-residue deletion in the ligase PxAEP3b. Replacing the 294–301 segment in

PxAEP3a with the corresponding sequence from PxAEP3b was found to improve its ability to cyclize kalata B1 and, thus, the 294–301 segment was named the marker of ligase activity (MLA).[397] Two additional replacements in the substrate pocket produced a chimeric PxAEP3a enzyme that fully acquired the ligase-type activity of PxAEP3b. The importance of these two segments was further demonstrated in studies with OaAEP1b (ligase-type) and OaAEP2 (hydrolase-type), where modifications in either the MLA or substrate pocket improved the ligase-type activity of OaAEP2 and a synergistic effect was identified when both regions were engineered.[397]

Studies on ligase-type AEPs have provided new insights into cyclotide processing that will assist with improving production in plants. Already, this area of the field is beginning to grow and, as mentioned above, recent work has focused on equipping plants that do not normally produce cyclotides with ligase-type AEPs to improve the yield of cyclic peptides.[399] In transgenic *N. benthamiana* plants, co-expressing the *Oak1* precursor with a ligase-type AEP was found to dramatically improve the production of cyclic kalata B1. Similarly, a multi-domain precursor was efficiency processed in the presence of a ligase-type AEP to produce cyclic kalata B2 and cyclic kalata B3, whereas the desired products were almost undetectable in the absence of a dedicated ligase. Additional co-expression experiments revealed that butelase 1 was able to process a cyclotide-encoding albumin-1 precursor that carried the sequence of Cter M or kalata B1.[399] OaAEP1b was also able to cyclize engineered kalata B1 variants encoded by a modified *Oak1* precursor, further expanding the scope of the cyclotide production *in planta*.

5. SYNTHESIS

5.1 Peptide α-thioesters produced via Boc chemistry

In the late 1990s, several groups reported the chemical synthesis of individual cyclotides from the bracelet or Möbius sub-groups.[11,12,16,18] This achievement was the culmination of key advances in synthetic methodology, together with the discovery of native chemical ligation (NCL)[442] and the application of intramolecular NCL for head-to-tail peptide cyclization.[443] These developments made it possible to assemble cyclotides as linear peptide precursors using solid phase synthesis, then carry out backbone cyclization via a chemoselective reaction in solution. The predominant synthesis strategy for the first cyclotides employed *t*-butyloxycarbonyl (Boc) chemistry and resin functionalized with a linker that

generated a peptide α-thioester upon cleavage. One approach for generating the required linker involved converting Boc-Gly-OH to its corresponding 3-thiopropionic acid ester and coupling this moiety to *p*-methylbenzhydrylamine (MBHA) resin, as shown in Figure 17.[444] This method was used in the initial syntheses of three bracelet cyclotides, cyclopsychotride A, circulin A and circulin B, with the linear chain designed to position Cys^{IV} at the N-terminus and a Gly residue at the C-terminus.[11,12,17,18] In reports of these syntheses, some losses in yield were noted due to premature cleavage of the thiol alkyl linker during synthesis, which amounted to approximately 20% in the synthesis of circulin B.[12]

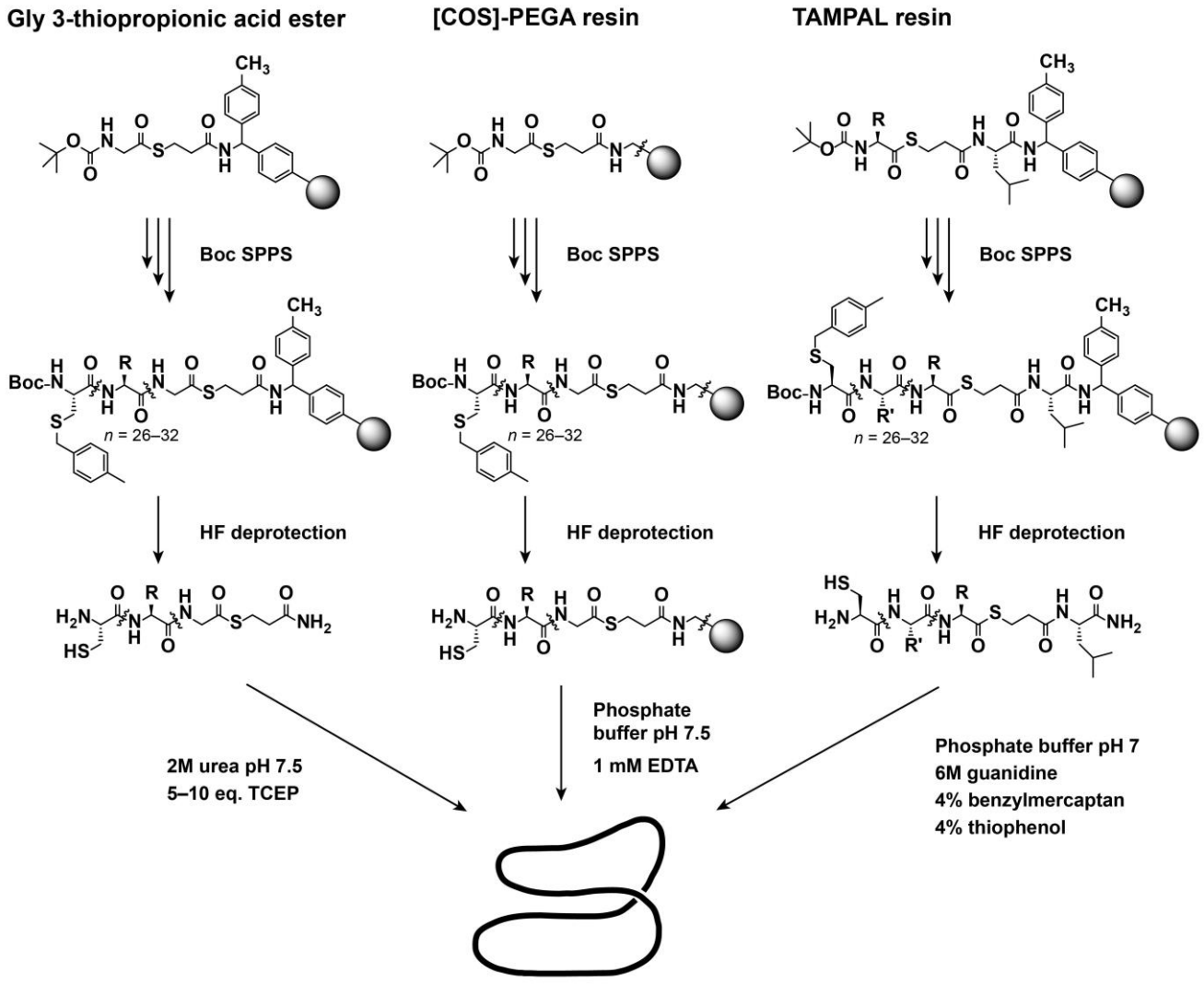

Figure 17. **Synthetic methods for producing cyclotides via Boc chemistry.** Three approaches are illustrated that use different linker chemistries to generate the desired peptide α-thioester. A Boc-Gly 3-thiopropionic acid ester linker can be attached to MBHA resin or PEGA resin to enable the production of peptide α-thioesters that can be cyclized in solution or on resin, respectively. Trityl-associated mercaptopropionic acid–leucine (TAMPAL) resin has also been developed to expand the range of amino acids that can be incorporated as the C-terminal thioester residue. In each approach, synthesis via Boc SPPS yields the resin-bound protected peptide α-thioester that contains an N-terminal Cys residue (shown with a *S*-methylbenzyl protecting group). After HF treatment, the deprotected peptide α-thioester can be cyclized by intramolecular native chemical ligation in solution, on resin, or after *in situ* thioester exchange in the presence of thioaryls, such as benzylmercaptan and thiophenol.

Another synthetic consideration that is especially relevant to cyclotides is correct disulfide pairing as oxidative folding of a peptide that contains six Cys residues can produce 15 potential isomers. By contrast, a peptide containing four Cys residues produces only three isomers. This feature was exploited in early syntheses of cyclopsychotride A, circulin A and circulin B through the use of orthogonal protecting groups for certain Cys residues to enable regioselective disulfide formation. Here, four Cys residues were *S*-methylbenzyl protected and the remaining two Cys residues were *S*-acetamidomethyl protected to separate the folding process into two steps.[11,12,17,18] Once the linear peptide chain had been assembled, the peptide α-thioester was deprotected and cleaved from the resin using HF and extracted in 8 M urea (pH 7.5) containing tris(2-carboxyethyl)phosphine (TCEP) to suppress the formation of intermolecular disulfide bonds. After dialysis against 2 M urea, cyclization via intramolecular NCL was carried out and the first two disulfide bonds were subsequently formed after diluting with H_2O to lower the concentration of urea to 1 M and adding 15% DMSO. The correct isomer was isolated by HPLC (~ 30% yield) and the final disulfide bond was formed by iodine oxidation at pH 4.

Another strategy for producing the resin-bound thioester linker was applied in the chemical synthesis of the Möbius cyclotide kalata B1.[16] This method involved coupling 3-bromopropanoic acid onto Gly-4-(oxymethyl)phenylacetamidomethyl (Gly-PAM) resin, which was then treated with thioactetic acid to install the desired thio-functionality. This moiety subsequently undergoes thiolysis by treatment with 2-mercaptoethanol to generate an exposed sulfhydryl that is accessible for coupling the first amino acid. In Figure 17, this synthesis protocol is shown using PEGA resin, which enables on-resin NCL reactions[445] as the resin has favorable swelling properties in aqueous and organic solvents, and is stable to HF treatment. Returning to the synthesis of kalata B1, the linear peptide chain was arranged to use the same ligation site as bracelet cyclotides (Cys^{IV} as the N-terminal residue) and assembled using Boc chemistry via the *in situ* neutralization protocol, with the completed peptide α-thioester liberated from the resin by HF cleavage. Cyclization via intramolecular NCL proceeded in aqueous buffer (pH 7.4) containing TCEP and oxidative folding was carried out in one step by dissolving the reduced, cyclic peptide in 0.1 M ammonium bicarbonate (pH 8.5) containing 1 mM GSH. Interestingly, including up to 50% (v/v) 2-propanol in the reaction buffer was found to improve the yield of correctly folded kalata B1. The addition of a co-solvent

was hypothesized to stabilize a local hydrophobic surface that forms during the folding process and is evident in the 3D structure of kalata B1 (Figure 11).

An alternative approach was also tested for the synthesis of kalata B1 that involved oxidative folding of the linear peptide followed by ligation of the free N- and C-termini using conventional coupling reagents.[16] This strategy parallels the biosynthetic pathway for cyclotides *in planta*, where oxidative folding occurs prior to cyclization. The rationale for applying this method to chemical synthesis was that formation of the cystine knot would bring the peptide's termini into proximity in order to promote cyclization. A different ligation site (Gly11–Gly12 in loop 2, Figure 1) was selected for this strategy as it would eliminate potential racemization and these residues form a β-turn in cyclic kalata B1 that is surface exposed. The corresponding linear peptide was produced via Boc chemistry and folded in ammonium bicarbonate buffer (pH 8.5) containing 50% 2-propanol and 1 mM GSH. However, the folding yield for linear kalata B1 was lower compared to the head-to-tail cyclized peptide, suggesting that cyclization imparts a degree of order that pre-organizes the Cys residues to achieve the correct connectivity.[16] Additionally, the optimal conditions for cyclization involved a rapid reaction (30 s) that was unable to reach completion as losses due to side reactions were observed in longer reactions since the peptide's sidechain protecting groups had been removed prior to folding.

On comparison, the synthesis schemes based on cyclization via intramolecular NCL followed by oxidative folding were higher yielding. Indeed, with subsequent advances in linker chemistry, such as the development of trityl-associated mercaptopropionic acid leucine (TAMPL) resin (Figure 17),[446] the synthesis of peptide α-thioesters via Boc chemistry was the primary route for chemical synthesis of cyclotides. In following studies, Boc chemistry was successfully used to synthesize a range of non-native cyclotides, including cyclotides with chimeric sequences[85] and libraries carrying point-mutations at each non-Cys residue,[125,170] and it continues to be used today, particularly for sequences that are challenging to assemble. Another approach for improving synthesis yields has been to use microwave-assisted methods, as has been applied for kalata B1.[107] However, with 9-fluorenylmethyloxycarbonyl (Fmoc) chemistry emerging as the preferred method for synthesis due to its use of less hazardous reagents, there has been broad interest in developing Fmoc-compatible methods for cyclotide synthesis.

5.2 Adapting cyclotide synthesis to Fmoc chemistry

Innovations enabling the synthesis of peptide α-thioesters using Fmoc chemistry were driven by its suitability for several new applications, including phosphopeptides and glycopeptides, that had proven challenging due to the harsh conditions encountered in Boc synthesis. However, the existing linkers used to synthesize peptide α-thioesters via Boc chemistry were sensitive to basic conditions, such as those used for Fmoc deprotection after each coupling reaction. Accordingly, there was a need to develop new linker chemistries and synthetic methodologies, several of which have been applied to synthesize cyclotides using Fmoc chemistry. One of the initial strategies was based on adapting the sulfonamide 'safety catch' linker, which is stable under acidic and basic conditions, to solid-phase peptide synthesis by generating an alkanesulfonamide linker.[447,448] Using this approach, the first amino acid to be loaded is coupled to the resin via an *N*-acyl sulfonamide link and peptide synthesis proceeds under standard conditions (Figure 18). Once the linear chain has been assembled, the resin is activated with iodoacetonitrile to generate an *N*-cyanomethyl derivative that can be cleaved using a thiol nucleophile to liberate the protected, linear peptide α-thioester. This method was used to synthesize the trypsin inhibitor cyclotide MCoTI-II, with linear peptide assembly employing an Asp–Gly dipeptide building block with *N*-2-hydroxy-4-methoxybenzyl protection of the amide bond to suppress aspartimide formation.[71] The resulting peptide α-thioester was cyclized by intramolecular NCL in 0.1 M phosphate buffer (pH 7.4) containing TCEP, with folding by air oxidation leading to efficient formation of the cystine knot. Following studies have also used this approach, or variations thereof, to synthesize MCoTI-II, engineered MCoTI-based cyclotides and cyclotide libraries via parallel synthesis.[108,217,261,300]

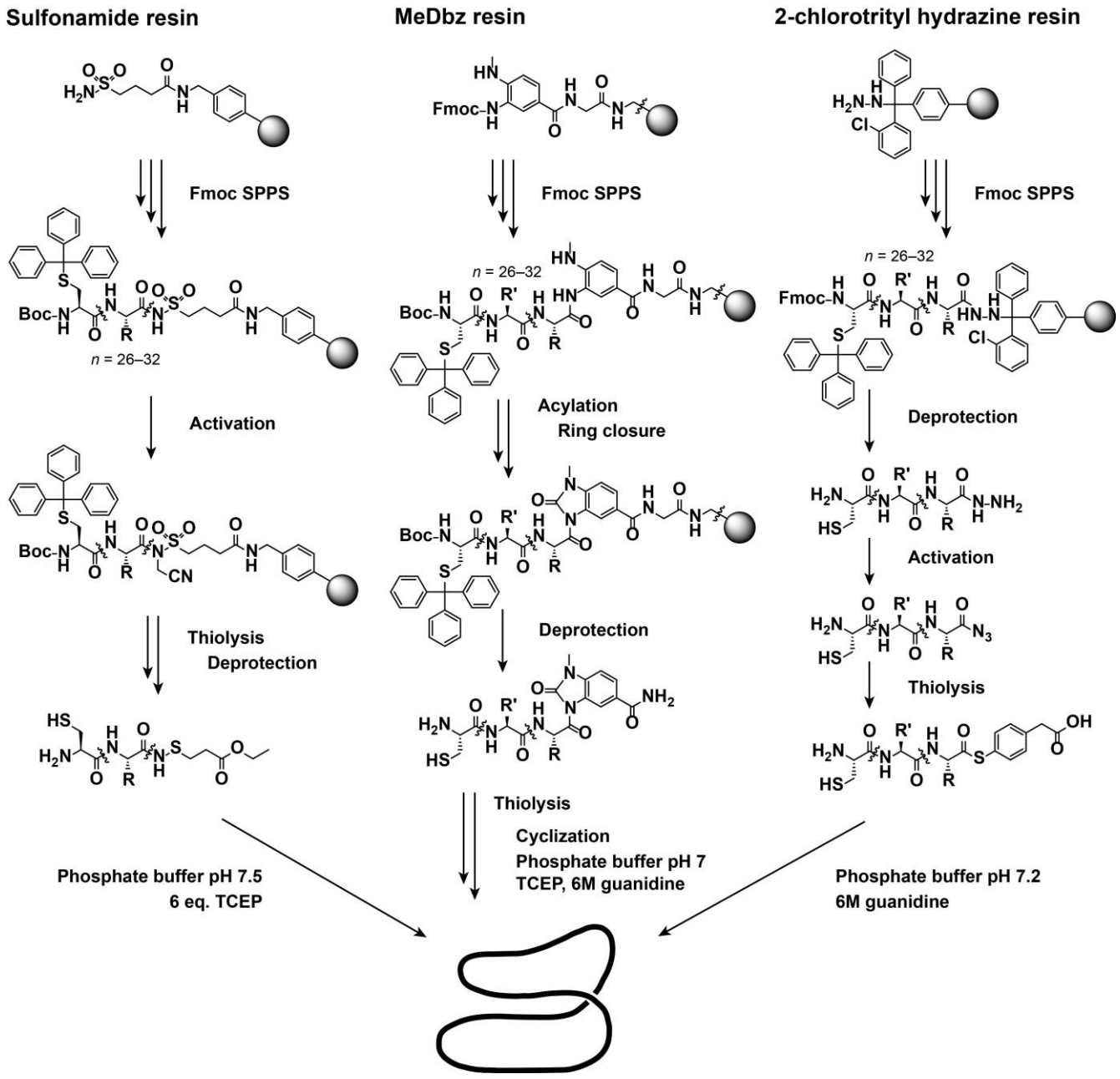

Figure 18. **Synthetic approaches for producing cyclotides via Fmoc chemistry.** Three methodologies are illustrated that use different linker chemistries to produce peptide thioesters or thioester precursors. For sulfonamide resin, the linear peptide chain is assembled using Fmoc SPPS with Boc N-protected Cys as the N-terminal residue. The sulfonamide linker is then activated using iodoacetonitrile, which enables cleavage (thiolysis) with ethyl 3-mercaptopropionate to generate a protected peptide thioester. Cleavage with TFA yields the deprotected peptide thioester that can be cyclized via intramolecular native chemical ligation. Peptide thioester precursors can be produced by a variety of methods, including 3-amino-4-(methylamino)benzoic acid (MeDbz) resin or 2-chlorotrityl hydrazine resin. For MeDbz resin, the attached peptide-MeDbz is treated with *p*-nitrophenyl chloroformate (acylation) followed by DIPEA (ring closure) to generate a peptide-MeNbz. After deprotection with TFA, the liberated peptide-MeNbz is converted to a thioester by treatment with (4-hydroxy)-thiophenol (thiolysis) and can undergo intramolecular native chemical ligation. For 2-chlorotrityl hydrazine resin, the assembled peptide hydrazide is deprotected prior to conversion to a peptide thioester. Treatment with sodium nitrite yields a peptide azide (activation), that can be converted to a peptide thioester by treatment with 4-mercaptophenylacetic acid (thiolysis) and cyclized by intramolecular native chemical ligation.

Another route for preparing cyclic peptides via Fmoc chemistry involves the synthesis of peptide–*N*-acylurea precursors that can be converted to the corresponding peptide α-thioester to allow intramolecular NCL.[449] In this approach, peptides are assembled onto resin bearing an *o*-aminoanilide linker that is introduced by coupling 3-Fmoc-4-diaminobenzoic acid (Fmoc-Dbz). Prior to cleavage and sidechain deprotection, the *o*-aminoanilide moiety is converted to *N*-acyl-benzimidazolinone (Nbz) by treatment with *p*-nitrophenyl chloroformate followed by *N*,*N*-diisopropylethylamine. The resulting peptide-Nbz is liberated from the resin by cleavage with trifluoroacetic acid and serves as a precursor for generating the desired peptide α-thioester via thiolysis, typically by treatment with 4-mercaptophenylacetic acid. Several cyclotides, including kalata B1, kalata B7 and MCoTI-II, have been successfully produced using this method,[243,346] including using microwave-based methods.[258] Recently, a second generation linker was developed to suppress unwanted branching due to acylation of the second amine on the Dbz moiety, which has been observed under certain conditions.[450] For the new linker, the *p*-amino group on Dbz was replaced by a less reactive methylamino group to generate Fmoc-3-amino-4-(methylamino)benzoic acid (Fmoc-MeDbz), as shown in Figure 18. Critically, the methylamino group is still amenable to acylation with *p*-nitrophenyl chloroformate and, thus, peptide-MeDbz precursors can be converted to the corresponding peptide-MeNbz using similar conditions to peptide-Dbz precursors. Subsequent thiolysis by treatment with (4-hydroxy)-thiophenol yields the desired peptide α-thioester. This method has been applied to synthesize kalata B1 and MCoTI-II as peptide-MeDbz precursors that were designed for cyclization between Cys and a β-branched residue (Cys3–Val4, kalata B1) or Cys and an aromatic residue (Cys27–Tyr28, MCoTI-II).[450]

Peptide hydrazides can also serve as precursors that undergo activation and thiolysis to generate peptide α-thioesters for intramolecular NCL.[451] This strategy involves Fmoc synthesis on a 2-Cl-(Trt)-$NHNH_2$ solid support that is prepared in one-step by treating 2-Cl-(Trt)-Cl resin with 5% hydrazine (Figure 18).[241] After assembly of the linear peptide chain, the desired peptide hydrazide is cleaved from the resin and sidechains are deprotected using trifluoroacetic acid. The C-terminal hydrazide is subsequently converted to an azide by treatment with $NaNO_2$ in phosphate buffer (pH 3, –10°C) and, after adjusting the pH to 7.0, the peptide α-thioester is produced by treatment with 4-mercaptophenylacetic acid. Prototypic cyclotides from each sub-group, namely kalata B1 (Möbius), cycloviolacin O2 (bracelet) and MCoTI-II (trypsin inhibitor), were synthesized using the peptide hydrazide approach, with cyclization of the

subsequent peptide α-thioester reaching completion within two hours.[241] Another type of thioester surrogate can be produced by Fmoc synthesis on 2-Cl-(Trt)-Cl resin that has been treated with 2-(butylamino)ethanethiol.[452] Here, cleavage of an assembled peptide from the resin yields a thioethylbutylamido (TEBA) peptide that can undergo a tandem N–S acyl shift and thiol–thioester exchange by treatment with sodium 2-mercaptoethane sulfonate in acidic conditions (pH 3, 40°C) to generate a MES-thioester. A kalata B1-TEBA precursor synthesized via this method was shown to undergo cyclization via intramolecular NCL at pH 7.[452] Recently, a method for Fmoc synthesis of peptide cryptothioesters was developed based on a *N*-(2-hydroxy-5-nitrobenzyl)cysteine (*N*-Hnb-Cys) moiety that undergoes an N–S acyl shift at near-neutral pH.[393] The *N*-Hnb-Cys group carries an S–StBu protecting group to provide temporal control over thioesterification and this approach has been used to synthesize several cyclotides, namely kalata B1, cycloviolacin O2 and Cter M.[393]

A final strategy that has been applied for Fmoc synthesis of cyclotides is based on activation of the C-terminal carboxyl group in an assembled linear peptide. In one approach, the activated carboxyl moiety is used to generate a thioester by treatment with *p*-acetamidothiophenol.[104] This method was used to synthesize cycloviolacin O2, whereby the linear peptide chain was assembled on NovaSyn TGT resin and the protected peptide was subsequently cleaved from the resin under mild conditions. The C-terminal carboxylate was activated using benzotriazol-1-yloxy tripyrrolidinophosphonium hexafluorophosphate (PyBOP) in the presence of DIEA, followed by addition of *p*-acetamidothiophenol to form the desired thioester. After sidechain deprotection, the resulting peptide α-thioester was cyclized via intramolecular NCL, followed by oxidative folding using an optimized buffer (pH 8.5) that contained 1 mM EDTA, 35% DMSO, GSH/cystamine and 6% Brij 35.[104] In a later study, the efficiency of linear peptide assembly and thioester synthesis were improved by using microwave-assisted methods, with the new method successfully used to synthesize kalata B1, MCoTI-II and cycloviolacin O2.[174] Another approach that utilizes activation of the C-terminal carboxyl group involves treating a protected peptide with HATU in the presence of DIPEA to generate a 1-oxy-7-azabenzotriazolate active ester.[278] This reaction is carried out using a relatively dilute concentration of peptide, such that an intramolecular reaction involving the peptide's N-terminal amino group (cyclization) is favored over an intermolecular reaction that would generate peptide dimers. Although the product yields from this approach are slightly lower than Boc synthesis followed by

intramolecular NCL, HATU-mediated C-terminal activation has been successfully applied to cyclize a range of naturally occurring and engineered cyclotides. However, as HATU is a guanidinium (or uronium) salt, potential side products can occur via reaction with the N-terminal amino group. If this side-reaction proves to be problematic for a given sequence, cyclization using alternative coupling reagents, such as phosphonium salts, should be explored.

5.3 Recombinant expression

As well as being producible by chemical synthesis, cyclotides are amenable to exogenous production via recombinant expression. It is possible to not only express cyclotide precursors in bacteria or yeast, but post-translational processing and cyclization can also be carried out *in vivo* using protein splicing. This technique derives from a self-catalyzed mechanism discovered in yeast, where certain proteins were observed to undergo spontaneous post-translational processing that resulted in excision of an internal peptide segment (intein) followed by ligation of the two remaining segments (exteins). This process can be adapted for head-to-tail cyclization by expressing the target sequence as a fusion protein that contains a C-terminal intein domain, as demonstrated for the expression of kalata B1 in *E. coli*.[70] Here, the fusion protein was arranged to have a single Met residue at the N-terminus (required to initiate translation), followed by the kalata B1 sequence and an engineered intein domain based on the *Saccharomyces cerevisiae* vacuolar membrane ATPase intein. The intein domain contains Cys as the first residue and, as with intramolecular NCL, the kalata B1 sequence is arranged to position Cys as the first residue.

Conversion of the kalata B1–intein fusion protein to cyclic kalata B1 commences with cleavage of the N-terminal Met by an endogenous enzyme, methionine aminopeptidase. This event unmasks an N-terminal Cys residue to allow intramolecular NCL. Next, a reversible N–S acyl shift occurs to generate a thioester linkage between the cyclotide domain and the intein. This rearrangement enables cleavage of the intein segment via nucleophilic attack that, when mediated by the N-terminal Cys residue, facilitates cyclization via intramolecular NCL. Initial experiments with several kalata B1 constructs indicated that *in vivo* intein cleavage was not accompanied by efficient cyclization.[70] However, the kalata B1–intein fusion protein could be purified and thioester cleavage carried out *in vitro* using ethyl mercaptan to successfully

generate cyclic kalata B1. This procedure was also used to express a range of kalata B1 mutants with point mutations in various loops and, in each case, a one-pot cyclization and folding reaction using the purified cyclotide–intein fusion generated the desired product, with conversion yields ranging from 10–60%.[70]

A similar approach was used to express MCoTI-II in *E. coli* using an engineered intein derived from *Mycobacterium xenopi* gyrase A.[92] Several cyclotide–intein fusion proteins were expressed in *E. coli* BL21 (DE3) cells and the desired products were isolated from cell lysates using either an intein pulldown or by affinity chromatography with immobilized trypsin. Interestingly, the major product from trypsin affinity purification was cyclic, oxidized MCoTI-II. Further experiments were subsequently performed to establish whether cyclization and folding had occurred inside the cell (or post-lysis) by including iodoacetamide in the lysis buffer to alkylate free thiols. This event would suppress cyclization and disulfide formation once cell lysis commenced. However, the presence of iodoacetamide did not impact on the production of cyclic, oxidized MCoTI-II, indicating that processing had occurred *in vivo*.[92] MCoTI-II was also expressed in an engineered *E. coli* strain (Origami 2) that is compatible with disulfide bond formation, which was reported to yield higher levels of cyclic, oxidized MCoTI-II.[92] In a following study, a library of MCoTI-I variants was expressed in *E. coli* Origami 2 cells, with control of intein cleavage and *in vivo* cyclization achieved by varying the culture temperature.[137] The MCoTI-I library was subsequently used to perform competitive binding assays with sepharose-bound trypsin and select variants that retained high affinity for the protease.

Another method that harnesses intein technology is protein trans-splicing. This mechanism was discovered following the identification of a split intein that was partitioned in two separate proteins and underwent self-catalyzed ligation to produce the *Synechocystis sp.* PCC6803 DnaE protein. Processing occurs when the two intein fragments self-associate to form an active intein domain, which catalyzes excision of the entire intein and ligation of the two DnaE extein segments. Protein trans-splicing has been adapted for expressing cyclic peptides, including MCoTI-I, which was expressed in *E. coli* Origami 2 cells using the *Nostoc puntiforme* PCC73102 DnaE split intein.[260] Here, the expression construct contained the MCoTI-I sequence placed between the two intein fragments that were arranged in reverse order (C-terminal intein fragment upstream of the MCoTI-I domain) to enable correct self-association. This precursor protein was processed *in vivo*, with the authors noting that protein trans-splicing yielded higher levels of recombinant MCoTI-I than expressed protein ligation using a single, intact intein.[260]

Subsequent studies have demonstrated some of the applications that are accessible with recombinant expression and protein trans-splicing. First, a nonproteinogenic amino acid, *p*-azidophenylalanine, was incorporated into a MCoTI-I variant to enable labelling of an expressed cyclotide using click chemistry.[260] Second, the potential of using expressed MCoTI-I variants to perform phenotypic screening was tested in a *Saccharomyces cerevisiae* model of α-synuclein-induced cytotoxicity.[312] Cells were transformed with a mixture of plasmids that encoded either MCoTI-I or an engineered cyclotide that contained a protective sequence against cytotoxicity (50,000-fold excess of the MCoTI-I plasmid). After inducing α-synuclein over-expression, surviving colonies were sequenced and 90% were found to encode the engineered cyclotide.[312] This finding demonstrates the considerable potential of protein trans-splicing to produce genetically encoded cyclotide libraries that can be used in functional screens.

5.4 Chemoenzymatic synthesis

The identification of several ligase-type enzymes has made it possible to extend biocatalytic cyclization to synthetic precursors that do not carry special modifications, chemical groups or domains. This approach is well-suited to the cyclization of precursors produced by routine solid-phase methods as the substrates of ligase-type enzymes are ordinary peptides that require as few as two additional amino acids at the C-terminus to install the relevant processing site. Accordingly, chemoenzymatic synthesis can be applied to a wide range of cyclotide precursors that have diverse sequences and chemical modifications, irrespective of whether they are folded or not. Additionally, the cyclization reaction retains exquisite site selectivity as the recognition sequences for ligase-type enzymes are often very specific. One class of enzymes that has been successfully used to cyclize synthetic precursors are ligase-type AEPs from cyclotide-producing plants.[289,304,397] In these studies, chemically synthesized peptides were used as model substrates to confirm the purified enzyme's ligase activity and characterize its specificity. In agreement with earlier *in planta* experiments, the findings from these assays confirmed the importance of the precursor's C-terminal P1↓P1′-P2′ motif as the minimal recognition sequence for correct processing. Additionally, AEPs have been shown to cyclize synthetic precursors that contain cyclotide sequences from separate plant families, provided that the precursor's processing site was modified to match the enzyme's

specificity.[289,304] With the recent characterization of an endogenous N-terminal processing enzyme, kalatase A (OaRD21A), it is now possible to reconstruct the processing of a synthetic kalata B1 precursor (LQLK-kalata B1-GI) using purified enzymes, where kalatase A first liberates the N-terminal LQLK propeptide and OaAEP1b subsequently cyclizes the newly generated kalata B1-GI intermediate.[434]

As outlined earlier, the identification of cyclotide processing enzymes from plants is a relatively recent event, and earlier studies relied on different enzymes to produce cyclotides via chemoenzymatic synthesis. One approach that is unique to members of the trypsin inhibitor sub-group involves cyclization at the scissile bond (PK↓IL, loop 1) using a protease that conventionally acts as a hydrolase, such as trypsin.[102,108] This unusual reaction is possible as trypsin inhibitor cyclotides are Laskowski (or standard mechanism) inhibitors and their mode of action involves cleavage and religation of the scissile bond. Accordingly, an enzyme that typically functions as a hydrolase, such as trypsin, can synthesize a peptide bond under very specific conditions, such as when tight binding of the cleaved N-terminus near the enzyme's catalytic machinery promotes re-synthesis of the scissile bond, as is the case for Laskowski inhibitors. This mechanism has been harnessed for cyclization of MCoTI-I and MCoTI-II, where a linear precursor containing Ile7 at the N-terminus (Lys6 at the C-terminus) was first folded to prevent proteolytic cleavage at an internal Lys or Arg residue, then successfully cyclized using sepharose-bound trypsin.[102,108] Further assays demonstrated that the cyclizing enzyme could be changed to chymotrypsin by substituting Lys6 with Phe to match the enzyme's specificity. However, one limitation of this approach is that the product of the reaction is a high affinity inhibitor of the cyclizing enzyme and, thus, the reaction typically requires near-equimolar concentrations of enzyme and substrate.

Another enzyme that has been utilized to cyclize synthetic precursors is the bacterial transpeptidase, sortase A. The natural function of sortase A is to attach various cell-surface proteins to the bacterial cell wall via a mechanism that commences with cleavage of the target protein at the recognition sequence LPXT↓G. This cleavage event generates an acyl-enzyme complex that subsequently undergoes nucleophilic attack by an incoming peptide segment that contains a poly-Gly motif at the N-terminus, leading to ligation of the two proteins and release of the enzyme. Placing the N-terminal poly-Gly motif and C-terminal LPXT↓G sequence in the same precursor enables an intramolecular reaction that leads to cyclization of synthetic peptides. Interestingly, native kalata B1 already contains a partial sortase A recognition sequence

in loop 6 (TRNGLPV). A substrate for sortase A-mediated cyclization was subsequently produced by adding three amino acids at both the N-terminus (GGG) and C-terminus (TGG).[287] This precursor was successfully cyclized by sortase A,[287] as was a recombinantly expressed MCoTI-II precursor.[288] A drawback of this approach is that the cyclization reaction is not traceless and the cyclic product retains part of the sortase A recognition sequence. However, this limitation is less significant for certain applications that involve sortase A, such as the production of chimeric molecules. For example, a recent study used sortase A to conjugate MCoTI-I to an alpaca-derived nanobody (VHH7) to promote targeted delivery of the cyclotide to antigen-presenting cells.[407] The VHH7 nanobody was recombinantly expressed with a C-terminal LPETGG-His_6 tag to install a sortase A recognition sequence. The purified protein was initially functionalized by coupling a GGGC-dibenzylcyclooctyne moiety via a conventional sortase A ligation reaction. The VHH7-GGGC-dibenzylcyclooctyne product was then conjugated to an azido-Lys bearing MCoTI-variant via a strain-promoted, copper-free click reaction.[407]

Specialized enzymes have also been engineered for chemoenzymatic synthesis, including several peptiligases that were produced by modifying the bacterial serine protease, subtilisin BPN′. The first-generation peptiligase was optimized by site-directed mutagensis to expand its specificity at the critical S1′ subsite. This process yielded several variants that accepted a broad range of chemically diverse P1′ residues, as well as other enzymes that tolerated specific residues that were less favored by the broader specificity ligases. The absence of strict sequence requirements means that peptiligases are capable of traceless ligation (or cyclization), with their major requirement being a C-terminal ester that can be installed during precursor synthesis. Using this approach, the peptiligase variant omniligase-1 was used to cyclize a chemically synthesized MCoTI-II precursor that contained a carboxamidomethyl ester at the C-terminus.[395] The reaction was also successful when performed on the crude precursor, and a one-pot system for cyclization and folding was used to produce MCoTI-II at a 1 gram scale. Here, the cyclization site was PK↓IL in loop 1, and a recent study demonstrated that MCoTI-II could also be cyclized by omniligase-1 at a site in loop 5 (GN↓GY) using a precursor equipped with a C-terminal hydroxymethylbenzoic acid ester.[433] The latter study also used omniligase-1 to cyclize kalata B1 at sites in loop 2 (GT↓CN) and loop 6 (RN↓GL), although the P2′ Asn residue in the first precursor was found to lower the yield of cyclic product by promoting hydrolysis (40% of initial substrate) rather than cyclization. At present, the chemoenzymatic synthesis and

conjugation of cyclotides is an area of significant interest, and it has exciting potential for supporting the production of designer cyclotides with enhanced or novel functions.

6. FUNCTION

6.1 Functions of native cyclotides

Biological function has been a common theme that has motivated the discovery of cyclotides, underpinned their well-defined structures, and provided the foundation for their applications in agriculture and medicine. Collectively, cyclotides have a very diverse range of functions, with many of the first cyclotides discovered during the rise of the 'natural products era' through their identification as active compounds in studies that screened plant extracts for medicinal properties. Kalata B1 is well-known for its discovery as an active molecule from an *O. affinis* extract that was used in African traditional medicine as a utertonic tea to accelerate childbirth.[1-4] A hemolytic peptide, identified as violapeptide I, was discovered by analyzing an extract prepared from *Viola arvensis*.[6] Circulin A and circulin B were isolated from an extract of the tropical plant *Chassalia parvifolia* based on their activity in anti-HIV assays.[7] Additional cyclotides with anti-HIV activity were identified in subsequent studies, including further cyclotides isolated from *C. parvifolia* (circulins C–F)[22] as well as new cyclotides isolated from *Leonia cymosa* (cycloviolins A–D)[23] and *Palicourea condensate* (palicourein).[25] Screening plant extracts for neurotensin antagonists led to the discovery of cyclopsychotride A in an extract of *Psychotria longipes*.[8] Synthetic cyclotides, particularly circulin B and cyclopsychotride A, were also found to have antimicrobial activity against several bacterial strains.[17] Finally, characterizing the repertoire of trypsin inhibitors in the seeds of *Momordica* plants identified two cyclotides, MCoTI-I and MCoTI-II, produced by *M. cochinchinensis*.[24]

As the number of known cyclotides continued to grow, reports of their insecticidal and environmental activities began to emerge. Kalata B1 was the first cyclotide identified to have insecticidal activity after observations that Australian bollworm, *Helicoverpa punctigera* larvae (as shown in Figure 2) failed to grow when they were fed an artificial diet containing purified kalata B1 (0.8 μmol per gram of feed).[29] Initial experiments exploring the mode of action for kalata B1 revealed that its insecticidal activity was not related to inhibition of digestive enzymes, including trypsin, chymotrypsin or α-amylase.

Subsequent studies identified that several cyclotides, including kalata B1, kalata B2, Cter M and psyleio A, also have activity against cotton bollworm (*Helicoverpa armigera*) larvae,[65,205,338] suggesting that insecticidal activity was common to a range of cyclotides from different plants. Using this assay as a model system, kalata B1 was shown to target epithelial cells in the larval midgut, causing substantial changes in gut morphology due to cell swelling, blebbing and lysis.[111] Insecticidal activity has also been described for parigidin-br1 against sugarcane borer (*Diatraea saccharalis*) larvae and cultured *Spodoptera frugiperda* (Sf9) cells, where mode of action studies also revealed disruption of the plasma membrane, cell swelling and lysis.[236]

Various cyclotides from Rubiaceae and Violaceae plants have also been shown to possess anthelmintic activity. For example, a series of *O. affinis* cyclotides was screened against gastrointestinal nematodes that infect sheep, including *Hemonchus contortus* and *Trichostrongylus colubriformis*.[109,169] The most potent inhibitor of larval development was kalata B6, followed by kalata B2 and B1, which displayed similar activity, whereas kalata B3 displayed minimal anthelmintic activity. The range of nematocidal cyclotides was expanded in a subsequent study, where *H. contortus* and *T. colubriformis* were screened against cyclotides from Violaceae plants, including cycloviolacins, varv peptides and vhl-1.[110] These assays revealed that several cyclotides were more potent than kalata B1, particularly those from *V. odorata* (cycloviolacin O2, O3, O8 and O13). Collectively, these cyclotides possess sequence variations in several loops and correlating sequence traits with anthelmintic activity revealed that cyclotides with three or four charged residues typically showed higher potency, irrespective of whether the cyclotide was from the bracelet or Möbius sub-group.[110] Certain cyclotides have also been tested against hookworm species known to infect humans or canines, with cycloviolacin O14 showing higher activity than kalata B6 or B1,[140] as well as schistosome strains, where kalata B2 was more active than kalata B1.[264] Beyond nematodes, studies have shown that kalata B1, kalata B2 and cycloviolacin O1 are toxic to molluscs, such as the golden apple snail,[112] and cycloviolacin O2 inhibits barnacle settlement in a non-toxic manner.[50]

Another activity that has been identified for numerous cyclotides is cytotoxicity against cancer cells. This function first emerged in a study that screened three cyclotides from Violaceae plants (varv A, varv F, and cycloviolacin O2) against a panel of cancer cell lines, including several cell lines that display resistance to chemotherapy drugs.[35] Cytotoxicity was assessed using a fluorescein diacetate hydrolysis assay after 72

hours culture, which revealed that cycloviolacin O2 showed the highest potency against all ten cell lines, with IC_{50} values in the range of 0.1–0.26 μM, whereas varv A and varv F had activity in the micromolar range. Two of the cell lines screened, U-937 GTB (lymphoma) and RPMI-8226/s (myeloma), were used in a subsequent study to identify cytotoxic molecules in an extract of *Viola tricolor*.[51] Activity-guided fractionation identified three cyclotides, two of which matched the known sequences of varv A or varv E, but the third sequence was novel and named vitri A. The most potent cyclotide was vitri A, which belongs to the bracelet sub-group (like cycloviolacin O2), whereas varv A, varv E, and varv F are all Möbius cyclotides. In a following study, additional cyclotides were isolated from *V. tricolor* and screened for cytotoxicity against cancer cells, where bracelet cyclotides were again found to be more cytotoxic.[180]

With the identification and characterization of cyclotides from additional plants, an increasing number of cyclotides have been found to be cytotoxic to cultured cancer cells. These include cyclotides from other Violaceae plants, including vibi G and H (*V. biflora*),[120] vaby A and D (*V. abyssinica*),[215] mela 1–7 (*Melicytus latifolius*),[317] vigno 5 (*V. ignobilis*),[331] and Poca A and B (*Pombalia calceolaria*).[411] Additional cyclotides produced by plants from the Rubiaceae family, psyle E (*Psychotria leptothyrsa*)[157] and hedyotide B7 (*Hedyotis biflora*),[280] and the Fabaceae family, cliotides (*Clitoria ternatea*),[269] are also cytotoxic to cancer cells. Collectively, these studies have provided several insights into the role of sequence and structure to cytotoxic activity, with positive net charge initially reported to be a key factor.[51] Similar findings emerged in studies on mela cyclotides, where Lys-rich Möbius cyclotides were more potent than their lysine-deficient counterparts.[317] However, a number of exceptions have also been identified, including cyclotides from *P. calceolaria* where Poca A (net charge −1) is more potent than cycloviolacin O4 (net charge +2),[411] and several cliotides, where CT19 and CT20 show relatively weak activity despite their net positive charge.[269] Interestingly, CT19 and CT20 have only four residues in loop 3 (compared to six residues in other bracelet cyclotides), indicating that other features are also likely to contribute to cytotoxicity against cancer cells.

Cyclotides have also been reported to have antimicrobial activity against a wide range of microorganisms.[17,178,270,366,375,391] None so far appear to be sufficiently potent for human clinical applications and, in general, reasonable potencies are only obtained in non-physiological (low salt) conditions. Nevertheless, promising results have been obtained in animal infection models in some cases,

despite low *in vitro* potency.[302] Activity testing has mainly focused on standard laboratory strains of bacteria and it is possible that biologically relevant antimicrobial activity will be against specific plant microbial pathogens.[381,390,401]

6.2 Linking structure to function

The known functions of cyclotides from each sub-group have implicated at least two types of molecular interactions in their mode-of-action. Based on their homology to well-characterized protease inhibitors (knottins) from related plants, trypsin inhibitor cyclotides block the active site of target enzymes via a protein–protein interaction. By contrast, the mode-of-action for Möbius and bracelet cyclotides involves membrane interactions. Unravelling the molecular basis for the various functions has been the overarching aim of a plethora of studies that have applied a range of approaches to examine the contribution of cyclotide structure, including primary structure, to bioactivity.

Cyclotides isolated directly from plants offer a unique opportunity to delve into structure–activity studies due to their natural sequence diversity. As outlined above, one area where this idea has been explored relates to the anthelmintic activity of Möbius and bracelet cyclotides from Violaceae plants, with cyclotides containing a higher number of basic residues tending to show higher potency.[110] More broadly, sequence analyses of cyclotides from different sub-groups and plant families have helped to pinpoint highly conserved residues that are likely to be important for function, including the critical Glu residue in loop 1 that is found in virtually all Möbius and bracelet cyclotides. An exception occurs in kalata B12, which has an Asp residue at this position, and this cyclotide is inactive in hemolysis assays at concentrations where kalata B1 is hemolytic.[212]

The importance of the conserved Glu residue in loop 1 has been explored further through targeted chemical modification of cycloviolacin O2.[80] Esterification of Glu to *O*-methyl Glu by treatment with acetyl chloride/MeOH led to a 48-fold loss in cytotoxicity against U937 cells, which surpassed the change in activity when the cyclotide's two Lys residues were *N*-acetylated (seven-fold).[80] Interestingly, chemical modification had a contrasting effect on the anthelmintic activity of cycloviolacin O2 as Lys acetylation was more detrimental to activity than Glu esterification.[110] These findings are consistent with assays

examining sequence-diverse cyclotides, where the correlation between net positive charge and bioactivity is more clear in anthelmintic assays compared to cancer cell cytotoxicity. In an earlier study, chemical modification was applied to kalata B1 to test the importance of an Arg residue for antimicrobial activity.[17] Kalata B1 has a single Arg residue, which was modified by treatment with *p*-hydroxyphenyl glyoxal and shown to diminish the cyclotide's activity against several microorganisms, including *Staphylococcus aureus*. A wide range of additional modifications (illustrated in Figure 19) have been made to the cyclotide framework to explore structure–function relationships and generate chemical probes.

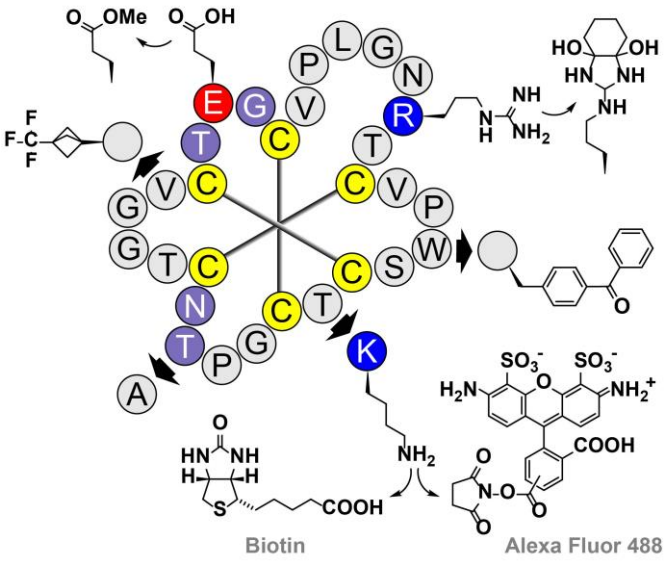

Figure 19. **Examining cyclotide structure–activity relationships using site-selective chemical modifications**. Selected chemical modifications are illustrated on a schematic diagram of kalata B1 (basic residues: blue; acidic residues: red; remaining residues in the bioactive face: purple). For cyclotides isolated from plants, Glu residues can be esterified by treatment with acetyl chloride in methanol, and Arg residues can be modified using 1,2-cyclohexanedione (shown) or 4-hydroxyphenyl glyoxal. Using chemical synthesis, point mutations can be introduced to perform an Ala-scan or Lys-scan. Replacing an amino acid with Lys, such as T20K, enables the production of labelled cyclotides by conjugation of a biotin or Alexa Fluor 488 tag. Additionally, non-proteinogenic amino acids can be introduced, including a 4-benzoyl-L-phenylalanine in place of Trp or trifluoromethyl bicyclopentylglycine in place of Val, to produce chemical probes for identifying or analyzing cyclotide interactions with various biomolecules. Figure adapted and updated from de Veer et al.[355]

Amongst these modifications are scanning mutagenesis studies that systematically introduced point mutations into kalata B1 with the aim of identifying residues that were essential for function. Initially, an Ala scan was performed using a library of 23 kalata B1 variants, where each non-Cys residue was individually mutated to Ala (Cys residues were not mutated to preserve the cystine knot).[125] Changes in function were assessed using bioassays for insecticidal activity, anthelmintic activity and hemolytic activity.[109,125] The three most important residues were all found in loop 1 (GET), which includes the highly conserved Glu residue that was identified in earlier studies. Two amino acids in loop 3 (Asn15 and Thr16)

were also shown to be key residues for activity, as well as Gly12 in loop 2. Interestingly, mapping these residues onto the 3D structure of kalata B1 revealed that five amino acids (Gly6, Glu7, Thr8, Asn15, and Thr16) clustered together to form a surface patch that was named the bioactive face. Several additional residues, including Arg28, three Val residues, and Pro3, were also found to influence anthelmintic and hemolytic activity. Observations made during the synthesis of the Ala-mutant library also contributed to identifying residues that were important for efficiently folding kalata B1 as mutations at certain positions yielded low amounts (Pro3, Gly12) or no detectable levels (Trp23, Pro24) of correctly folded product.[125]

Kalata B1 has also been the focus of a lysine-scanning study, which contributed to clarifying the role of several residues outside the bioactive face.[170] Introducing a charged residue at each non-Cys position was particularly useful for examining the role of hydrophobic residues. By testing the anthelmintic activity of each Lys-mutant, a second region was defined that was important for activity and named the hydrophobic face, where Val4, Val10, Trp23, and Val25 were found to be key amino acids. Interestingly, the activity screen also identified six residues that formed a single cluster where mutation to Lys led to improved activity.[170] Accordingly, this region was named the amendable face. Certain mutations were also shown to have an additive effect, which was most evident in a triple mutant where Gly1, Thr20 and Asn29 were each replaced by Lys.

Several of the residues that form the bioactive face and hydrophobic face in kalata B1 are also conserved in other cyclotides from the Möbius sub-group, as shown in Figure 10. In the bioactive face, the three residues in loop 1 are almost completely conserved (Ser occasionally replaces Thr), whereas in loop 3, Thr16 is highly conserved, but Asn15 is replaced by Tyr in approximately 40% of sequences, including kalata B7. In the hydrophobic face, Trp23 and Val25 (loop 5) are the most common residues at these positions, followed by Tyr and Ile, respectively, whereas Val10 (loop 2) is replaced by Phe in 50% of sequences. Some similarities are also evident in the bracelet sub-group, particularly in loop 1, where Glu is conserved and Ala occasionally replaces Gly, but Ser (80%) is more common than Thr. However, loop 3 is extended in bracelet cyclotides (typically six residues) and it has different sequence features compared to Möbius cyclotides. In NMR structures of kalata B1 and kalata B7, Glu (loop 1) forms intramolecular hydrogen bonds with the backbone NH of Thr16 and Asn15/Tyr15, as shown in Figure 20.[41,124,263] In cycloviolacin O1 and cycloviolacin O2, the corresponding Glu residue forms hydrogen bonds with the first

two or three residues of loop 3 (via backbone NH atoms or Oγ when a Ser or Thr residue is present) that stabilize a 3_{10} helix.[41,146] Subsequent analyses of the *O*-methyl Glu variant of cycloviolacin O2 illustrated the critical role of these interactions, as loop 3 became flexible and disordered without the stabilizing hydrogen bonds coordinated by Glu, offering a structural rationale for the loss in bioactivity that accompanied Glu esterification.[146] Another key difference occurs in loop 5, which is noticeably more hydrophilic in bracelet cyclotides and lacks an aromatic residue, although Val still precedes Cys^{VI} as seen in the Möbius sub-group. At present, a systematic point mutant scan has yet to be reported for a bracelet cyclotide, with the findings from such a study likely to provide further clarity on the similarities and differences between the two sub-groups.

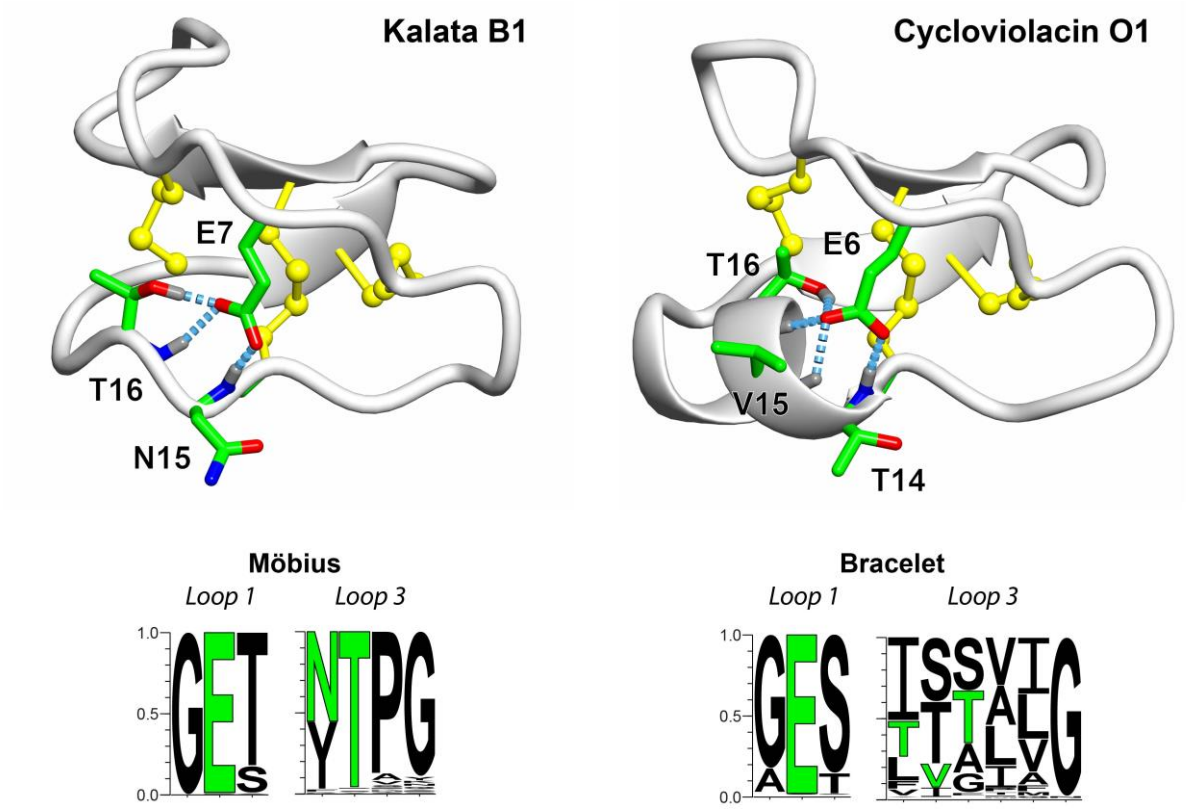

Figure 20. **Stabilizing interactions involving the conserved Glu residue in Möbius and bracelet cyclotides.** The high-resolution NMR structures of kalata B1 (PDB 1NB1) and cycloviolacin O1 (PDB 1NBJ) are shown as ribbon diagrams, with disulfide bonds shown in ball-and-stick model. In kalata B1, the conserved Glu residue (Glu7) is proposed to form hydrogen bonds with the backbone NH of Asn15 and Thr16, together with Oγ of Thr16. In cycloviolacin O1, Glu6 forms hydrogen bonds with the backbone NH of Thr14, Val15 and Thr16, as well as Oγ of Thr16, to stabilize a short helix in loop 3. Hydrogen bonds shown for each cyclotide are based on structural analyses by Rosengren et al.[41] The logo diagrams (below) illustrate sequence diversity in loops 1 and 3 in the Möbius and bracelet sub-groups (amino acids shown in the structure above are colored green). In Möbius cyclotides, Thr is highly conserved in loop 3, whereas Asn is replaced by Tyr in approximately 40% of sequences. The bracelet sub-group shows higher diversity in loop 3, although Ser or Thr is often the second (75%) and third residue (65%) in this loop. Glu is highly conserved in loop 1 for both sub-groups.

In addition to sequence modifications, the role of structure-defining covalent bonds has been explored in relation to function. One structural feature that has attracted longstanding interest is the head-to-tail cyclic backbone. Initial studies focused on kalata B1 and examined the effect of breaking the cyclic backbone in each of the peptide's six loops by synthesizing a series of full-length linear permutants.[20] Disrupting the backbone in either loop 1 or loop 4 was found to prevent efficient folding, indicating that these loops are important for promoting correct disulfide connectivity. Additionally, several of the linear permutants displayed different HPLC retention times suggesting that, despite being correctly folded, they were not identical in structure. Subsequent changes in function were assessed by performing hemolytic assays, which revealed that each of the linear permutants lacked activity.[20] This finding was explored further by characterizing the hemolytic activity and solution structure of a linear kalata B1 variant that lacked five residues in loop 6.[44] Although the overall fold of the linear variant was similar to cyclic kalata B1, the $Cys^{I–IV}$ disulfide bond and Glu7 were found to adopt two conformations (an indication of increased flexibility) and the molecule showed much weaker hemolytic activity. The naturally occurring acyclotide violacin A also shows weaker hemolytic activity, with the authors suggesting that one contributing factor to the loss of activity was a decrease in hydrophobicity.[83] This effect is not necessarily related to charge introduced by the free N- and C-terminus as linear kalata B1 variants that are *N*-acetylated and *C*-amidated still lack hemolytic activity.[54] Further studies have shown that the anti-HIV activity[48] and insecticidal activity[111] of kalata B1 also depend on its cyclic backbone. By contrast, the potent activity of trypsin inhibitor cyclotides does not rely on the presence of a cyclic backbone, although this finding likely reflects their different mode of action compared to Möbius and bracelet cyclotides.[61]

Another structural feature that has been examined in SAR studies is the cystine knot. One approach used to explore the role of the cystine knot involved testing the activity of two-disulfide intermediates that were generated during chemical synthesis.[17] Cyclic peptides containing two disulfide bonds based on cyclopsychotride ($Cys^{III–VI}$ absent), and kalata B1 or circulin B ($Cys^{II–V}$ absent) were screened in antimicrobial assays and found to have reasonably similar activity to their corresponding three-disulfide peptides. Consistent with these results, a two-disulfide kalata B1 mutant that was produced by mutating Cys^{I} and Cys^{IV} to Ala shows a similar 3D structure to native kalata B1.[38] By contrast, loss of all three

disulfide bonds is detrimental to activity, as indicated by U937 cytotoxicity assays performed using a reduced and *S*-alkylated variant of cycloviolacin O2.[80] More broadly, the effect of global structure on function has been examined by chemically synthesizing the D-enantiomer of kalata B1. Interestingly, this peptide showed only slightly weaker activity than L-kalata B1 in a range of bioassays, including anthelmintic, anti-HIV and hemolytic assays.[109,211] Additionally, hemolytic assays performed using different ratios of L- and D-kalata B1 revealed that certain enantiomer mixtures produced weaker activity than D-kalata B1 alone, suggesting that self-association might play an important role for kalata B1 and its mode of action.[211]

6.3 Defining the mode-of-action for membrane-active cyclotides

As new insights into the role of key residues and features continued to emerge, the next challenge was to identify the specific molecular targets of cyclotides, particularly those from the Möbius and bracelet sub-groups. These cyclotides were anticipated to target lipid membranes, and the first evidence supporting this hypothesis arose in studies that examined cyclotide binding to lipid mixtures that were representative of different membrane types. Using surface plasmon resonance (SPR), kalata B1 and kalata B6 were both shown to interact with immobilized lipids.[66] Additionally, examining the affinity of each cyclotide for various lipids revealed a degree of binding selectivity, as kalata B1 and kalata B6 both displayed higher affinity for dimyristoyl-L-α-phosphatidylethanolamine compared to other lipids that contained a phosphatidylcholine or phosphatidylglycerol head group. Interactions between kalata B1 and lipid membranes were also analyzed using NMR spectroscopy to examine cyclotide binding to dodecylphosphocholine (DPC) micelles.[89] Fluctuations in kalata B1 ^{1}H chemical shifts suggested that membrane interaction occurred via surface-association rather than deep insertion into the micelle. A model of the cyclotide–micelle complex was subsequently produced by examining attenuation of NOE cross-peaks upon incorporation of 5- and 16-doxylstearate relaxation probes into the DPC micelle. These data indicated that the hydrophobic face of kalata B1 (Val10 together with portions of loop 5 and 6) was embedded within the micelle.[89] Interestingly, several of these residues were also found to be important in

a liposome leakage assay, where the activity of kalata B1 was diminished when each amino acid from the hydrophobic face was mutated to Ala, particularly Trp23 and Val25 located in loop 5.[148]

In addition to the studies on Möbius cyclotides, other studies have characterized the binding interactions between bracelet cyclotides and membranes. These investigations were prompted by the potent cytotoxicity of cycloviolacin O2 against cancer cell lines, including observations that treating U-937 cells with cycloviolacin O2 resulted in rapid cell death that was accompanied by disruption of the cell membrane.[100] Changes in membrane integrity were examined further by performing leakage assays with HeLa cells or liposomes, which revealed that cycloviolacin O2 was active against simple membranes with defined lipid composition as well as complex membranes in living cells. A later study examined cyclotide interactions with a broader range of lipids, and found that cycloviolacin O2 was more active against liposomes when anionic lipids were included in the formulation compared to liposomes comprised solely of zwitterionic phosphocholine-type lipids.[185] This effect was shown to be related to charge as Lys *N*-acetylation led to diminished activity. Additionally, Glu esterification led to improved activity against anionic lipid-containing liposomes, but weaker activity against liposomes comprised of *E. coli* polar lipids, indicating that Glu6 influences interactions with different types of membranes. The structural basis for cycloviolacin O2–membrane interactions has been explored by NMR spectroscopy using DPC micelles.[147] Here, the signal attenuation profile in the presence of 5- and 16-doxylstearate relaxation probes indicated that loops 1, 2, and 3 were located at the peptide–micelle interface. This binding mode was different to several Möbius cyclotides, including kalata B1,[89] kalata B2,[147] kalata B7,[124] and varv-F,[149] where loops 1, 2 and 5 contributed to micelle interactions, and loop 3 appeared to be solvent-exposed. However, the helical structure of loop 3 in cycloviolacin O2, and other bracelet cyclotides, is more suited to interaction with lipids, and this feature may contribute to the differences in binding mode for bracelet and Möbius cyclotides.

As noted above, one of the key findings to emerge from studying cyclotide–membrane interactions was the observation that several cyclotides showed higher affinity for certain lipids. To explore this phenomenon in greater detail, SPR experiments were performed to examine the interaction between kalata B1 and immobilized phosphatidylcholine lipid bilayers that included additional lipids with different biophysical properties.[184] Kalata B1 showed weak binding to neutral phosphatidylcholine bilayers, anionic bilayers and phosphatidylinositol-containing bilayers. However, membrane binding affinity was found to

strongly correlate with the presence of phosphatidylethanolamine (PE) lipids, including bilayers that were representative of mammalian-type and bacterial-type membranes. A subsequent study demonstrated that a wider range of cyclotides from the Möbius and bracelet sub-groups display preferential binding to PE lipids, including kalata B2, B6, B7 (Möbius), and cycloviolacin O2, kalata B5, B8, B9, and tricyclon A (bracelet).[230,232] Interestingly, an earlier study also found that interaction between cycloviolacin O2 and bilayers comprised of *E. coli* polar lipids resulted in selective release of PE lipids from the bilayer.[185] The interaction between kalata B1 and PE lipids was further analyzed by NMR spectroscopy to compare peptide ^{1}H chemical shifts in the presence of increasing concentrations of lipid.[184] These experiments revealed that protons displaying altered chemical shifts were mainly located within the bioactive face of kalata B1, and when the experiment was repeated with an inactive mutant E7D that does not bind PE, no chemical shift changes were observed. This finding further clarifies the significance of the conserved Glu residue in loop 1 and indicates that its previously identified role in maintaining structure[146] is important for interaction with PE lipids.

Characterizing the binding of mutant cyclotides to immobilized lipid bilayers has provided further insights into the relationship between membrane interactions and bioactivity. Initial studies focused on a series of mutants reported as part of the kalata B1 lysine scan and examined their binding to PE-containing bilayers using SPR. Strikingly, variants with mutations located in the bioactive face or hydrophobic face were found to display weaker membrane binding, with the decrease in affinity for PE-containing lipids correlating with the previously reported loss in bioactivity.[184] By contrast, Lys mutants showing improved bioactivity compared to kalata B1 displayed higher binding to PE-containing bilayers, indicating a close correlation between interaction with PE lipids and biological function for kalata B1. A similar relationship was identified by studying additional kalata B1 variants, including several peptides with relatively conservative mutations. Variants containing mutations in the bioactive face (G6A, E7D, N15D, and T16S) showed weaker binding to immobilized lipid bilayers,[184,231,284] which was consistent with their diminished bioactivity. Interestingly, inserting an additional Trp residue into loop 5 or replacing Asn15 with Tyr (loop 3) led to improvements in both membrane binding and activity in hemolytic or cytotoxicity assays.[284] The N15Y mutation produced the largest change in activity for kalata B1, and this replacement is found in approximately 40% of naturally occurring Möbius cyclotides, including kalata B7. Indeed, mutating Tyr15

in kalata B7 to Ser or Ala was shown to decrease the cyclotide's ability to bind and permeabilize PE-containing liposomes.[346]

The interaction between cyclotides and PE lipids is not only relevant to their bioactivity, it is also a key event that influences the ability of kalata B1 to internalize into cells. Kalata B1 was first shown to cross cell membranes in experiments that examined the uptake of fluorescently-labelled cyclotides.[187] These assays were performed with Lys point-mutants as native kalata B1 does not contain an exposed amino group that can be used for labelling, for example, with biotin or Alexa Fluor 488. The use of Lys mutants also enabled a comparison of active (T20K) and inactive (V25K) kalata B1 mutants. In MCF-7 cells, T20K was found to internalize more efficiently than V25K, indicating that cell penetration by kalata B1 was influenced by PE binding. Additionally, cellular uptake was inhibited when the temperature was lowered to 277K, but not by treatment with a macropinocytosis inhibitor, suggesting that kalata B1 entered cells by endocytosis. In a following study, the mechanism for internalization into cells was explored further using additional kalata B1 variants that contained a Lys mutation within the bioactive face.[308] T20K was shown to internalize into HeLa cells at a peptide concentration that was non-toxic and did not permeabilize membranes, whereas the inactive mutants E7K, T16K, and V25K all showed considerably lower rates of uptake. Cellular entry of unlabeled kalata B1 was confirmed using LC-MRM mass spectrometry, where it was detected in membrane-associated and cytosolic fractions. The decrease in cellular uptake at lower temperature (277K) was also shown to be a result of changes in membrane fluidity, as well as inhibition of endocytosis that was partially dependent on both dynamin and actin. These findings indicated that kalata B1 enters cells either by direct translocation or endocytosis, with both processes relying on initial binding to the membrane via PE lipids.

6.4 Trypsin inhibitor cyclotides repurpose loop 1 to enable enzyme inhibition

Unlike Möbius and bracelet cyclotides, several aspects of the mode of action for trypsin inhibitor cyclotides could be inferred from related peptides that displayed similar structure and function. Examining the sequence[24] and solution structure[27,28] of trypsin inhibitor cyclotides isolated from *M. cochinchinensis* seeds revealed strong homology to several knottins from related plants that were potent trypsin inhibitors,

but lacked a head-to-tail cyclic backbone. These inhibitors were classed as Laskowski (or standard mechanism) inhibitors and were known to inhibit trypsin by binding within the enzyme active site via an exposed loop, as seen in structures of trypsin-knottin complexes determined by X-ray crystallography. The inhibitor's binding loop resembles a favored cleavage sequence within a protein substrate, and Laskowski inhibitors are described as having a substrate-like mechanism, to the extent that they are cleaved at the scissile bond. However, unlike ordinary substrates, the newly generated termini at the cleavage site remain tightly bound, which promotes religation of the scissile bond using the enzyme's catalytic machinery rather than hydrolysis of the acyl-enzyme complex. Indeed, trypsin can be used to cyclize MCoTI-II when the acyclic precursor is arranged so that the P1 Lys and P1′ Ile residues are located at the C- and N-terminus, respectively, as described in Section 5.4.[102]

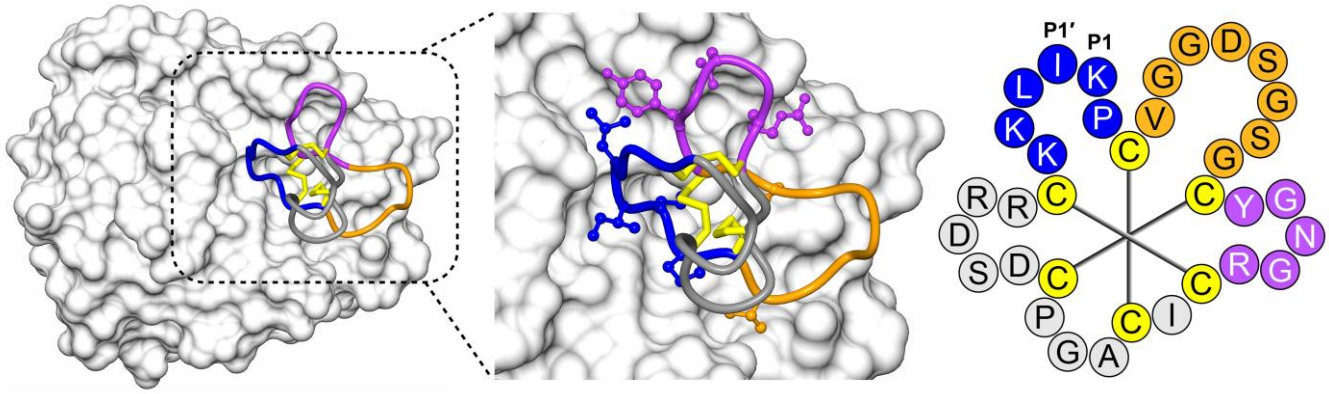

Figure 21. **Residues from three loops contribute to binding of MCoTI-II to trypsin.** The structure of MCoTI-II (ribbon diagram) in complex with trypsin (surface representation, grey) shows the three contact loops: loop 1 (blue), loop 5 (purple), and loop 6 (orange). In the insert, selected contact residues from these loops are shown in ball-and-stick model, and the cystine knot is shown in stick representation (yellow). The sequence of MCoTI-II is shown to the right, with loops colored according to the structure graphic. The position of the scissile bond is indicated by labelling the P1 Lys and P1′ Ile residues in loop 1.

Just as loop 1 has a critical role in PE-binding for Möbius and bracelet cyclotides, sequences of MCoTI-I and MCoTI-II indicate that the scissile bond for trypsin inhibitor cyclotides is also located in loop 1. Interestingly, loop 1 in trypsin inhibitor cyclotides is twice the length of Möbius and bracelet cyclotides, which reflects that it has evolved for a different function and class of molecular targets. The structure of MCoTI-II bound to trypsin has been determined by X-ray crystallography, which confirmed that MCoTI-II has a similar binding mode to acyclic knottins, with loop 1 being the primary binding loop (Figure 21).[255] Additional residues in loops 5 and 6 were also found to be contact residues, including a Ser residue in loop

6 that forms part of cyclization loop and is not present in acyclic knottins. The contribution of key contact residues towards inhibitory activity and selectivity has been studied using a series of synthetic MCoTI-II mutants. The major specificity determinant in many trypsin inhibitors is the P1 residue, which is typically Lys or Arg. Replacing P1 Lys in MCoTI-II with Phe was shown to convert the cyclotide into a potent chymotrypsin inhibitor,[108] whereas replacing Lys with Ala abolished the cyclotide's activity against several enzymes, including trypsin,[108,266] but generated a potent inhibitor of elastase.[145] Mutating other residues in loop 1 to Ala had varying effects on trypsin inhibitory activity, with P1′ Ile and P2′ Leu also found to be important, whereas P2 Pro and P3′ Lys were more tolerant of replacement.[266] Larger segments of MCoTI-II have also been replaced using corresponding loops from an acyclic knottin to generate cyclotide–knottin hybrid peptides.[114] Further details on MCoTI-II engineering studies are described in sections 7.2 and 7.3 below.

Although trypsin inhibitor cyclotides primarily function as enzyme inhibitors, MCoTI-I and MCoTI-II have also been shown to internalize into cells. This property is shared with Möbius and bracelet cyclotides, but occurs via separate mechanisms as trypsin inhibitor cyclotides lack many of the key residues that mediate binding to PE lipids. Nonetheless, differences in lipid binding probably contribute to the lack of cytotoxic or hemolytic activity identified for MCoTI-II in a range of assays. Initial studies examining cellular uptake of MCoTI-II demonstrated that biotin-labelled MCoTI-II internalized into MCF-7 cells and RAW264.7 macrophages more efficiently than kalata B1.[98] Additionally, cellular uptake appeared to occur via macropinocytosis as MCoTI-II was observed to co-localize with tetramethylrhodamine-dextran, and internalization was blocked when energy-dependent endocytic processes were inhibited by lowering the temperature to 277K. A following study demonstrated that MCoTI-I is also internalized by HeLa cells,[190] with analyses performed using live cell imaging as opposed to paraformaldehyde-fixed cells. Co-localization with markers for different endocytic pathways indicated that MCoTI-I entered cells by macropinocytosis, but also by lipid-dependent and clathrin-mediated pathways to a lesser extent. Further insights into the cellular uptake of trypsin inhibitor cyclotides emerged from examining the internalization of Lys to Ala mutants based on MCoTI-II.[187] Compared to native MCoTI-II, the mutant peptides typically showed lower rates of internalization, suggesting that cellular uptake was influenced by positive charge. Interactions with various lipids were subsequently assessed, and MCoTI-II was found to selectively bind

to phosphatidylinositol (3,4,5)-trisphosphate and phosphatidic acid. The ability of MCoTI-I and MCoTI-II to enter cells without causing membrane disruption, together with their low toxicity, highlights their considerable promise as scaffolds for targeting intracellular proteins or pathways.

7. APPLICATIONS

7.1 Applications based on natural function

The unique structures and diverse functions of cyclotides have paved the way for ongoing studies that are investigating the potential of cyclotides as novel pharmaceuticals or agricultural commodities. One area of exploration that has been particularly successful relates to efforts to harness the natural bioactivity of cyclotides to develop new drug leads and bioinsecticides. The discovery that kalata B1 inhibits the proliferation of activated human peripheral lymphocytes prompted suggestions that certain cyclotides could serve as novel immunosuppressive agents.[216] This activity was of interest as the anti-proliferative effect of kalata B1 was cytostatic, rather than involving apoptosis or necrosis. A subsequent study examined the role of specific residues using kalata B1 mutants, and found that variants with mutations in the amendable face (G18K, T20K or N29K) retained anti-proliferative activity, whereas mutations in the bioactive face (T8K) or hydrophobic face (V10A or V10K) were detrimental to activity.[257] Mode-of-action studies were subsequently performed using T20K kalata B1 and an inactive mutant (V10K). These experiments revealed that inhibition of T-cell proliferation was accompanied by diminished interleukin-2 signaling, including lower levels of secreted interleukin-2 and lower expression of its cognate receptor, as well as lower secretion of interferon-γ and tumor necrosis factor-α. Although several aspects of this mechanism remain to be fully elucidated, a recent study used a photo-reactive crosslinking probe to search for proteins that bound to kalata B1 in T-cell lysates.[372] The probe was produced by replacing Trp23 in kalata B1 with 4-benzoyl-L-phenylalanine (Figure 19), and analyzing interacting proteins revealed that kalata B1 bound to 14-3-3 proteins, which was shown to alter Akt/PI3K/Foxo3a signaling in a luciferase reporter assay.

Encouraged by these findings, the immunosuppressive activity of the lead variant T20K was subsequently assessed *in vivo* using an experimental autoimmune encephalomyelitis (EAE) mouse model of multiple sclerosis. Initially, T-cells isolated from EAE mice were treated with T20K, which was shown

to inhibit their proliferation *ex vivo* and decrease secretion of interleukin-2, as well as cytokines associated with Th1 and Th17-type autoimmunity, namely interferon-γ and interleukin 17A.[348] T20K was also shown to have a protective effect in EAE mice, with intraperitoneal administration (10 mg/kg) found to delay the onset of disease and decrease the severity of clinical symptoms. Histological analyses revealed that this effect was accompanied by a pronounced decrease in the infiltration of immune cells into the spinal cord and protection of neurons from demyelination. Remarkably, oral administration of T20K (20 mg/kg) was also shown to have a therapeutic effect in EAE mice on both clinical symptoms and spinal cord inflammation. This finding is exciting and raises the possibility of delivery via alternative routes to injection. Currently, T20K is being developed by Cyxone and it is anticipated that phase I clinical trials will commence in 2019.[426]

Another application that utilizes the natural bioactivity of cyclotides involves their use in novel bioinsecticides. As described earlier, a number of plants produce cyclotides that have insecticidal activity, including butterfly pea.[205,206] Studies have shown that separate parts of the butterfly pea plant produce different arrays of cyclotides, with cyclotides enriched in seeds and roots typically having different biophysical properties to those expressed in leaves and flowers.[333] Cyclotide-containing extracts from aerial parts of the plant are more active in vesicle leakage assays, including for vesicles that mimic the lipid composition of insect guts, whereas cyclotides extracts from roots were more active against nematodes.[333] These findings indicate that certain cyclotides in butterfly pea are subject to tissue-specific expression, where they are specialized to protect the plant against distinct types of pests in their local microenvironments. An extract from butterfly pea has now been commercialized as the bioinsecticide Sero-X, which was recently approved for use on macadamia nut and cotton crops in Australia.

7.2 Applications based on re-directed function

Cyclotides have been used to develop new chemical tools or pharmaceutical leads by shifting their natural activity to new targets. This line of investigation has been most thoroughly examined in the context of protease inhibitor engineering using MCoTI-II. As their name suggests, trypsin inhibitor cyclotides have high affinity for the prototypic serine protease trypsin. However, gene duplication events over millions of

years have given rise to a superfamily of serine proteases that show high structural homology to trypsin but are specialized for separate physiological functions. As MCoTI-II is structurally optimized for binding within the active site of trypsin, it represents a promising scaffold for targeting the active sites of structurally related proteases. Additionally, it is amenable to sequence modification in most loops, as seen in sequences of naturally occurring trypsin inhibitor cyclotides from separate *Momordica* species illustrated in Figure 22. Moreover, the ability of MCoTI-II to penetrate cells and its multiple contact loops provide a unique opportunity to target proteases that appear particularly challenging due to their cellular localization or close similarity to related enzymes.

Initial engineering studies based on MCoTI-II focused on substituting key binding residues to improve its activity against new target proteases. One target was β-tryptase, an enzyme produced by mast cells that is implicated in allergic inflammation, including asthma. Native MCoTI-II is a potent inhibitor of β-tryptase and engineered inhibitors have been produced using two different strategies. In one approach, a tripeptide motif Lys-Lys-Val was substituted into loop 6 of MCoTI-II[179] or a MCoTI–knottin hybrid scaffold[114] to generate β-tryptase inhibitors with low nanomolar K_i values. In another study, the length of loop 6 was decreased by four residues (deleting Ser-Asp-Gly-Gly) to weaken the inhibitor's activity against trypsin, while retaining its potent activity against β-trypase.[145] In the latter study, MCoTI-based inhibitors for neutrophil elastase, a target for several diseases that feature chronic inflammation, including chronic obstructive pulmonary disorder, were also produced by substituting the specificity-determining P1 Lys residue for Val or Ala.[145]

Another protease that has been targeted using engineered MCoTI-based inhibitors is matripase, a membrane-anchored protease that is over-expressed in several cancers. Inhibitors for matriptase were developed by substituting P4 Val to Arg, which brought about a 10-fold improvement in activity, combined with a P1′ Ile to Ala replacement, which was performed to decrease off-target activity against trypsin.[266] Figure 22 illustrates several of the substitutions that have been carried out in engineered MCoTI-variants. This range of substitutions highlights the flexible nature of the framework, which has been expanded even further by modifications introduced in grafting studies (Section 7.3).

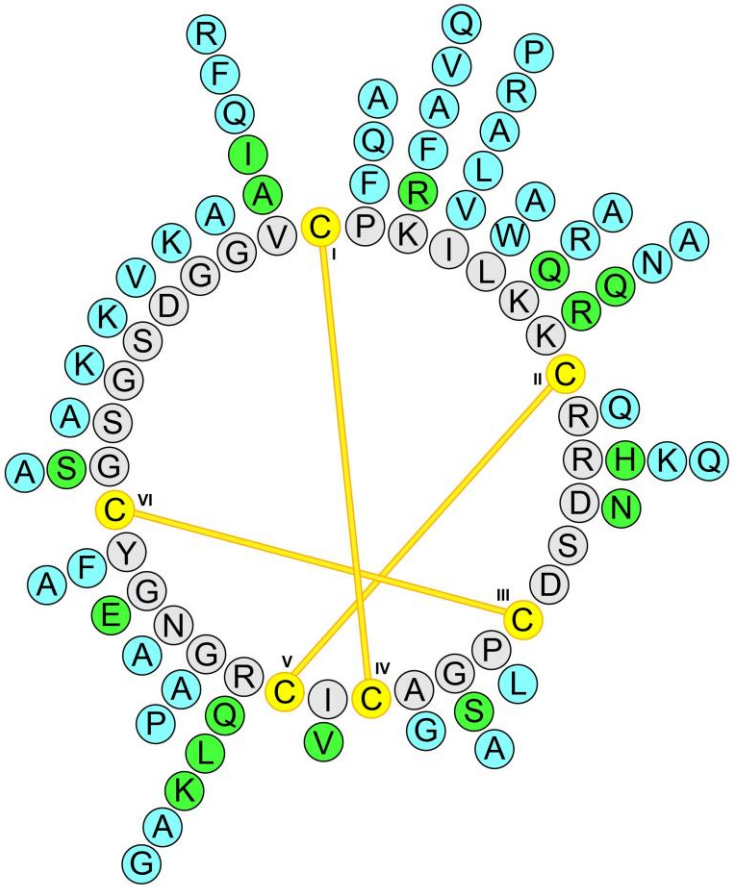

Figure 22. **Sequence variation found in naturally occurring trypsin inhibitor cyclotides and engineered variants.** The sequence of MCoTI-II is shown in grey circles using single letter amino acid code (clockwise direction). Cys residues are highlighted in yellow circles and are completely conserved to maintain the I-IV, II-V, III-VI disulfide connectivity that forms the cystine knot. Sequence variations found in naturally occurring trypsin inhibitor cyclotides are shown in green circles and residue substitutions introduced in engineered variants are also shown (cyan). Note that the most extensively substituted residues are in loop 1 (between Cys^{I} and Cys^{II}), as well as the P4 Val residue in loop 6 (between Cys^{VI} and Cys^{I}).

Another engineering strategy applied to MCoTI-II capitalizes on the inhibitor's substrate-like mechanism and is based on substituting the P4–P1 residues (Val3–Lys6) with a highly preferred cleavage sequence for the new target. This approach draws on existing substrate specificity data for the protease of interest and involves screening a non-combinatorial library of tetrapeptide substrates to identify candidate sequences that are optimized for subsite cooperativity. Using this strategy, MCoTI-based inhibitors were developed for coagulation factor XIIa,[347] a key protease in the intrinsic pathway of the coagulation system that has emerged as a novel target for preventing thrombosis. The selectivity of the first-generation inhibitor was refined by substituting P2′ Leu to Trp (loop 1) as well as replacing Gly1 with Lys (loop 6), with these modifications identified by a cyclic peptide library screen and computer-aided design, respectively.[347]

In another recent study, a substrate-guided approach was also used to generate MCoTI-based inhibitors for kallikrein-related peptidase 4 (KLK4), a protease that is over-expressed in prostate cancer. Substitutions at three positions (P1, P2 and P4) yielded an engineered variant that displayed exceptional selectivity over closely-related proteases, including KLK5, KLK7, KLK14, plasma kallikrein, plasmin and coagulation factor XIIa.[408] Cellular uptake assays revealed that the new variant was internalized into cells with slightly higher efficiency that MCoTI-II. Interestingly, in the case of both coagulation factor XIIa and KLK4, the P2 Pro residue that is highly conserved in trypsin inhibitor cyclotides and acyclic knottins was successfully targeted for optimization, indicating that it is a viable option in future engineering studies.

Sequence optimization of MCoTI-II has been carried out on a broader scale using genetically encoded sequence-diverse libraries produced by yeast surface display. This is a particularly powerful approach as it provides access to a much broader range of unique sequences than can be practically obtained using chemical synthesis. Yeast surface display has been used to construct libraries of MCoTI-variants by expressing a fusion protein that comprises the inhibitor coding sequence linked to the *Saccharomyces cerevisiae* Aga2p protein via the human influenza hemagglutinin epitope and a Gly-Ser linker.[256] In this construct, the inhibitor is displayed on the cell-surface as an acyclic knottin, which enables the introduction of a cMyc tag at the C-terminus. Sequence diversity is subsequently introduced at designated positions during PCR amplification by the use of NNK codons. This strategy was used to produce MCoTI-based inhibitors for matriptase, where the primary focus for sequence optimization was the P1′–P4′ (Ile7–Lys10) segment in loop 1, and varying levels of sequence variation were also permitted in loops 2, 5 and 6.[256] After incubating the immobilized library with matriptase, cells expressing matriptase-binding peptides were isolated by fluorescence-activated cell sorting and, after several rounds of enrichment, four MCoTI-variants were identified by sequencing and selected for further characterization. Sequence changes from native MCoTI-II were predominantly located in loops 1 and 6, with a single replacement found in loop 5 for two variants. Each of the identified variants displayed potent activity against matriptase (K_i values in the low to sub-nanomolar range), demonstrating the considerable potential of the screening approach.

7.3 Applications based on grafting to introduce new functions

Another broad application of cyclotides stems from their beneficial molecular properties, including strong resistance to degradation, well-defined structures and tolerance to sequence modification. Several of these characteristics, particularly high stability, are rarely seen in ordinary peptides, prompting suggestions that cyclotides represent promising engineering scaffolds that can be adapted for a range of new functions. To date, the main approach for equipping cyclotides with new biological activities has involved inserting an epitope from a bioactive peptide or protein into the cyclotide framework. This process is termed "grafting" (Figure 23) and leads to the production of a chimeric cyclotide that combines the properties of the ultra-stable scaffold with the specific function of the bioactive epitope. Cyclotide grafting has been extensively reviewed in previous articles,[251,363,418-420] and the reader is referred to these reviews for further information. The following section will focus on several applications that demonstrate the unique opportunities enabled by cyclotides.

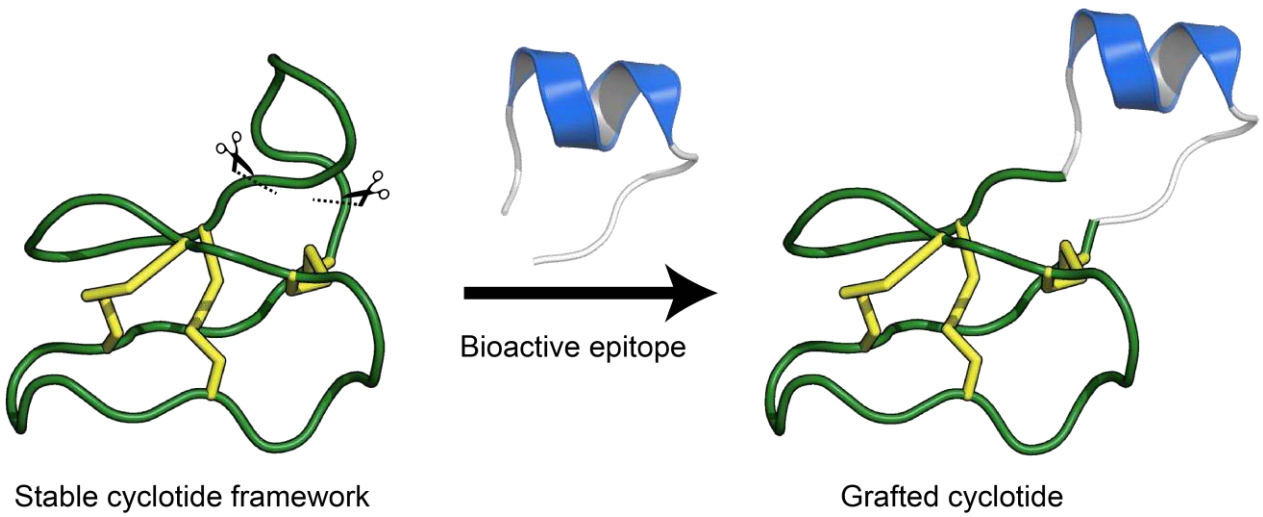

Figure 23. **Schematic diagram illustrating the concept of grafting an epitope into a cyclotide scaffold.** A bioactive epitope, shown here as a small helix, with desired bioactivity (discovered using screening, computational design, phage display or derived from a bioactive epitope of a larger protein) is inserted into a stable cyclotide framework, resulting in a new grafted peptide that has the desired bioactivity as well as stability.

One application of grafted cyclotides that has attracted significant interest is their ability to deliver cargoes inside cells. Although many proteins have limited access to the intracellular space when added exogenously, several cyclotides, including kalata B1, MCoTI-I, and MCoTI-II, have been shown to be internalized by cells. Therefore, grafting epitopes into certain cyclotide frameworks can serve to, not only stabilize the bioactive epitope, but enable delivery across membranes. This approach has been used to produce grafted cyclotides that modulate the p53 pathway via blocking the binding of its endogenous

inhibitors, Mdm2 and MdmX.[261] The grafted cyclotides were designed by inserting a previously identified α-helical peptide that binds with high affinity to Mdm2 and MdmX into loop 6 of MCoTI-I. This scaffold was selected as trypsin inhibitor cyclotides are internalized by cells in a non-toxic manner that does not cause membrane disruption. NMR experiments indicated that the 17-amino acid grafted epitope did not markedly alter the structure of the MCoTI-I scaffold (loops 1–5) and was not detrimental to oxidative folding to form the cystine knot. The grafted cyclotide was shown to bind with high affinity to Mdm2 and MdmX, such that it blocked the binding of either inhibitor to the transactivation domain of p53 at nanomolar concentrations. Activity was also demonstrated in cellular assays, where the grafted cyclotide lowered the viability of p53-competent cancer cells, with further analyses revealing that cytotoxicity was mediated by stabilization of p53 and activation of downstream signaling pathways that initiated cell cycle arrest and apoptosis. Encouraged by these results, the grafted cyclotide was tested in a tumor xenograft model, where mice carrying established tumors were treated by intravenous injection (40 mg/kg). The MCoTI-variant was shown to dramatically suppress tumor growth and activate the p53 pathway, indicating that grafted cyclotides can successfully reach their intended intracellular targets *in vivo*.

Another application of interest for grafted cyclotides relates to their potential to demonstrate oral activity. The first indication that certain cyclotides might be orally active can be traced to kalata B1 and traditional medicine, where a tea brewed from *O. affinis* leaves is given to induce uterine contractions and accelerate childbirth. A grafted cyclotide that was produced using the kalata B1 framework has also been reported to have oral activity.[238] This peptide emerged from a study developing bradykinin B_1 receptor antagonists as a treatment for chronic pain, and was designed by grafting a nine-amino acid epitope into loop 6 of kalata B1. In competitive binding assays, the grafted cyclotide was shown to prevent the bradykinin B_1 receptor from binding an endogenous agonist, [des-Arg9] bradykinin, which was accompanied by inhibition of B_1 receptor-mediated signaling.

The analgesic activity of the kalata B1-variant was subsequently assessed in mice using an abdominal constriction model. Intraperitoneal injection (1 mg/kg) of the grafted cyclotide was found to provide higher pain relief than the linear B_1 receptor antagonist epitope or a grafted, acyclic permutant. A similar level of pain relief was achieved when the grafted cyclotide was delivered by oral administration (10 mg/kg), whereas the acyclic kalata B1-variant had considerably weaker oral activity and the linear

epitope was not active. Although the grafted cyclotide showed oral activity, the oral bioavailability of cyclotides, and macrocyclic peptides in general, is quite low. To some extent, cyclotides overcome this challenge by having exceptionally high potency. As noted earlier, the kalata B1-variant T20K also shows oral activity,[348] and the field will be closely following the progress of this molecule through clinical trials, as well as other developments relating to peptide oral bioavailability.

In addition to grafting selective epitopes into a cyclotide framework, cyclotide grafting has also been applied to adjust the selectivity of bioactive peptides that have broad-range activity. One area where this approach has been used is the development of grafted cyclotides that target the melanocortin system,[218] which comprises a family of five G protein-coupled receptors (GPCRs) and their endogenous agonists. Individual melanocortin receptors (MCRs) are involved in modulating key physiological processes, ranging from metabolism and food intake to inflammation and immunity, and are activated by non-specific peptide ligands that share a common pharmacophore: His-Phe-Arg-Trp. In a physiological setting, selective MCR activation is enabled by tissue-specific expression of their peptide agonists, which is difficult to replicate in a pharmacological setting where a therapeutic peptide would be administered systemically and may have a broad biodistribution. Grafting the MCR pharmacophore into a cyclotide framework offers the opportunity to lock the bioactive epitope into a specific conformation and generate new agonists that are, not only stable, but have altered receptor selectivity. This concept was demonstrated by grafting the His-Phe-Arg-Trp pharamacophore (flanked on either side by a Gly residue) into loop 6 of kalata B1. Compared to an endogenous MCR agonist, the grafted cyclotide showed similar binding affinity for MC4R, which is a therapeutic target for obesity, and displayed much weaker binding to off-target MCRs.[218]

Recent findings from additional studies have provided further support for the idea that cyclotides represent promising design frameworks for selectively targeting a range of GPCRs. The native sequence and structure of loop 3 in kalata B7 has been identified to closely resemble human oxytocin.[263] Consistent with this finding, kalata B7 was shown to activate the human oxytocin receptor, and further assays revealed that a nine-residue peptide epitope based on residues 14–22 of kalata B7 displayed considerably higher activity than the full-length cyclotide, confirming that the bioactive epitope resided within loop 3. In another study, a 14-amino acid epitope was grafted into loop 6 of MCoTI-I to produce a potent antagonist of the chemokine receptor CXCR4, which was shown to block the entry and replication of HIV-1 in human MT4

lymphocytes.[217] The lead molecule from this study was subsequently modified by conjugating the metal chelating moiety 1,4,7,10-tetraazacyclododecane-1,4,7,10-tetraaceticacid (DOTA) to a Lys residue in loop 1 to enable the production of a radiolabeled bioimaging probe.[374] Incubating the grafted MCoTI-DOTA peptide with the radionuclide $^{64}Cu(OAc)_2$ generated a CXCR4-targeted probe that was suitable for PET-CT imaging and retained equivalent *in vitro* receptor binding affinity. Subsequent *in vivo* studies using CXCR4-overexpressing U87 xenografts in mice demonstrated rapid and specific binding of the radiolabeled probe to CXCR4-positive tumor cells, whereas a DOTA-conjugated MCoTI-I control peptide was rapidly cleared via the kidneys.[374] This finding highlights a key difference for cyclotides compared to monoclonal antibodies as, due to their smaller size, non-bound probe can be rapidly cleared from circulation, yet they retain high target affinity and are stable in serum.

A final application that relates to cyclotide grafting involves the use of display technologies that enable *in situ* sequence optimization. In contrast to grafting applications, which are based on rational design (outlined above), this approach employs recombinant DNA techniques to generate libraries with vast sequence diversity that can be screened against a target of interest. One method that has been successfully used to express and screen genetically encoded cyclotide libraries is bacterial display. An engineered variant of the outer membrane protein OmpX (named eCPX) was used to display the peptide library on the cell surface, with the encoded cyclotide displayed as an acyclic peptide to enable expression of the cyclotide-eCPX construct as a single fusion protein.[200] Sequence diversity was introduced using NNS codons and the library was screened by successive binding and amplification steps in a similar way to yeast surface display (section 7.2).[256]

Using this approach, grafted cyclotides based on kalata B1 were developed that target the serine protease thrombin or the growth factor receptor neuropilin-1.[200,254] For the thrombin-binding peptides, sequence optimization was targeted to loop 6 of kalata B1, which yielded 29 individual hits that were clustered into five consensus groups.[200] Two sequences from separate consensus groups were chemically synthesized as head-to-tail cyclic peptides and shown to target the thrombin active site with relatively high affinity. The neuropilin-1 antagonists were identified using a two-phase design strategy, where an initial display library was focused on optimizing loop 6. Hits from three consensus groups were synthesized and tested for neuropilin-1 binding, with the lead molecule used to design a second-generation display library

that focused on engineering loop 5, together with selected residues in loops 1 and 2.[254] The second library was also screened in the presence of trypsin to select for variants that showed higher resistance to enzymatic degradation. Sequences identified in this screen were found to bind to neuropilin-1 with improved affinity (K_D values in the range of 30–60 nM) and were more resistant to trypsin degradation. Additionally, the role of the cyclic backbone for binding affinity and biological activity was assessed using cyclic and acyclic forms of one of the lead molecules. Although both variants showed similar K_D values for binding to neuropilin-1, the cyclic peptide was found to be more potent in HUVEC migration assays, where activity was based on blocking the interaction between neuropilin-1 and vascular endothelial growth factor.[254]

8. OUTLOOK

Cyclotides continue to attract interest as topologically interesting and stable peptides that have a wide range of potential applications in medicine and agriculture. With robust methods available for their structure determination and chemical synthesis, together with emerging approaches to make them via chemoenzymatic or recombinant means, the tools are in place to exploit these interesting biomolecules for human benefit. In common with a diverse range of other macrocycles that are currently of interest in the pharmaceutical industry, such as stapled peptides, cyclotides (~ 3000 Da) fill an important molecular weight gap between small molecule drugs (< 500 Da) and biologics (>5000 Da), and with their exceptional stability and amenability to grafting, they have considerable potential as drug leads. We also propose that their natural origin as plant-derived peptides offers a unique possibility for their large scale and eco-friendly manufacture. Thus, one of the exciting prospects for the future is to foster the expression of 'designer' cyclotides, and indeed other cyclic peptides, using plants as bio-factories for producing high value pharmaceuticals or agrichemicals. Initial success in this field was reported recently with the expression in transgenic plants of an orally active candidate for multiple sclerosis, [T20K]kalata B1,[399] and a picomolar plasmin inhibitor based on sunflower trypsin inhibitor-1 (SFTI-1).[441]

Plant biofactories not only provide a 'greener' way to produce bioactive peptides that can be harvested from biomass and formulated into pharmaceutical products such as tablets, but also offer the potential for novel delivery routes, for example incorporating peptide-based medicines into foods. The

expression of bioactive peptides into edible seeds, where the seed essentially becomes a 'biopill', in particular, offers great potential for the economical supply of next generation medicines into developing countries. Seeds are typically stable and readily transported and have the potential to overcome some of the limitations of cold-chain transport of conventional peptide and protein formulations.

As well as these types of blue sky applications of cyclotides there are many opportunities for more conventional formulations of cyclotides. One area that is just beginning to be developed, for example, is in the formuation of cyclotides into nanoparticles. One recent paper[438] demonstrated that nanostructured cyclotides exhibited antitumor activity and sustained drug release. That example involved the incorporation of cyclotides kalata B2 and parigidin-br1 into the polymers Eudragit® L 100-55 and RS 30 D but we anticipate that this is an area that will expand into other formuations in the near future. Such formulation research is likely to be applied not only in the pharmaceutical field but also to cyclotide-based agrichemicals. The exceptional stability of cyclotides makes them suitable for a wide range of formulation options.

The possibility to develop medical and agricultural applications of cyclotides has arisen because of the important advances made over the last two decades in our understanding of the chemistry and molecular biology of cyclotides. But there remain unanswered questions on the chemistry, biology and evolution of cyclotides. One question on their chemistry is why are post-translational modifications apparently not common in this class of peptides yet seem to be quite frequent in other classes of similarly sized bioactive peptides such as the conotoxins? One possibility is that cyclotides achieve exceptional stabilization and favorable biophysical properties via their CCK motif so that no further modifications are required. Another possibility that needs to be considered is that perhaps such modifications are in fact more common that previously thought but have been overlooked. With just a few papers having reported post-translational modifications of cyclotides it is probably timely to explore in more detail the prevelance of such modifications amongst the natural cyclotide repoitoire.

Why are bracelet cyclotides more prevalent in nature than Mobius cyclotides, but more difficult to fold *in vitro*? So far there has only been limited success in folding bracelet cyclotides *in vitro* yet they outnumber Mobius cyclotides 2:1 in nature. We speculate that the cis X-Pro peptide bond in loop 5 of Mobius cyclotides might act as a seeding structure for folding but this suggestion has yet to be explored in detail and indeed the whole field of cyclotide folding is underexplored. We foreshadow great opportunies

to use computational approaches to explore cyclotide folding, given their small size and well defined structures and the steadily improving speed of computer hardware for molecular dynamics simulations.

Key biological questions that remain unanswered include- why does a single plant produce so many cyclotide variants, are there other native functions of cyclotides not so far discovered, and are cyclotides up-regulated in response to specific biotic or abiotic stresses? Related to the first of these questions is the question- are there perhaps synergistic effects between members of the suite of cyclotides in a given plant? So far most studies of cyclotide bioactivity have focused on individual isolated or synthesized components. We anticipate that with advances in synthetic and bioanalytical capability future studies will be able to explore cyclotide mixtures in more detail. We also anticipate that a wider range of screening options facilitated by access to cyclotide mixtures and libraries might indeed uncover new biological activities. Furthermore, with decreasing sequencing costs, more extensive transcriptome analyses of multiple plant tissues under a wide range of stresses will be a valuable area of cyclotide research.

Evolutionary questions include why are cyclotides ubiquitous in the Violaceae family, but sparse in other plant families? Why do monocots produce acyclotides, but not cyclotides? Studies of the enzymes involved in cyclotide biosynthesis are currently an active area of research and may assist in understanding aspects of cyclotide evolution. The increasing availability of plant genomes, which are often much larger and less tractable than the genomes of other organisms, will also undoubtedly help shed light on these evolutionaly questions. More broadly, we hope that the description of cyclotides provided in this article will help stimulate further work to answer other questions about these fascinating macrocyclic peptides.

AUTHOR INFORMATION

Corresponding Author

*Email: d.craik@imb.uq.edu.au

Notes

The authors declare no competing financial interest.

Biographies

Simon de Veer is a National Health and Medical Research Council (NHMRC) Early Career Fellow at the Institute for Molecular Bioscience (IMB), located at The University of Queensland (UQ), Brisbane, Australia. He received his PhD from Queensland University of Technology, and his research focuses on the use of naturally occurring cyclic peptides, including cyclotides, as design templates for targeting enzymes and cell-surface receptors.

Meng-Wei Kan undertook her PhD in medicinal chemistry at the School of Chemistry and Molecular Biosciences at UQ and joined David Craik's group at IMB as a senior research administration officer in 2013. Her research interests are in applications of peptide chemistry in medicine and agriculture, with a particular focus on cyclic peptides, including cyclotides.

David Craik is a Professor of Chemistry at IMB, UQ. He obtained his PhD in organic chemistry from La Trobe University in Australia and undertook postdoctoral studies at Florida State and Syracuse Universities, USA, before taking up a lectureship at the Victorian College of Pharmacy in 1983. He moved to UQ in 1995 to set up a biomolecular NMR laboratory and is currently an Australian Research Council Laureate Fellow. His research focuses on applications of cyclic peptides, toxins and NMR in drug design. He is a Fellow of the Australian Academy of Science and has received numerous awards for his research, including the Hirschmann Award from the American Chemical Society.

ACKNOWLEDGEMENTS

Work in our laboratory on cyclotides is funded by grants from the Australian Research Council (ARC; DP150100443) and the National Health and Medical Research Council (NHMRC; GNT1084965 and GNT1164412). DJC is an ARC Australian Laureate Fellow (FL150100146) and SJD is a NHMRC Early Career Fellow (GNT1120066).

REFERENCES

(1) Gran, L. An oxytocic principle found in *Oldenlandia affinis* DC. *Medd. Nor. Farm. Selsk.* **1970**, *12*, 173–180.

(2) Gran, L. Oxytocic principles of *Oldenlandia affinis*. *Lloydia* **1973**, *36*, 174–178.

(3) Gran, L. Isolation of oxytocic peptides from *Oldenlandia affinis* by solvent extraction of tetraphenylborate complexes and chromatography on sephadex LH-20. *Lloydia* **1973**, *36*, 207–208.

(4) Gran, L. On the effect of a polypeptide isolated from "Kalata-Kalata" (*Oldenlandia affinis* DC) on the oestrogen dominated uterus. *Acta Pharmacol. Toxicol.* **1973**, *33*, 400–408.

(5) Sletten, K.; Gran, L. Some molecular properties of kalatapeptide B-1 A uterotonic polypeptide isolated from *Oldenlandia affinis* DC. *Medd. Nor. Farm. Selsk.* **1973**, *7-8*, 69–82.

(6) Schöpke, T.; Hasan Agha, M. I.; Kraft, R.; Otto, A.; Hiller, K. Hämolytisch aktive komponenten aus *Viola tricolor* L. und *Viola arvensis* Murray. *Sci. Pharm.* **1993**, *61*, 145–153.

(7) Gustafson, K. R.; Sowder, R. C.; Henderson, L. E.; Parsons, I. C.; Kashman, Y.; Cardellina, J. H.; McMahon, J. B.; Buckheit, R. W.; Pannell, L. K.; Boyd, M. R. Circulins A and B: Novel HIV-inhibitory macrocyclic peptides from the tropical tree *Chassalia parvifolia*. *J. Am. Chem. Soc.* **1994**, *116*, 9337–9338.

(8) Witherup, K. M.; Bogusky, M. J.; Anderson, P. S.; Ramjit, H.; Ransom, R. W.; Wood, T.; Sardana, M. Cyclopsychotride A, A biologically active, 31-residue cyclic peptide isolated from *Psychotria longipes*. *J. Nat. Prod.* **1994**, *57*, 1619–1625.

(9) Saether, O.; Craik, D. J.; Campbell, I. D.; Sletten, K.; Juul, J.; Norman, D. G. Elucidation of the primary and three-dimensional structure of the uterotonic polypeptide kalata B1. *Biochemistry* **1995**, *34*, 4147–4158.

(10) Derua, R.; Gustafson, K. R.; Pannell, L. K. Analysis of the disulfide linkage pattern in circulin A and B, HIV-inhibitory macrocyclic peptides. *Biochem. Biophys. Res. Commun.* **1996**, *228*, 632–638.

(11) Tam, J. P.; Lu, Y.-A. Synthesis of large cyclic cystine-knot peptide by orthogonal coupling strategy using unprotected peptide precursors. *Tetrahedron Lett.* **1997**, *38*, 5599-5602.

(12) Tam, J. P.; Lu, Y.-A. A biomimetic strategy in the synthesis and fragmentation of cyclic protein. *Protein Sci.* **1998**, *7*, 1583–1592.

(13) Claeson, P.; Göransson, U.; Johansson, S.; Luijendijk, T.; Bohlin, L. Fractionation protocol for the isolation of polypeptides from plant biomass. *J. Nat. Prod.* **1998**, *61*, 77–81.

(14) Craik, D. J.; Daly, N. L.; Bond, T.; Waine, C. Plant cyclotides: A unique family of cyclic and knotted proteins that defines the cyclic cystine knot structural motif. *J. Mol. Biol.* **1999**, *294*, 1327–1336.

(15) Göransson, U.; Luijendijk, T.; Johansson, S.; Bohlin, L.; Claeson, P. Seven novel macrocyclic polypeptides from *Viola arvensis*. *J. Nat. Prod.* **1999**, *62*, 283–286.

(16) Daly, N. L.; Love, S.; Alewood, P. F.; Craik, D. J. Chemical synthesis and folding pathways of large cyclic polypeptides: Studies of the cystine knot polypeptide kalata B1. *Biochemistry* **1999**, *38*, 10606–10614.

(17) Tam, J. P.; Lu, Y. A.; Yang, J. L.; Chiu, K. W. An unusual structural motif of antimicrobial peptides containing end-to-end macrocycle and cystine-knot disulfides. *Proc. Natl. Acad. Sci. U. S. A.* **1999**, *96*, 8913–8918.

(18) Tam, J. P.; Lu, Y.-A.; Yu, Q. Thia zip reaction for synthesis of large cyclic peptides: Mechanisms and applications. *J. Am. Chem. Soc.* **1999**, *121*, 4316–4324.

(19) Daly, N. L.; Koltay, A.; Gustafson, K., R.; Boyd, M. R.; Casas-Finet, J. R.; Craik, D. J. Solution structure by NMR of circulin A: A macrocyclic knotted peptide having anti-HIV activity. *J. Mol. Biol.* **1999**, *285*, 333–345.

(20) Daly, N. L.; Craik, D. J. Acyclic permutants of naturally occurring cyclic proteins. Characterization of cystine knot and β-sheet formation in the macrocyclic polypeptide kalata B1. *J. Biol. Chem.* **2000**, *275*, 19068–19075.

(21) Gran, L.; Sandberg, F.; Sletten, K. *Oldenlandia affinis* (R&S) DC. A plant containing uteroactive peptides used in African traditional medicine. *J. Ethnopharmacol.* **2000**, *70*, 197–203.

(22) Gustafson, K. R.; Walton, L. K.; Sowder, R. C.; Johnson, D. G.; Pannell, L. K.; Cardellina, J. H.; Boyd, M. R. New circulin macrocyclic polypeptides from *Chassalia parvifolia*. *J. Nat. Prod.* **2000**, *63*, 176–178.

(23) Hallock, Y. F.; Sowder, R. C.; Pannell, L. K.; Hughes, C. B.; Johnson, D. G.; Gulakowski, R.; Cardellina, J. H.; Boyd, M. R. Cycloviolins A-D, anti-HIV macrocyclic peptides from *Leonia cymosa*. *J. Org. Chem.* **2000**, *65*, 124–128.

(24) Hernandez, J. F.; Gagnon, J.; Chiche, L.; Nguyen, T. M.; Andrieu, J. P.; Heitz, A.; Trinh Hong, T.; Pham, T. T.; Le Nguyen, D. Squash trypsin inhibitors from *Momordica cochinchinensis* exhibit an atypical macrocyclic structure. *Biochemistry* **2000**, *39*, 5722–5730.
(25) Bokesch, H. R.; Pannell, L. K.; Cochran, P. K.; Sowder, R. C.; McKee, T. C.; Boyd, M. R. A novel anti-HIV macrocyclic peptide from *Palicourea condensata*. *J. Nat. Prod.* **2001**, *64*, 249–250.
(26) Broussalis, A. M.; Göransson, U.; Coussio, J. D.; Ferraro, G.; Martino, V.; Claeson, P. First cyclotide from *Hybanthus* (Violaceae). *Phytochemistry* **2001**, *58*, 47–51.
(27) Felizmenio-Quimio, M. E.; Daly, N. L.; Craik, D. J. Circular proteins in plants: Solution structure of a novel macrocyclic trypsin inhibitor from *Momordica cochinchinensis*. *J. Biol. Chem.* **2001**, *276*, 22875–22882.
(28) Heitz, A.; Hernandez, J. F.; Gagnon, J.; Hong, T. T.; Pham, T. T.; Nguyen, T. M.; Le-Nguyen, D.; Chiche, L. Solution structure of the squash trypsin inhibitor MCoTI-II. A new family for cyclic knottins. *Biochemistry* **2001**, *40*, 7973–7983.
(29) Jennings, C.; West, J.; Waine, C.; Craik, D.; Anderson, M. Biosynthesis and insecticidal properties of plant cyclotides: The cyclic knotted proteins from *Oldenlandia affinis*. *Proc. Natl. Acad. Sci. U. S. A.* **2001**, *98*, 10614–10619.
(30) Craik, D. J. Plant cyclotides: Circular, knotted peptide toxins. *Toxicon* **2001**, *39*, 1809–1813.
(31) Craik, D. J.; Daly, N. L.; Waine, C. The cystine knot motif in toxins and implications for drug design. *Toxicon* **2001**, *39*, 43–60.
(32) Trabi, M.; Craik, D. J. Circular proteins – no end in sight. *Trends Biochem. Sci.* **2002**, *27*, 132–138.
(33) Craik, D. J.; Anderson, M. A.; Barry, D. G.; Clark, R. J.; Daly, N. L.; Jennings, C. V.; Mulvenna, J. Discovery and structures of the cyclotides: Novel macrocyclic peptides from plants. *Lett. Pept. Sci.* **2002**, *8*, 119–128.
(34) Craik, D. J.; Simonsen, S.; Daly, N. L. The cyclotides: Novel macrocyclic peptides as scaffolds in drug design. *Curr. Opin. Drug Discov. Devel.* **2002**, *5*, 251–260.
(35) Lindholm, P.; Göransson, U.; Johansson, S.; Claeson, P.; Gulbo, J.; Larsson, R.; Bohlin, L.; Backlund, A. Cyclotides: A novel type of cytotoxic agents. *Mol. Cancer Ther.* **2002**, *1*, 365–369.
(36) Skjeldal, L.; Gran, L.; Sletten, K.; Volkman, B. F. Refined structure and metal binding site of the kalata B1 peptide. *Arch. Biochem. Biophys.* **2002**, *399*, 142–148.
(37) Craik, D. J.; Barry, D. G.; Clark, R. J.; Daly, N. L.; Sando, L. Structure-function studies of the plant cyclotides: The role of a circular protein backbone. *Toxin Rev.* **2003**, *22*, 555–576.
(38) Daly, N. L.; Clark, R. J.; Craik, D. J. Disulfide folding pathways of cystine knot proteins. Tying the knot within the circular backbone of the cyclotides. *J. Biol. Chem.* **2003**, *278*, 6314–6322.
(39) Daly, N. L.; Clark, R. J.; Göransson, U. Diversity in the disulfide folding pathways of cystine knot peptides. *Lett. Pep. Sci.* **2003**, *10*, 523–531.
(40) Göransson, U.; Craik, D. J. Disulfide mapping of the cyclotide kalata B1. Chemical proof of the cyclic cystine knot motif. *J. Biol. Chem.* **2003**, *278*, 48188–48196.
(41) Rosengren, K. J.; Daly, N. L.; Plan, M. R.; Waine, C.; Craik, D. J. Twists, knots, and rings in proteins. Structural definition of the cyclotide framework. *J. Biol. Chem.* **2003**, *278*, 8606–8616.
(42) Göransson, U.; Broussalis, A. M.; Claeson, P. Expression of *Viola* cyclotides by liquid chromatography-mass spectrometry and tandem mass spectrometry sequencing of intercysteine loops after introduction of charges and cleavage sites by aminoethylation. *Anal. Biochem.* **2003**, *318*, 107–117.
(43) Svangård, E.; Göransson, U.; Smith, D.; Verma, C.; Backlund, A.; Bohlin, L.; Claeson, P. Primary and 3-D modelled structures of two cyclotides from *Viola odorata*. *Phytochemistry* **2003**, *64*, 135–142.
(44) Barry, D. G.; Daly, N. L.; Clark, R. J.; Sando, L.; Craik, D. J. Linearization of a naturally occurring circular protein maintains structure but eliminates hemolytic activity. *Biochemistry* **2003**, *42*, 6688–6695.
(45) Avrutina, O.; Schmoldt, H.-U.; Kolmar, H.; Diederichsen, U. Fmoc-assisted synthesis of a 29-residue cystine-knot trypsin inhibitor containing a guaninyl amino acid at the P1-position. *Eur. J. Org. Chem.* **2004**, *2004*, 4931–4935.
(46) Barry, D. G.; Daly, N. L.; Bokesch, H. R.; Gustafson, K. R.; Craik, D. J. Solution structure of the cyclotide palicourein: Implications for the development of a pharmaceutical framework. *Structure* **2004**, *12*, 85–94.
(47) Colgrave, M. L.; Craik, D. J. Thermal, chemical, and enzymatic stability of the cyclotide kalata B1: The importance of the cyclic cystine knot. *Biochemistry* **2004**, *43*, 5965–5975.
(48) Daly, N. L.; Gustafson, K. R.; Craik, D. J. The role of the cyclic peptide backbone in the anti-HIV activity of the cyclotide kalata B1. *FEBS Lett.* **2004**, *574*, 69–72.

(49) Dutton, J. L.; Renda, R. F.; Waine, C.; Clark, R. J.; Daly, N. L.; Jennings, C. V.; Anderson, M. A.; Craik, D. J. Conserved structural and sequence elements implicated in the processing of gene-encoded circular proteins. *J. Biol. Chem.* **2004**, *279*, 46858–46867.
(50) Göransson, U.; Sjögren, M.; Svangård, E.; Claeson, P.; Bohlin, L. Reversible antifouling effect of the cyclotide cycloviolacin O2 against barnacles. *J. Nat. Prod.* **2004**, *67*, 1287–1290.
(51) Svangård, E.; Göransson, U.; Hocaoglu, Z.; Gullbo, J.; Larsson, R.; Claeson, P.; Bohlin, L. Cytotoxic cyclotides from *Viola tricolor*. *J. Nat. Prod.* **2004**, *67*, 144–147.
(52) Trabi, M.; Craik, D. J. Tissue-specific expression of head-to-tail cyclized miniproteins in Violaceae and structure determination of the root cyclotide *Viola hederacea* root cyclotide1. *Plant Cell* **2004**, *16*, 2204–2216.
(53) Trabi, M.; Svangård, E.; Herrmann, A.; Göransson, U.; Claeson, P.; Craik, D. J.; Bohlin, L. Variations in cyclotide expression in *Viola* species. *J. Nat. Prod.* **2004**, *67*, 806–810.
(54) Simonsen, S. M.; Daly, N. L.; Craik, D. J. Capped acyclic permutants of the circular protein kalata B1. *FEBS Lett.* **2004**, *577*, 399–402.
(55) Nourse, A.; Trabi, M.; Daly, N. L.; Craik, D. J. A comparison of the self-association behavior of the plant cyclotides kalata B1 and kalata B2 via analytical ultracentrifugation. *J. Biol. Chem.* **2004**, *279*, 562–570.
(56) Craik, D. J.; Daly, N. L.; Mulvenna, J.; Plan, M. R.; Trabi, M. Discovery, structure and biological activities of the cyclotides. *Curr. Protein Pept. Sci.* **2004**, *5*, 297–315.
(57) Göransson, U.; Svangård, E.; Claeson, P.; Bohlin, L. Novel strategies for isolation and characterization of cyclotides: The discovery of bioactive macrocyclic plant polypeptides in the Violaceae. *Curr. Protein Pept. Sci.* **2004**, *5*, 317–329.
(58) Gustafson, K. R.; McKee, T. C.; Bokesch, H. R. Anti-HIV cyclotides. *Curr. Protein Pept. Sci.* **2004**, *5*, 331–340.
(59) Chiche, L.; Heitz, A.; Gelly, J. C.; Gracy, J.; Chau, P. T.; Ha, P. T.; Hernandez, J. F.; Le-Nguyen, D. Squash inhibitors: From structural motifs to macrocyclic knottins. *Curr. Protein Pept. Sci.* **2004**, *5*, 341–349.
(60) Craik, D. J.; Daly, N. L. Oxidative folding of the cystine knot motif in cyclotide proteins. *Protein Pept. Lett.* **2005**, *12*, 147–152.
(61) Avrutina, O.; Schmoldt, H. U.; Gabrijelcic-Geiger, D.; Le Nguyen, D.; Sommerhoff, C. P.; Diederichsen, U.; Kolmar, H. Trypsin inhibition by macrocyclic and open-chain variants of the squash inhibitor MCoTI-II. *Biol. Chem.* **2005**, *386*, 1301–1306.
(62) Basse, C. W. Dissecting defense-related and developmental transcriptional responses of maize during *Ustilago maydis* infection and subsequent tumor formation. *Plant Physiol.* **2005**, *138*, 1774–1784.
(63) Chen, B.; Colgrave, M. L.; Daly, N. L.; Rosengren, K. J.; Gustafson, K. R.; Craik, D. J. Isolation and characterization of novel cyclotides from *Viola hederaceae*: Solution structure and anti-HIV activity of vhl-1, a leaf-specific expressed cyclotide. *J. Biol. Chem.* **2005**, *280*, 22395–22405.
(64) Colgrave, M. L.; Jones, A.; Craik, D. J. Peptide quantification by matrix-assisted laser desorption ionisation time-of-flight mass spectrometry: Investigations of the cyclotide kalata B1 in biological fluids. *J. Chromatogr. A* **2005**, *1091*, 187–193.
(65) Jennings, C. V.; Rosengren, K. J.; Daly, N. L.; Plan, M.; Stevens, J.; Scanlon, M. J.; Waine, C.; Norman, D. G.; Anderson, M. A.; Craik, D. J. Isolation, solution structure, and insecticidal activity of kalata B2, a circular protein with a twist: Do möbius strips exist in nature? *Biochemistry* **2005**, *44*, 851–860.
(66) Kamimori, H.; Hall, K.; Craik, D. J.; Aguilar, M. I. Studies on the membrane interactions of the cyclotides kalata B1 and kalata B6 on model membrane systems by surface plasmon resonance. *Anal. Biochem.* **2005**, *337*, 149–153.
(67) Koltay, A.; Daly, N. L.; Gustafson, K. R.; Craik, D. J. Structure of circulin B and implications for antimicrobial activity of the cyclotides. *Int. J. Pept. Res. Therap.* **2005**, *11*, 99–106.
(68) Mulvenna, J. P.; Sando, L.; Craik, D. J. Processing of a 22 kDa precursor protein to produce the circular protein tricyclon A. *Structure* **2005**, *13*, 691–701.
(69) Simonsen, S. M.; Sando, L.; Ireland, D. C.; Colgrave, M. L.; Bharathi, R.; Göransson, U.; Craik, D. J. A continent of plant defense peptide diversity: Cyclotides in Australian *Hybanthus* (Violaceae). *Plant Cell* **2005**, *17*, 3176–3189.
(70) Kimura, R. H.; Tran, A.-T.; Camarero, J. A. Biosynthesis of the cyclotide kalata B1 by using protein splicing. *Angew. Chem. Int. Ed.* **2006**, *118*, 987–990.

(71) Thongyoo, P.; Tate, E. W.; Leatherbarrow, R. J. Total synthesis of the macrocyclic cysteine knot microprotein MCoTI-II. *Chem. Commun.* **2006**, 2848–2850.
(72) Čemažar, M.; Craik, D. J. Factors influencing the stability of cyclotides: Proteins with a circular backbone and cystine knot motif. *Int. J. Pept. Res. Ther.* **2006**, *12*, 253–260.
(73) Craik, D. J. Seamless proteins tie up their loose ends. *Science* **2006**, *311*, 1563–1564.
(74) Craik, D. J.; Čemažar, M.; Daly, N. L. The cyclotides and related macrocyclic peptides as scaffolds in drug design. *Curr. Opin. Drug Discov. Devel.* **2006**, *9*, 251–260.
(75) Craik, D. J.; Čemažar, M.; Wang, C. K.; Daly, N. L. The cyclotide family of circular miniproteins: Nature's combinatorial peptide template. *Biopolymers: Pept. Sci.* **2006**, *84*, 250–266.
(76) Tan, N. H.; Zhou, J. Plant cyclopeptides. *Chem. Rev.* **2006**, *106*, 840–895.
(77) Gunasekera, S.; Daly, N. L.; Anderson, M. A.; Craik, D. J. Chemical synthesis and biosynthesis of the cyclotide family of circular proteins. *IUBMB Life* **2006**, *58*, 515–524.
(78) Werle, M.; Schmitz, T.; Haung, H.-L.; Wentzel, A.; Kolmar, H.; Bernkop-Schnurch, A. The potential of cystine-knot microproteins as novel pharmacophoric scaffolds in organ peptide drug delivery. *J. Drug Target.* **2006**, *14*, 137–146.
(79) Daly, N. L.; Clark, R. J.; Plan, M. R.; Craik, D. J. Kalata B8, a novel antiviral circular protein, exhibits conformational flexibility in the cystine knot motif. *Biochem. J.* **2006**, *393*, 619–626.
(80) Herrmann, A.; Svangård, E.; Claeson, P.; Gullbo, J.; Bohlin, L.; Göransson, U. Key role of glutamic acid for the cytotoxic activity of the cyclotide cycloviolacin O2. *Cell. Mol. Life Sci.* **2006**, *63*, 235–245.
(81) Chen, B.; Colgrave, M. L.; Wang, C.; Craik, D. J. Cycloviolacin H4, a hydrophobic cyclotide from *Viola hederaceae*. *J. Nat. Prod.* **2006**, *69*, 23–28.
(82) Ireland, D. C.; Colgrave, M. L.; Craik, D. J. A novel suite of cyclotides from *Viola odorata*: Sequence variation and the implications for structure, function and stability. *Biochem. J.* **2006**, *400*, 1–12.
(83) Ireland, D. C.; Colgrave, M. L.; Nguyencong, P.; Daly, N. L.; Craik, D. J. Discovery and characterization of a linear cyclotide from *Viola odorata*: Implications for the processing of circular proteins. *J. Mol. Biol.* **2006**, *357*, 1522–1535.
(84) Čemažar, M.; Daly, N. L.; Haggblad, S.; Lo, K. P.; Yulyaningsih, E.; Craik, D. J. Knots in rings: The circular knotted protein *Momordica cochinchinensis* trypsin inhibitor-II folds via a stable two-disulfide intermediate. *J. Biol. Chem.* **2006**, *281*, 8224–8232.
(85) Clark, R. J.; Daly, N. L.; Craik, D. J. Structural plasticity of the cyclic-cystine-knot framework: Implications for biological activity and drug design. *Biochem. J.* **2006**, *394*, 85–93.
(86) Mulvenna, J. P.; Mylne, J. S.; Bharathi, R.; Burton, R. A.; Shirley, N. J.; Fincher, G. B.; Anderson, M. A.; Craik, D. J. Discovery of cyclotide-like protein sequences in graminaceous crop plants: Ancestral precursors of circular proteins? *Plant Cell* **2006**, *18*, 2134–2144.
(87) Mulvenna, J. P.; Wang, C.; Craik, D. J. CyBase: A database of cyclic protein sequence and structure. *Nucleic Acids Res.* **2006**, *34*, D192–D194.
(88) Nair, S. S.; Romanuka, J.; Billeter, M.; Skjeldal, L.; Emmett, M. R.; Nilsson, C. L.; Marshall, A. G. Structural characterization of an unusually stable cyclic peptide, kalata B2 from *Oldenlandia affinis*. *Biochim. Biophys. Acta* **2006**, *1764*, 1568–1576.
(89) Shenkarev, Z. O.; Nadezhdin, K. D.; Sobol, V. A.; Sobol, A. G.; Skjeldal, L.; Arseniev, A. S. Conformation and mode of membrane interaction in cyclotides - Spatial structure of kalata B1 bound to a dodecylphosphocholine micelle. *FEBS J.* **2006**, *273*, 2658–2672.
(90) Seydel, P.; Dörnenburg, H. Establishment of *in vitro* plants, cell and tissue cultures from *Oldenlandia affinis* for the production of cyclic peptides. *Plant Cell Tissue Organ Cult.* **2006**, *85*, 247–255.
(91) Seydel, P.; Gruber, C. W.; Craik, D. J.; Dörnenburg, H. Formation of cyclotides and variations in cyclotide expression in *Oldenlandia affinis* suspension cultures. *Appl. Microbiol. Biotechnol.* **2007**, *77*, 275–284.
(92) Camarero, J. A.; Kimura, R. H.; Woo, Y.-H.; Shekhtman, A.; Cantor, J. Biosynthesis of a fully functional cyclotide inside living bacterial cells. *ChemBioChem* **2007**, *8*, 1363–1366.
(93) Craik, D. J.; Čemažar, M.; Daly, N. L. The chemistry and biology of cyclotides. *Curr. Opin. Drug Discov. Devel.* **2007**, *10*, 176–184.
(94) Craik, D. J.; Clark, R. J.; Daly, N. L. Potential therapeutic applications of the cyclotides and related cystine knot mini-proteins. *Expert Opin. Investig. Drugs* **2007**, *16*, 595–604.
(95) Craik, D. J.; Daly, N. L. NMR as a tool for elucidating the structures of circular and knotted proteins. *Mol. Biosyst.* **2007**, *3*, 257–265.

(96) Pelegrini, P. B.; Quirino, B. F.; Franco, O. L. Plant cyclotides: An unusual class of defense compounds. *Peptides* **2007**, *28*, 1475–1481.
(97) Gruber, C. W.; Čemažar, M.; Anderson, M. A.; Craik, D. J. Insecticidal plant cyclotides and related cystine knot toxins. *Toxicon* **2007**, *49*, 561–575.
(98) Greenwood, K. P.; Daly, N. L.; Brown, D. L.; Stow, J. L.; Craik, D. J. The cyclic cystine knot miniprotein MCoTI-II is internalized into cells by macropinocytosis. *Int. J. Biochem. Cell Biol.* **2007**, *39*, 2252–2264.
(99) Plan, M. R. R.; Göransson, U.; Clark, R. J.; Daly, N. L.; Colgrave, M. L.; Craik, D. J. The cyclotide fingerprint in *Oldenlandia affinis*: Elucidation of chemically modified, linear and novel macrocyclic peptides. *ChemBioChem* **2007**, *8*, 1001–1011.
(100) Svangård, E.; Burman, R.; Gunasekera, S.; Lovborg, H.; Gullbo, J.; Göransson, U. Mechanism of action of cytotoxic cyclotides: Cycloviolacin O2 disrupts lipid membranes. *J. Nat. Prod.* **2007**, *70*, 643–647.
(101) Saska, I.; Gillon, A. D.; Hatsugai, N.; Dietzgen, R. G.; Hara-Nishimura, I.; Anderson, M. A.; Craik, D. J. An asparaginyl endopeptidase mediates *in vivo* protein backbone cyclisation. *J. Biol. Chem.* **2007**, *282*, 29721–29728.
(102) Thongyoo, P.; Jaulent, A. M.; Tate, E. W.; Leatherbarrow, R. J. Immobilized protease-assisted synthesis of engineered cysteine-knot microproteins. *ChemBioChem* **2007**, *8*, 1107–1109.
(103) Gruber, C. W.; Čemažar, M.; Clark, R. J.; Horibe, T.; Renda, R. F.; Anderson, M. A.; Craik, D. J. A novel plant protein-disulfide isomerase involved in the oxidative folding of cystine knot defense proteins. *J. Biol. Chem.* **2007**, *282*, 20435–20446.
(104) Aboye, T. L.; Clark, R. J.; Craik, D. J.; Göransson, U. Ultra stable peptide scaffolds for protein engineering – synthesis and folding of the circular cystine knotted cyclotide cycloviolacin O2. *ChemBioChem* **2008**, *9*, 103–113.
(105) Čemažar, M.; Gruber, C. W.; Craik, D. J. Oxidative folding of cyclic cystine knot proteins. *Antioxid. Redox Signal.* **2008**, *10*, 103–111.
(106) Čemažar, M.; Joshi, A.; Daly, N. L.; Mark, A. E.; Craik, D. J. The structure of a two-disulfide intermediate assists in elucidating the oxidative folding pathway of a cyclic cystine knot protein. *Structure* **2008**, *16*, 842–851.
(107) Čemažar, M.; Craik, D. J. Microwave-assisted Boc-solid phase peptide synthesis of cyclic cysteine-rich peptides. *J. Pept. Sci.* **2008**, *14*, 683–689.
(108) Thongyoo, P.; Roque-Rosell, N.; Leatherbarrow, R. J.; Tate, E. W. Chemical and biomimetic total syntheses of natural and engineered MCoTI cyclotides. *Org. Biomol. Chem.* **2008**, *6*, 1462–1470.
(109) Colgrave, M. L.; Kotze, A. C.; Huang, Y. H.; O'Grady, J.; Simonsen, S. M.; Craik, D. J. Cyclotides: Natural, circular plant peptides that possess significant activity against gastrointestinal nematode parasites of sheep. *Biochemistry* **2008**, *47*, 5581–5589.
(110) Colgrave, M. L.; Kotze, A. C.; Ireland, D. C.; Wang, C. K.; Craik, D. J. The anthelmintic activity of the cyclotides: Natural variants with enhanced activity. *ChemBioChem* **2008**, *9*, 1939–1945.
(111) Barbeta, B. L.; Marshall, A. T.; Gillon, A. D.; Craik, D. J.; Anderson, M. A. Plant cyclotides disrupt epithelial cells in the midgut of lepidopteran larvae. *Proc. Natl. Acad. Sci. U. S. A.* **2008**, *105*, 1221–1225.
(112) Plan, M. R. R.; Saska, I.; Cagauan, A. G.; Craik, D. J. Backbone cyclised peptides from plants show molluscicidal activity against the rice pest *Pomacea canaliculata* (golden apple snail). *J. Agric. Food Chem.* **2008**, *56*, 5237–5241.
(113) Dörnenburg, H. Plant cell culture technology – harnessing a biological approach for competitive cyclotides production. *Biotechnol. Lett.* **2008**, *30*, 1311–1321.
(114) Avrutina, O.; Schmoldt, H. U.; Gabrijelcic-Geiger, D.; Wentzel, A.; Frauendorf, H.; Sommerhoff, C. P.; Diederichsen, U.; Kolmar, H. Head-to-tail cyclized cystine-knot peptides by a combined recombinant and chemical route of synthesis. *ChemBioChem* **2008**, *9*, 33–37.
(115) Gillon, A. D.; Saska, I.; Jennings, C. V.; Guarino, R. F.; Craik, D. J.; Anderson, M. A. Biosynthesis of circular proteins in plants. *Plant J.* **2008**, *53*, 505–515.
(116) Gruber, C. W.; Elliott, A. G.; Ireland, D. C.; Delprete, P. G.; Dessein, S.; Göransson, U.; Trabi, M.; Wang, C. K.; Kinghorn, A. B.; Robbrecht, E.; et al. Distribution and evolution of circular miniproteins in flowering plants. *Plant Cell* **2008**, *20*, 2471–2483.
(117) Gunasekera, S.; Foley, F. M.; Clark, R. J.; Sando, L.; Fabri, L. J.; Craik, D. J.; Daly, N. L. Engineering stabilized vascular endothelial growth factor-A antagonists: Synthesis, structural characterization, and bioactivity of grafted analogues of cyclotides. *J. Med. Chem.* **2008**, *51*, 7697–7704.

(118) Combelles, C.; Gracy, J.; Heitz, A.; Craik, D. J.; Chiche, L. Structure and folding of disulfide-rich miniproteins: Insights from molecular dynamics simulations and MM-PBSA free energy calculations. *Proteins* **2008**, *73*, 87–103.
(119) Heitz, A.; Avrutina, O.; Le-Nguyen, D.; Diederichsen, U.; Hernandez, J. F.; Gracy, J.; Kolmar, H.; Chiche, L. Knottin cyclization: Impact on structure and dynamics. *BMC Struct. Biol.* **2008**, *8*, 54.
(120) Herrmann, A.; Burman, R.; Mylne, J. S.; Karlsson, G.; Gullbo, J.; Craik, D. J.; Clark, R. J.; Göransson, U. The alpine violet, *Viola biflora*, is a rich source of cyclotides with potent cytotoxicity. *Phytochemistry* **2008**, *69*, 939–952.
(121) Mylne, J. S.; Craik, D. J. ^{15}N cyclotides by whole plant labeling. *Biopolymers: Pept. Sci.* **2008**, *90*, 575–580.
(122) Saska, I.; Colgrave, M. L.; Jones, A.; Anderson, M. A.; Craik, D. J. Quantitative analysis of backbone-cyclised peptides in plants. *J. Chromatogr. B Analyt. Technol. Biomed. Life Sci.* **2008**, *872*, 107–114.
(123) Xu, W. Y.; Tang, J.; Ji, C. J.; He, W. J.; Tan, N. H. Application of TLC chemical method to detection of cyclotides in plants. *Chinese Sci. Bull.* **2008**, *53*, 1671–1674.
(124) Shenkarev, Z. O.; Nadezhdin, K. D.; Lyukmanova, E. N.; Sobol, V. A.; Skjeldal, L.; Arseniev, A. S. Divalent cation coordination and mode of membrane interaction in cyclotides: NMR spatial structure of ternary complex Kalata B7/Mn^{2+}/DPC micelle. *J. Inorg. Biochem.* **2008**, *102*, 1246–1256.
(125) Simonsen, S. M.; Sando, L.; Rosengren, K. J.; Wang, C. K.; Colgrave, M. L.; Daly, N. L.; Craik, D. J. Alanine scanning mutagenesis of the prototypic cyclotide reveals a cluster of residues essential for bioactivity. *J. Biol. Chem.* **2008**, *283*, 9805–9813.
(126) Wang, C. K.; Colgrave, M. L.; Gustafson, K. R.; Ireland, D. C.; Göransson, U.; Craik, D. J. Anti-HIV cyclotides from the Chinese medicinal herb *Viola yedoensis*. *J. Nat. Prod.* **2008**, *71*, 47–52.
(127) Wang, C. K.; Kaas, Q.; Chiche, L.; Craik, D. J. CyBase: A database of cyclic protein sequences and structures, with applications in protein discovery and engineering. *Nucleic Acids Res.* **2008**, *36*, D206–D210.
(128) Tokuoka, T. Molecular phylogenetic analysis of Violaceae (Malpighiales) based on plastid and nuclear DNA sequences. *J. Plant Res.* **2008**, *121*, 253–260.
(129) Gran, L.; Sletten, K.; Skjeldal, L. Cyclic peptides from *Oldenlandia affinis* DC. Molecular and biological properties. *Chem. Biodivers.* **2008**, *5*, 2014–2022.
(130) Ireland, D. C.; Wang, C. K.; Wilson, J. A.; Gustafson, K. R.; Craik, D. J. Cyclotides as natural anti-HIV agents. *Biopolymers: Pept. Sci.* **2008**, *90*, 51–60.
(131) Kolmar, H. Alternative binding proteins: Biological activity and therapeutic potential of cystine-knot miniproteins. *FEBS J.* **2008**, *275*, 2684–2690.
(132) Craik, D. J. Circling the enemy: Cyclic proteins in plant defence. *Trends Plant Sci.* **2009**, *14*, 328–335.
(133) Daly, N. L.; Craik, D. J.: Folding motifs of cystine-rich peptides. In *Oxidative Folding of Proteins and Peptides*; Buchner, J., Moroder, L., Ed.; RSC Publishing: London, 2009; pp 318–344.
(134) Daly, N. L.; Craik, D. J. Design and therapeutic applications of cyclotides. *Future Med. Chem.* **2009**, *1*, 1613–1622.
(135) Daly, N. L.; Rosengren, K. J.; Craik, D. J. Discovery, structure and biological activities of cyclotides. *Adv. Drug Deliv. Rev.* **2009**, *61*, 918–930.
(136) Wang, C. K.; Huang, Y.-H.; Greenwood, K.; Craik, D. J.: Membrane binding of cyclotides. In *Membrane Active Peptides: Methods and Results on Structure and Function*; Castanho, M., Ed.; IUL Publishers: La Jolla, USA, 2009; Chapter 22; pp 597–672.
(137) Austin, J.; Wang, W.; Puttamadappa, S.; Shekhtman, A.; Camarero, J. A. Biosynthesis and biological screening of a genetically encoded library based on the cyclotide MCoTI-I. *ChemBioChem* **2009**, *10*, 2663–2670.
(138) Chan, L. Y.; Wang, C. K.; Major, J. M.; Greenwood, K. P.; Lewis, R. J.; Craik, D. J.; Daly, N. L. Isolation and characterization of peptides from *Momordica cochinchinensis* seeds. *J. Nat. Prod.* **2009**, *72*, 1453–1458.
(139) Trabi, M.; Mylne, J. S.; Sando, L.; Craik, D. J. Circular proteins from Melicytus (Violaceae) refine the conserved protein and gene architecture of cyclotides. *Org. Biomol. Chem.* **2009**, *7*, 2378–2388.
(140) Colgrave, M. L.; Kotze, A. C.; Kopp, S.; McCarthy, J. S.; Coleman, G. T.; Craik, D. J. Anthelmintic activity of cyclotides: *In vitro* studies with canine and human hookworms. *Acta Trop.* **2009**, *109*, 163–166.

(141) Dumont, E. l.; Laurent, A. l. D.; Loos, P.-F.; Assfeld, X. Analyzing the selectivity and successiveness of a two-electron capture on a multiply disulfide-linked protein. *J. Chem. Theory Comput.* **2009**, *5*, 1700–1708.
(142) Sze, S. K.; Wang, W.; Meng, W.; Yuan, R.; Guo, T.; Zhu, Y.; Tam, J. P. Elucidating the structure of cyclotides by partial acid hydrolysis and LC-MS/MS analysis. *Anal. Chem.* **2009**, *81*, 1079–1088.
(143) Gruber, C. W.; Čemažar, M.; Mechler, A.; Martin, L. L.; Craik, D. J. Biochemical and biophysical characterization of a novel plant protein disulfide isomerase. *Biopolymers: Pept. Sci.* **2009**, *92*, 35–43.
(144) Gunasekera, S.; Daly, N.; Clark, R.; Craik, D. J. Dissecting the oxidative folding of circular cystine knot miniproteins: Development of hybrid cyclotide scaffolds for protein engineering. *Antioxid. Redox Signal.* **2009**, *11*, 971–980.
(145) Thongyoo, P.; Bonomelli, C.; Leatherbarrow, R. J.; Tate, E. W. Potent inhibitors of β-tryptase and human leukocyte elastase based on the MCoTI-II scaffold. *J. Med. Chem.* **2009**, *52*, 6197–6200.
(146) Göransson, U.; Herrmann, A.; Burman, R.; Haugaard-Jönsson, L. M.; Rosengren, K. J. The conserved Glu in the cyclotide cycloviolacin O2 has a key structural role. *ChemBioChem* **2009**, *10*, 2354–2360.
(147) Wang, C. K.; Colgrave, M. L.; Ireland, D. C.; Kaas, Q.; Craik, D. J. Despite a conserved cystine knot motif, different cyclotides have different membrane binding modes. *Biophys. J.* **2009**, *97*, 1471–1481.
(148) Huang, Y.-H.; Colgrave, M. L.; Daly, N. L.; Keleshian, A.; Martinac, B.; Craik, D. J. The biological activity of the prototypic cyclotide kalata B1 is modulated by the formation of multimeric pores. *J. Biol. Chem.* **2009**, *284*, 20699–20707.
(149) Wang, C. K.; Hu, S. H.; Martin, J. L.; Sjogren, T.; Hajdu, J.; Bohlin, L.; Claeson, P.; Göransson, U.; Rosengren, K. J.; Tang, J.; et al. Combined X-ray and NMR analysis of the stability of the cyclotide cystine knot fold that underpins its insecticidal activity and potential use as a drug scaffold. *J. Biol. Chem.* **2009**, *284*, 10672–10683.
(150) Zhang, J.; Hu, M.; Li, J. T.; Guan, J. P.; Yang, B.; Shu, W. S.; Liao, B. A transcriptional profile of metallophyte *Viola baoshanensis* involved in general and species-specific cadmium-defense mechanisms. *J. Plant Physiol.* **2009**, *166*, 862–870.
(151) Zhang, J.; Liao, B.; Craik, D. J.; Li, J. T.; Hu, M.; Shu, W. S. Identification of two suites of cyclotide precursor genes from metallophyte *Viola baoshanensis*: cDNA sequence variation, alternative RNA splicing and potential cyclotide diversity. *Gene* **2009**, *431*, 23–32.
(152) Dörnenburg, H. Progress in kalata peptide production via plant cell bioprocessing. *Biotechnol. J.* **2009**, *4*, 632–645.
(153) Dörnenburg, H. Cyclotide synthesis and supply: From plant to bioprocess. *Biopolymers: Pept. Sci.* **2010**, *94*, 602–610.
(154) Broussalis, A. M.; Clemente, S.; Ferraro, G. E. *Hybanthus parviflorus* (Violaceae): Insecticidal activity of a South American plant. *Crop Prot.* **2010**, *29*, 953–956.
(155) Burman, R.; Gruber, C. W.; Rizzardi, K.; Herrmann, A.; Craik, D. J.; Gupta, M. P.; Göransson, U. Cyclotide proteins and precursors from the genus *Gloeospermum*: Filling a blank spot in the cyclotide map of Violaceae. *Phytochemistry* **2010**, *71*, 13–20.
(156) Burman, R.; Svedlund, E.; Felth, J.; Hassan, S.; Herrmann, A.; Clark, R. J.; Craik, D. J.; Bohlin, L.; Claeson, P.; Göransson, U.; et al. Evaluation of toxicity and anti-tumour activity of cycloviolacin O2 in mice. *Biopolymers: Pept. Sci.* **2010**, *94*, 626–634.
(157) Gerlach, S. L.; Burman, R.; Bohlin, L.; Mondal, D.; Göransson, U. Isolation, characterization, and bioactivity of cyclotides from the Micronesian plant *Psychotria leptothyrsa*. *J. Nat. Prod.* **2010**, *73*, 1207–1213.
(158) Gerlach, S. L.; Rathinakumar, R.; Chakravarty, G.; Göransson, U.; Wimley, W. C.; Darwin, S. P.; Mondal, D. Anticancer and chemosensitizing abilities of cycloviolacin O2 from *Viola odorata* and psyle cyclotides from *Psychotria leptothyrsa*. *Biopolymers: Pept. Sci.* **2010**, *94*, 617–625.
(159) Gruber, C. W. Global cyclotide adventure: A journey dedicated to the discovery of circular peptides from flowering plants. *Biopolymers: Pept. Sci.* **2010**, *94*, 565–572.
(160) Colgrave, M. L.; Poth, A. G.; Kaas, Q.; Craik, D. J. A new 'era' for cyclotide sequencing. *Biopolymers: Pept. Sci.* **2010**, *94*, 592–601.
(161) Cascales, L.; Craik, D. J. Naturally occurring circular proteins: Distribution, biosynthesis and evolution. *Org. Biomol. Chem.* **2010**, *8*, 5035–5047.
(162) Clark, R. J.; Craik, D. J. Native chemical ligation applied to the synthesis and bioengineering of circular peptides and proteins. *Biopolymers: Pept. Sci.* **2010**, *94*, 414–422.

(163) Conlan, B. F.; Gillon, A. D.; Craik, D. J.; Anderson, M. A. Circular proteins and mechanisms of cyclization. *Biopolymers: Pept. Sci.* **2010**, *94*, 573–583.
(164) Henriques, S. T.; Craik, D. J. Cyclotides as templates in drug design. *Drug Discov. Today* **2010**, *15*, 57–64.
(165) Craik, D. J.; Mylne, J. S.; Daly, N. L. Cyclotides: Macrocyclic peptides with applications in drug design and agriculture. *Cell. Mol. Life Sci.* **2010**, *67*, 9–16.
(166) Garcia, A. E.; Camarero, J. A. Biological activities of natural and engineered cyclotides, a novel molecular scaffold for peptide-based therapeutics. *Curr. Mol. Pharmacol.* **2010**, *3*, 153–163.
(167) Jagadish, K.; Camarero, J. A. Cyclotides, a promising molecular scaffold for peptide-based therapeutics. *Biopolymers: Pept. Sci.* **2010**, *94*, 611–616.
(168) Ireland, D. C.; Clark, R. J.; Daly, N. L.; Craik, D. J. Isolation, sequencing, and structure-activity relationships of cyclotides. *J. Nat. Prod.* **2010**, *73*, 1610–1622.
(169) Colgrave, M. L.; Huang, Y. H.; Craik, D. J.; Kotze, A. C. Cyclotide interactions with the nematode external surface. *Antimicrob. Agents Chemother.* **2010**, *54*, 2160–2166.
(170) Huang, Y. H.; Colgrave, M. L.; Clark, R. J.; Kotze, A. C.; Craik, D. J. Lysine-scanning mutagenesis reveals a previously unidentified amendable face of the cyclotide kalata B1 for the optimisation of nematocidal activity. *J. Biol. Chem.* **2010**, *285*, 10797–10805.
(171) Kaas, Q.; Craik, D. J. Analysis and classification of circular proteins in CyBase. *Biopolymers: Pept. Sci.* **2010**, *94*, 584–591.
(172) Mylne, J. S.; Wang, C. K.; van der Weerden, N. L.; Craik, D. J. Cyclotides are a component of the innate defence of *Oldenlandia affinis*. *Biopolymers: Pept. Sci.* **2010**, *94*, 635–646.
(173) Qin, Q.; McCallum, E. J.; Kaas, Q.; Suda, J.; Saska, I.; Craik, D. J.; Mylne, J. S. Identification of candidates for cyclotide biosynthesis and cyclisation by expressed sequence tag analysis of *Oldenlandia affinis*. *BMC Genomics* **2010**, *11*, 111.
(174) Park, S.; Gunasekera, S.; Aboye, T. L.; Göransson, U. An efficient approach for the total synthesis of cyclotides by microwave assisted Fmoc-SPPS. *Int. J. Pept. Res. Ther.* **2010**, *16*, 167–176.
(175) Daly, N. L.; Chen, B.; Nguyencong, P.; Craik, D. J. Structure and activity of the leaf-specific cyclotide vhl-2. *Aust. J. Chem.* **2010**, *63*, 771–778.
(176) Gao, Y.; Cui, T.; Lam, Y. Synthesis and disulfide bond connectivity-activity studies of a kalata B1-inspired cyclopeptide against dengue NS2B-NS3 protease. *Bioorg. Med. Chem.* **2010**, *18*, 1331–1336.
(177) Plan, M. R.; Rosengren, K. J.; Sando, L.; Daly, N. L.; Craik, D. J. Structural and biochemical characteristics of the cyclotide kalata B5 from *Oldenlandia affinis*. *Biopolymers: Pept. Sci.* **2010**, *94*, 647–658.
(178) Pränting, M.; Lööv, C.; Burman, R.; Göransson, U.; Andersson, D. I. The cyclotide cycloviolacin O2 from *Viola odorata* has potent bactericidal activity against Gram-negative bacteria. *J. Antimicrob. Chemother.* **2010**, *65*, 1964–1971.
(179) Sommerhoff, C. P.; Avrutina, O.; Schmoldt, H. U.; Gabrijelcic-Geiger, D.; Diederichsen, U.; Kolmar, H. Engineered cystine knot miniproteins as potent inhibitors of human mast cell tryptase β. *J. Mol. Biol.* **2010**, *395*, 167–175.
(180) Tang, J.; Wang, C. K.; Pan, X.; Yan, H.; Zeng, G.; Xu, W.; He, W.; Daly, N. L.; Craik, D. J.; Tan, N. Isolation and characterization of cytotoxic cyclotides from *Viola tricolor*. *Peptides* **2010**, *31*, 1434–1440.
(181) Tang, J.; Wang, C. K.; Pan, X.; Yan, H.; Zeng, G.; Xu, W.; He, W.; L., D. N.; Craik, D. J.; Tan, N. Isolation and characterization of bioactive cyclotides from *Viola labridorica*. *Helv. Chim. Acta* **2010**, *93*, 2287–2295.
(182) Xiang, B.; Du, G. H.; Wang, X. C.; Zhang, S. X.; Qin, X. Y.; Kong, J. Q.; Cheng, K. D.; Li, Y. J.; Wang, W. Elucidating the structure of two cyclotides of *Viola tianshanica* maxim by MALDI TOF/TOF MS analysis. *Acta Pharm. Sin.* **2010**, *45*, 1402–1409.
(183) Puttamadappa, S. S.; Jagadish, K.; Shekhtman, A.; Camarero, J. A. Backbone dynamics of cyclotide MCoTI-I free and complexed with trypsin. *Angew. Chem. Int. Ed.* **2010**, *49*, 7030–7034.
(184) Henriques, S. T.; Huang, Y. H.; Rosengren, K. J.; Franquelim, H. G.; Carvalho, F. A.; Johnson, A.; Sonza, S.; Tachedjian, G.; Castanho, M. A. R. B.; Daly, N. L.; et al. Decoding the membrane activity of the cyclotide kalata B1: The importance of phosphatidylethanolamine phospholipids and lipid organization on hemolytic and anti-HIV activities. *J. Biol. Chem.* **2011**, *286*, 24231–24241.
(185) Burman, R.; Strömstedt, A. A.; Malmsten, M.; Göransson, U. Cyclotide-membrane interactions: Defining factors of membrane binding, depletion and disruption. *Biochim. Biophys. Acta, Biomembr.* **2011**, *1808*, 2665–2673.

(186) Burman, R.; Herrmann, A.; Tran, R.; Kivela, J. E.; Lomize, A.; Gullbo, J.; Göransson, U. Cytotoxic potency of small macrocyclic knot proteins: Structure-activity and mechanistic studies of native and chemically modified cyclotides. *Org. Biomol. Chem.* **2011**, *9*, 4306–4314.
(187) Cascales, L.; Henriques, S. T.; Kerr, M. C.; Huang, Y. H.; Sweet, M. J.; Daly, N. L.; Craik, D. J. Identification and characterization of a new family of cell-penetrating peptides. Cyclic cell-penetrating peptides. *J. Biol. Chem.* **2011**, *286*, 36932–36943.
(188) Chan, L. Y.; Gunasekera, S.; Henriques, S. T.; Worth, N. F.; Le, S. J.; Clark, R. J.; Campbell, J. H.; Craik, D. J.; Daly, N. L. Engineering pro-angiogenic peptides using stable disulfide-rich cyclic scaffolds. *Blood* **2011**, *118*, 6709–6717.
(189) Conlan, B. F.; Gillon, A. D.; Barbeta, B. L.; Anderson, M. A. Subcellular targeting and biosynthesis of cyclotides in plant cells. *Am. J. Bot.* **2011**, *98*, 2018–2026.
(190) Contreras, J.; Elnagar, A. Y. O.; Hamm-Alvarez, S. F.; Camarero, J. A. Cellular uptake of cyclotide MCoTI-I follows multiple endocytic pathways. *J. Control. Release* **2011**, *155*, 134–143.
(191) Conlan, B. F.; Anderson, M. A. Circular micro-proteins and mechanisms of cyclization. *Curr. Pharm. Des.* **2011**, *17*, 4318–4328.
(192) Craik, D. J.; Conibear, A. C. The chemistry of cyclotides. *J. Org. Chem.* **2011**, *76*, 4805–4817.
(193) Daly, N. L.; Craik, D. J. Bioactive cystine knot proteins. *Curr. Opin. Chem. Biol.* **2011**, *15*, 362–368.
(194) Daly, N. L.; Gruber, C. W.; Göransson, U.; Craik, D. J.: Cystine knot folding in cyclotides. In *Protein Rev*; Ventura, S. and Chang, R. W., Eds.; Springer: New York, USA, 2011; Chapter 3; pp 43–61.
(195) Daly, N. L.; Rosengren, K. J.; Henriques, S. T.; Craik, D. J. NMR and protein structure in drug design: Application to cyclotides and conotoxins. *Eur. Biophys. J.* **2011**, *40*, 359–370.
(196) Gracy, J.; Chiche, L. Structure and modeling of knottins, a promising molecular scaffold for drug discovery. *Curr. Pharm. Des.* **2011**, *17*, 4337–4350.
(197) Gruber, C. W.; O'Brien, M. Uterotonic plants and their bioactive constituents. *Planta Med.* **2011**, *77*, 207–220.
(198) Katoh, T.; Goto, Y.; Reza, M. S.; Suga, H. Ribosomal synthesis of backbone macrocyclic peptides. *Chem. Commun.* **2011**, *47*, 9946–9958.
(199) Smith, A. B.; Daly, N. L.; Craik, D. J. Cyclotides: A patent review. *Expert Opin. Ther. Pat.* **2011**, *21*, 1657–1672.
(200) Getz, J. A.; Rice, J. J.; Daugherty, P. S. Protease-resistant peptide ligands from a knottin scaffold library. *ACS Chem. Biol.* **2011**, *6*, 837–844.
(201) Ghassempour, A.; Ghahramanzamaneh, M.; Hashempour, H.; Kargosha, K. Multidimensional liquid chromatography for separation of cyclotides in *Viola ignobilis*. *Acta Chromatogr.* **2011**, *23*, 641–651.
(202) Hashempour, H.; Ghassempour, A.; Daly, N. L.; Spengler, B.; Rompp, A. Analysis of cyclotides in *Viola ignobilis* by nano liquid chromatography fourier transform mass spectrometry. *Protein Pept. Lett.* **2011**, *18*, 747–752.
(203) He, W.; Chan, L. Y.; Zeng, G.; Daly, N. L.; Craik, D. J.; Tan, N. Isolation and characterization of cytotoxic cyclotides from *Viola philippica*. *Peptides* **2011**, *32*, 1719–1723.
(204) Poth, A. G.; Colgrave, M. L.; Philip, R.; Kerenga, B.; Daly, N. L.; Anderson, M. A.; Craik, D. J. Discovery of cyclotides in the Fabaceae plant family provides new insights into the cyclization, evolution, and distribution of circular proteins. *ACS Chem. Biol.* **2011**, *6*, 345–355.
(205) Poth, A. G.; Colgrave, M. L.; Lyons, R. E.; Daly, N. L.; Craik, D. J. Discovery of an unusual biosynthetic origin for circular proteins in legumes. *Proc. Natl. Acad. Sci. U. S. A.* **2011**, *108*, 10127–10132.
(206) Nguyen, G. K. T.; Zhang, S.; Ngan, T. K. N.; Phuong, Q. T. N.; Chiu, M. S.; Hardjojo, A.; Tam, J. P. Discovery and characterization of novel cyclotides originated from chimeric precursors consisting of albumin-1 chain a and cyclotide domains in the Fabaceae family. *J. Biol. Chem.* **2011**, *286*, 24275–24287.
(207) Nguyen, G. K. T.; Zhang, S.; Wang, W.; Wong, C. T. T.; Ngan, T. K. N.; Tam, J. P. Discovery of a linear cyclotide from the bracelet subfamily and its disulfide mapping by top-down mass spectrometry. *J. Biol. Chem.* **2011**, *286*, 44833–44844.
(208) Ovesen, R. G.; Brandt, K. K.; Göransson, U.; Nielsen, J.; Hansen, H. C.; Cedergreen, N. Biomedicine in the environment: Cyclotides constitute potent natural toxins in plants and soil bacteria. *Environ. Toxicol. Chem.* **2011**, *30*, 1190–1196.

(209) Ovesen, R. G.; Nielsen, J.; Bruun Hansen, H. C. Biomedicine in the environment: Sorption of the cyclotide kalata B2 to montmorillonite, goethite, and humic acid. *Environ. Toxicol. Chem.* **2011**, *30*, 1785–1792.
(210) Ovesen, R. G.; Göransson, U.; Hansen, S. H.; Nielsen, J.; Hansen, H. C. B. A liquid chromatography-electrospray ionization-mass spectrometry method for quantification of cyclotides in plants avoiding sorption during sample preparation. *J. Chromatogr. A* **2011**, *1218*, 7964–7970.
(211) Sando, L.; Henriques, S. T.; Foley, F.; Simonsen, S. M.; Daly, N. L.; Hall, K. N.; Gustafson, K. R.; Aguilar, M. I.; Craik, D. J. A synthetic mirror image of kalata B1 reveals that cyclotide activity is independent of a protein receptor. *ChemBioChem* **2011**, *12*, 2456–2462.
(212) Wang, C. K.; Clark, R. J.; Harvey, P. J.; Rosengren, K. J.; Čemažar, M.; Craik, D. J. The role of conserved Glu residue on cyclotide stability and activity: A structural and functional study of kalata B12, a naturally occurring Glu to Asp mutant. *Biochemistry* **2011**, *50*, 4077–4086.
(213) Wong, C. T.; Taichi, M.; Nishio, H.; Nishiuchi, Y.; Tam, J. P. Optimal oxidative folding of the novel antimicrobial cyclotide from *Hedyotis biflora* requires high alcohol concentrations. *Biochemistry* **2011**, *50*, 7275–7283.
(214) Aboye, T. L.; Clark, R. J.; Burman, R.; Roig, M. B.; Craik, D. J.; Göransson, U. Interlocking disulfides in circular proteins: Toward efficient oxidative folding of cyclotides. *Antioxid. Redox Signal.* **2011**, *14*, 77–86.
(215) Yeshak, M. Y.; Burman, R.; Asres, K.; Göransson, U. Cyclotides from an extreme habitat: Characterization of cyclic peptides from *Viola abyssinica* of the Ethiopian highlands. *J. Nat. Prod.* **2011**, *74*, 727–731.
(216) Gründemann, C.; Koehbach, J.; Huber, R.; Gruber, C. W. Do plant cyclotides have potential as immunosuppressant peptides? *J. Nat. Prod.* **2012**, *75*, 167–174.
(217) Aboye, T. L.; Ha, H.; Majumder, S.; Christ, F.; Debyser, Z.; Shekhtman, A.; Neamati, N.; Camarero, J. A. Design of a novel cyclotide-based CXCR4 antagonist with anti-human immunodeficiency virus (HIV)-1 activity. *J. Med. Chem.* **2012**, *55*, 10729–10734.
(218) Eliasen, R.; Daly, N. L.; Wulff, B. S.; Andresen, T. L.; Conde-Frieboes, K. W.; Craik, D. J. Design, synthesis, structural and functional characterization of novel melanocortin agonists based on the cyclotide kalata B1. *J. Biol. Chem.* **2012**, *287*, 40493–40501.
(219) Conibear, A. C.; Daly, N. L.; Craik, D. J. Quantification of small cyclic disulfide-rich peptides. *Biopolymers: Pept. Sci.* **2012**, *98*, 518–524.
(220) Čemažar, M.; Kwon, S.; Mahatmanto, T.; Ravipati, A. S.; Craik, D. J. Discovery and applications of disulfide-rich cyclic peptides. *Curr. Top. Med. Chem.* **2012**, *12*, 1534–1545.
(221) Conlan, B. F.; Colgrave, M. L.; Gillon, A. D.; Guarino, R.; Craik, D. J.; Anderson, M. A. Insights into processing and cyclization events associated with biosynthesis of the cyclic peptide kalata B1. *J. Biol. Chem.* **2012**, *287*, 28037–28046.
(222) Aboye, T. L.; Camarero, J. A. Biological synthesis of circular polypeptides. *J. Biol. Chem.* **2012**, *287*, 27026–27032.
(223) Craik, D. J. Host-defense activities of cyclotides. *Toxins* **2012**, *4*, 139–156.
(224) Craik, D. J.; Henriques, S. T.; Mylne, J. S.; Wang, C. K.: Cyclotide isolation and characterization. In *Methods in Enzymology - Natural Product Biosynthesis by Microorganisms and Plants, Part B*; Hopwood, D. A., Ed.; Academic Press, 2012; Vol. 516; Chapter 3; pp 37–62.
(225) Craik, D. J.; Swedberg, J. E.; Mylne, J. S.; Čemažar, M. Cyclotides as a basis for drug design. *Expert Opin. Drug Discov.* **2012**, *7*, 179–194.
(226) Gerlach, S. L.; Mondal, D. The bountiful biological activities of cyclotides. *Chron. Young Sci.* **2012**, *3*, 169–177.
(227) Göransson, U.; Burman, R.; Gunasekera, S.; Strömstedt, A. A.; Rosengren, K. J. Circular proteins from plants and fungi. *J. Biol. Chem.* **2012**, *287*, 27001–27006.
(228) Pinto, M. F. S.; Fensterseifer, I. C. M.; Franco, O. L.: Plant cyclotides: An unusual protein family with multiple functions. In *Prog Biol Control*; Mérillon, J. M. and Ramawat, K. G., Eds.; Springer Netherlands, 2012; Vol. 12; Chapter 14; pp 333–344.
(229) Reinwarth, M.; Nasu, D.; Kolmar, H.; Avrutina, O. Chemical synthesis, backbone cyclization and oxidative folding of cystine-knot peptides - Promising scaffolds for applications in drug design. *Molecules* **2012**, *17*, 12533–12552.
(230) Henriques, S. T.; Craik, D. J. Importance of the cell membrane on the mechanism of action of cyclotides. *ACS Chem. Biol.* **2012**, *7*, 626–636.

(231) Hall, K.; Lee, T. H.; Daly, N. L.; Craik, D. J.; Aguilar, M. I. Gly_6 of kalata B1 is critical for the selective binding to phosphatidylethanolamine membranes. *Biochim. Biophys. Acta, Biomembr.* **2012**, *1818*, 2354–2361.
(232) Henriques, S. T.; Huang, Y. H.; Castanho, M. A. R. B.; Bagatolli, L. A.; Sonza, S.; Tachedjian, G.; Daly, N. L.; Craik, D. J. Phosphatidylethanolamine binding is a conserved feature of cyclotide-membrane interactions. *J. Biol. Chem.* **2012**, *287*, 33629–33643.
(233) Wang, C. K.; Wacklin, H. P.; Craik, D. J. Cyclotides insert into lipid bilayers to form membrane pores and destabilize the membrane through hydrophobic and phosphoethanolamine-specific interactions. *J. Biol. Chem.* **2012**, *287*, 43884–43898.
(234) Mylne, J. S.; Chan, L. Y.; Chanson, A. H.; Daly, N. L.; Schaefer, H.; Bailey, T. L.; Nguyencong, P.; Cascales, L.; Craik, D. J. Cyclic peptides arising by evolutionary parallelism via asparaginyl-endopeptidase–mediated biosynthesis. *Plant Cell* **2012**, *24*, 2765–2778.
(235) Nguyen, G. K. T.; Lim, W. H.; Nguyen, P. Q. T.; Tam, J. P. Novel cyclotides and uncyclotides with highly shortened precursors from *Chassalia chartacea* and effects of methionine oxidation on bioactivities. *J. Biol. Chem.* **2012**, *287*, 17598–17607.
(236) Pinto, M. F. S.; Fensterseifer, I. C. M.; Migliolo, L.; Sousa, D. A.; de Capdville, G.; Arboleda-Valencia, J. W.; Colgrave, M. L.; Craik, D. J.; Magalhaes, B. S.; Dias, S. C.; et al. Identification and structural characterization of novel cyclotide with activity against an insect pest of sugar cane. *J. Biol. Chem.* **2012**, *287*, 134–147.
(237) Poth, A. G.; Mylne, J. S.; Grassl, J.; Lyons, R. E.; Millar, A. H.; Colgrave, M. L.; Craik, D. J. Cyclotides associate with leaf vasculature and are the products of a novel precursor in *Petunia* (Solanaceae). *J. Biol. Chem.* **2012**, *287*, 27033–27046.
(238) Wong, C. T. T.; Rowlands, D. K.; Wong, C. H.; Lo, T. W. C.; Nguyen, G. K. T.; Li, H. Y.; Tam, J. P. Orally active peptidic bradykinin B-1 receptor antagonists engineered from a cyclotide scaffold for inflammatory pain treatment. *Angew. Chem. Int. Ed.* **2012**, *51*, 5620–5624.
(239) Yeshak, M. Y.; Burman, R.; Eriksson, C.; Göransson, U. Optimization of cyclotide extraction parameters. *Phytochem Lett.* **2012**, *5*, 776–781.
(240) Zheng, J. S.; Chang, H. N.; Shi, J.; Liu, L. Chemical synthesis of a cyclotide via intramolecular cyclization of peptide O-esters. *Sci. China Chem.* **2012**, *55*, 64–69.
(241) Zheng, J. S.; Tang, S.; Guo, Y.; Chang, H. N.; Liu, L. Synthesis of cyclic peptides and cyclic proteins via ligation of peptide hydrazides. *ChemBioChem* **2012**, *13*, 542–546.
(242) Cowper, B.; Craik, D. J.; Macmillan, D. Making ends meet: Chemically mediated circularization of recombinant proteins. *ChemBioChem* **2013**, *14*, 809–812.
(243) Akcan, M.; Craik, D. J.: Synthesis of Cyclic Disulfide-Rich Peptides. In *Peptide Synthesis and Applications*; Jensen, K. J., Tofteng Shelton, P. and Pedersen, S. L., Eds.; Humana Press, 2013; Vol. 1047; Chapter 6; pp 89–101.
(244) Borra, R.; Camarero, J. A. Recombinant expression of backbone-cyclized polypeptides. *Biopolymers: Pept. Sci.* **2013**, *100*, 502–509.
(245) Craik, D. J.; Malik, U. Cyclotide biosynthesis. *Curr. Opin. Chem. Biol.* **2013**, *17*, 546–554.
(246) Craik, D. J. Joseph Rudinger memorial lecture: Discovery and applications of cyclotides. *J. Pept. Sci.* **2013**, *19*, 393–407.
(247) Craik, D. J.; Fairlie, D. P.; Liras, S.; Price, D. The future of peptide-based drugs. *Chem. Biol. Drug Des.* **2013**, *81*, 136–147.
(248) Demartini, D. R.; Pasquali, G.; Carlini, C. R. An overview of proteomics approaches applied to biopharmaceuticals and cyclotides research. *J. Proteomics* **2013**, *93*, 224–233.
(249) Schroeder, C. I.; Swedberg, J. E.; Craik, D. J. Recent progress towards pharmaceutical applications of disulfide-rich cyclic peptides. *Curr. Protein Pept. Sci.* **2013**, *14*, 532–542.
(250) Koehbach, J.; Gruber, C. W. From ethnopharmacology to drug design. *Commun. Integr. Biol.* **2013**, *6*, e27583.
(251) Poth, A. G.; Chan, L. Y.; Craik, D. J. Cyclotides as grafting frameworks for protein engineering and drug design applications. *Biopolymers: Pept. Sci.* **2013**, *100*, 480–491.
(252) Gerlach, S. L.; Göransson, U.; Kaas, Q.; Craik, D. J.; Mondal, D.; Gruber, C. W. A systematic approach to document cyclotide distribution in plant species from genomic, transcriptomic, and peptidomic analysis. *Biopolymers: Pept. Sci.* **2013**, *100*, 433–437.

(253) Gerlach, S. L.; Yeshak, M.; Göransson, U.; Roy, U.; Izadpanah, R.; Mondal, D. Cycloviolacin O2 (CyO2) suppresses productive infection and augments the antiviral efficacy of nelfinavir in HIV-1 infected monocytic cells. *Biopolymers: Pept. Sci.* **2013**, *100*, 471–479.
(254) Getz, J. A.; Cheneval, O.; Craik, D. J.; Daugherty, P. S. Design of a cyclotide antagonist of neuropilin-1 and -2 that potently inhibits endothelial cell migration. *ACS Chem. Biol.* **2013**, *8*, 1147–1154.
(255) Daly, N. L.; Thorstholm, L.; Greenwood, K. P.; King, G. J.; Rosengren, K. J.; Heras, B.; Martin, J. L.; Craik, D. J. Structural insights into the role of the cyclic backbone in a squash trypsin inhibitor. *J. Biol. Chem.* **2013**, *288*, 36141–36148.
(256) Glotzbach, B.; Reinwarth, M.; Weber, N.; Fabritz, S.; Tomaszowski, M.; Fittler, H.; Christmann, A.; Avrutina, O.; Kolmar, H. Combinatorial optimization of cystine-knot peptides towards high-affinity inhibitors of human matriptase-1. *PLoS One* **2013**, *8*, e76956.
(257) Gründemann, C.; Thell, K.; Lengen, K.; Garcia-Käufer, M.; Huang, Y.-H.; Huber, R.; Craik, D. J.; Schabbauer, G.; Gruber, C. W. Cyclotides suppress human T-lymphocyte proliferation by an interleukin 2-dependent mechanism. *PLoS One* **2013**, *8*, e68016.
(258) Gunasekera, S.; Aboye, T.; Madian, W.; El-Seedi, H.; Göransson, U. Making ends meet: Microwave-accelerated synthesis of cyclic and disulfide rich proteins via in situ thioesterification and native chemical ligation. *Int. J. Pept. Res. Ther.* **2013**, *19*, 43–54.
(259) Hashempour, H.; Koehbach, J.; Daly, N. L.; Ghassempour, A.; Gruber, C. W. Characterizing circular peptides in mixtures: Sequence fragment assembly of cyclotides from a violet plant by MALDI-TOF/TOF mass spectrometry. *Amino Acids* **2013**, *44*, 581–595.
(260) Jagadish, K.; Borra, R.; Lacey, V.; Majumder, S.; Shekhtman, A.; Wang, L.; Camarero, J. A. Expression of fluorescent cyclotides using protein trans-splicing for easy monitoring of cyclotide–protein interactions. *Angew. Chem. Int. Ed.* **2013**, *52*, 3126–3131.
(261) Ji, Y.; Majumder, S.; Millard, M.; Borra, R.; Bi, T.; Elnagar, A. Y.; Neamati, N.; Shekhtman, A.; Camarero, J. A. In vivo activation of the p53 tumor suppressor pathway by an engineered cyclotide. *J. Am. Chem. Soc.* **2013**, *135*, 11623–11633.
(262) Koehbach, J.; Attah, A. F.; Berger, A.; Hellinger, R.; Kutchan, T. M.; Carpenter, E. J.; Rolf, M.; Sonibare, M. A.; Moody, J. O.; Wong, G. K.-S.; et al. Cyclotide discovery in Gentianales revisited—identification and characterization of cyclic cystine-knot peptides and their phylogenetic distribution in Rubiaceae plants. *Biopolymers: Pept. Sci.* **2013**, *100*, 438–452.
(263) Koehbach, J.; O'Brien, M.; Muttenthaler, M.; Miazzo, M.; Akcan, M.; Elliott, A. G.; Daly, N. L.; Harvey, P. J.; Arrowsmith, S.; Gunasekera, S.; et al. Oxytocic plant cyclotides as templates for peptide G protein-coupled receptor ligand design. *Proc. Natl. Acad. Sci. U. S. A.* **2013**, *110*, 21183–21188.
(264) Malagón, D.; Botterill, B.; Gray, D. J.; Lovas, E.; Duke, M.; Gray, C.; Kopp, S. R.; Knott, L. M.; McManus, D. P.; Daly, N. L.; et al. Anthelminthic activity of the cyclotides (kalata B1 and B2) against schistosome parasites. *Biopolymers: Pept. Sci.* **2013**, *100*, 461–470.
(265) Nguyen, G. K.; Lian, Y. L.; Pang, E. W. H.; Phuong, Q. T. N.; Tran, T. D.; Tam, J. P. Discovery of linear cyclotides in monocot plant *Panicum laxum* of Poaceae family provides new insights into evolution and distribution of cyclotides in plants. *J. Biol. Chem.* **2013**, *288*, 3370–3380.
(266) Quimbar, P.; Malik, U.; Sommerhoff, C. P.; Kaas, Q.; Chan, L. Y.; Huang, Y.-H.; Grundhuber, M.; Dunse, K.; Craik, D. J.; Anderson, M. A.; et al. High-affinity cyclic peptide matriptase inhibitors. *J. Biol. Chem.* **2013**, *288*, 13885–13896.
(267) Rosengren, K. J.; Daly, N. L.; Harvey, P. J.; Craik, D. J. The self-association of the cyclotide kalata B2 in solution is guided by hydrophobic interactions. *Biopolymers: Pept. Sci.* **2013**, *100*, 453–460.
(268) Schrank, E.; Wagner, G. E.; Zangger, K. Solution NMR studies on the orientation of membrane-bound peptides and proteins by paramagnetic probes. *Molecules* **2013**, *18*, 7407–7435.
(269) Sen, Z.; Zhan, X. K.; Jing, J.; Yi, Z.; Wanqi, Z. Chemosensitizing activities of cyclotides from *Clitoria ternatea* in paclitaxel-resistant lung cancer cells. *Oncol. Lett.* **2013**, *5*, 641–644.
(270) Zarrabi, M.; Dalirfardouei, R.; Sepehrizade, Z.; Kermanshahi, R. K. Comparison of the antimicrobial effects of semipurified cyclotides from Iranian *Viola odorata* against some of plant and human pathogenic bacteria. *J. Appl. Microbiol.* **2013**, *115*, 367–375.
(271) Arnison, P. G.; Bibb, M. J.; Bierbaum, G.; Bowers, A. A.; Bugni, T. S.; Bulaj, G.; Camarero, J. A.; Campopiano, D. J.; Challis, G. L.; Clardy, J.; et al. Ribosomally synthesized and post-translationally modified peptide natural products: Overview and recommendations for a universal nomenclature. *Nat. Prod. Rep.* **2013**, *30*, 108–160.

(272) Ackerman, S. E.; Currier, N. V.; Bergen, J. M.; Cochran, J. R. Cystine-knot peptides: Emerging tools for cancer imaging and therapy. *Expert Rev. Proteomics* **2014**, *11*, 561–572.
(273) Burman, R.; Gunasekera, S.; Strömstedt, A. A.; Göransson, U. Chemistry and biology of cyclotides: Circular plant peptides outside the box. *J. Nat. Prod.* **2014**, *77*, 724–736.
(274) Góngora-Benítez, M.; Tulla-Puche, J.; Albericio, F. Multifaceted roles of disulfide bonds. Peptides as therapeutics. *Chem. Rev.* **2014**, *114*, 901–926.
(275) Northfield, S. E.; Wang, C. K.; Schroeder, C. I.; Durek, T.; Kan, M. W.; Swedberg, J. E.; Craik, D. J. Disulfide-rich macrocyclic peptides as templates in drug design. *Eur. J. Med. Chem.* **2014**, *77*, 248–257.
(276) Thell, K.; Hellinger, R.; Schabbauer, G.; Gruber, C. W. Immunosuppressive peptides and their therapeutic applications. *Drug Discov. Today* **2014**, *19*, 645–653.
(277) Wang, C. K.; Gruber, C. W.; Čemažar, M.; Siatskas, C.; Tagore, P.; Payne, N.; Sun, G.; Wang, S.; Bernard, C. C.; Craik, D. J. Molecular grafting onto a stable framework yields novel cyclic peptides for the treatment of multiple sclerosis. *ACS Chem. Biol.* **2014**, *9*, 156–163.
(278) Cheneval, O.; Schroeder, C. I.; Durek, T.; Walsh, P.; Huang, Y.-H.; Liras, S.; Price, D. A.; Craik, D. J. Fmoc-based synthesis of disulfide-rich cyclic peptides. *J. Org. Chem.* **2014**, *79*, 5538–5544.
(279) Hemu, X.; Qiu, Y. B.; Tam, J. P. Peptide macrocyclization through amide-to-amide transpeptidation. *Tetrahedron* **2014**, *70*, 7707–7713.
(280) Ding, X. M.; Bai, D. S.; Qian, J. J. Novel cyclotides from *Hedyotis biflora* inhibit proliferation and migration of pancreatic cancer cell in vitro and in vivo. *Med. Chem. Res.* **2014**, *23*, 1406–1413.
(281) Gray, K.; Elghadban, S.; Thongyoo, P.; Owen, K. A.; Szabo, R.; Bugge, T. H.; Tate, E. W.; Leatherbarrow, R. J.; Ellis, V. Potent and specific inhibition of the biological activity of the type-II transmembrane serine protease matriptase by the cyclic microprotein MCoTI-II. *Thromb. Haemost.* **2014**, *112*, 402–411.
(282) Hellinger, R.; Koehbach, J.; Fedchuk, H.; Sauer, B.; Huber, R.; Gruber, C. W.; Gründemann, C. Immunosuppressive activity of an aqueous Viola tricolor herbal extract. *J. Ethnopharmacol.* **2014**, *151*, 299–306.
(283) D'Souza, C.; Henriques, S. T.; Wang, C. K.; Craik, D. J. Structural parameters modulating the cellular uptake of disulfide-rich cyclic cell-penetrating peptides: MCoTI-II and SFTI-1. *Eur. J. Med. Chem.* **2014**, *88*, 10–18.
(284) Henriques, S. T.; Huang, Y.-H.; Chaousis, S.; Wang, C. K.; Craik, D. J. Anticancer and toxic properties of cyclotides are dependent on phosphatidylethanolamine phospholipid targeting. *ChemBioChem* **2014**, *15*, 1956–1965.
(285) Nawae, W.; Hannongbua, S.; Ruengjitchatchawalya, M. Defining the membrane disruption mechanism of kalata B1 via coarse-grained molecular dynamics simulations. *Sci. Rep.* **2014**, *4*, 3933.
(286) Nawae, W.; Hannongbua, S.; Ruengjitchatchawalya, M. Dynamic scenario of membrane binding process of kalata B1. *PLoS One* **2014**, *9*, e114473.
(287) Jia, X.; Kwon, S.; Wang, C. I.; Huang, Y. H.; Chan, L. Y.; Tan, C. C.; Rosengren, K. J.; Mulvenna, J. P.; Schroeder, C. I.; Craik, D. J. Semienzymatic cyclization of disulfide-rich peptides using sortase A. *J. Biol. Chem.* **2014**, *289*, 6627–6638.
(288) Stanger, K.; Maurer, T.; Kaluarachchi, H.; Coons, M.; Franke, Y.; Hannoush, R. N. Backbone cyclization of a recombinant cystine-knot peptide by engineered Sortase A. *FEBS Lett.* **2014**, *588*, 4487–4496.
(289) Nguyen, G. K. T.; Wang, S. J.; Qiu, Y. B.; Hemu, X.; Lian, Y. L.; Tam, J. P. Butelase 1 is an Asx-specific ligase enabling peptide macrocyclization and synthesis. *Nat. Chem. Biol.* **2014**, *10*, 732–738.
(290) Kedarisetti, P.; Mizianty, M. J.; Kaas, Q.; Craik, D. J.; Kurgan, L. Prediction and characterization of cyclic proteins from sequences in three domains of life. *Biochim. Biophys. Acta, Proteins Proteomics* **2014**, *1844*, 181–190.
(291) Liu, M. Z.; Yang, Y.; Zhang, S. X.; Tang, L.; Wang, H. M.; Chen, C. J.; Shen, Z. F.; Cheng, K. D.; Kong, J. Q.; Wang, W. A cyclotide against influenza A H1N1 virus from *Viola yedoensis*. *Acta Pharm. Sin.* **2014**, *49*, 905–912.
(292) Mahatmanto, T.; Poth, A. G.; Mylne, J. S.; Craik, D. J. A comparative study of extraction methods reveals preferred solvents for cystine knot peptide isolation from *Momordica cochinchinensis* seeds. *Fitoterapia* **2014**, *95*, 22–33.
(293) Park, S.; Strömstedt, A. A.; Göransson, U. Cyclotide structure–activity relationships: Qualitative and quantitative approaches linking cytotoxic and anthelmintic activity to the clustering of physicochemical forces. *PLoS One* **2014**, *9*, e91430.

(294) Taylor, C. M.; Northfield, S. E.; Wang, C. K.; Craik, D. J. Native peptide folding dominates over stereoelectronic effects of prolyl hydroxylation in loop 5 of the macrocyclic peptide kalata B1. *Tetrahedron* **2014**, *70*, 7669–7674.
(295) Wang, C. K.; King, G. J.; Northfield, S. E.; Ojeda, P. G.; Craik, D. J. Racemic and quasi-racemic X-ray structures of cyclic disulfide-rich peptide drug scaffolds. *Angew. Chem. Int. Ed.* **2014**, *53*, 11236–11241.
(296) Wang, C. K.; Northfield, S. E.; Swedberg, J. E.; Harvey, P. J.; Mathiowetz, A. M.; Price, D. A.; Liras, S.; Craik, D. J. Translational diffusion of cyclic peptides measured using pulsed-field gradient NMR. *J. Phys. Chem. B* **2014**, *118*, 11129–11136.
(297) Xu, W.; Wang, B.; Lin, Y.; Li, Y.; Su, Z.; He, W.; Tan, N.; Wang, Q. Emulsions stabilized by mini cyclic proteins for bioactive compound delivery. *RSC Adv.* **2014**, *4*, 48000–48003.
(298) Craik, D. J. (Ed.) *Advances in Botanical Research: Plant Cyclotides*; Academic Press: London, 2015; Vol. 76.
(299) Mollica, A.; Costante, R.; Stefanucci, A.; Novellino, E. Cyclotides: A natural combinatorial peptide library or a bioactive sequence player? *J. Enzyme Inhib. Med. Chem.* **2015**, *30*, 575–580.
(300) Aboye, T.; Kuang, Y.; Neamati, N.; Camarero, J. A. Rapid parallel synthesis of bioactive folded cyclotides by using a tea-bag approach. *ChemBioChem* **2015**, *16*, 827–833.
(301) Chan, L. Y.; Craik, D. J.; Daly, N. L. Cyclic thrombospondin-1 mimetics: Grafting of a thrombospondin sequence into circular disulfide-rich frameworks to inhibit endothelial cell migration. *Biosci. Rep.* **2015**, *35*, e00270.
(302) Fensterseifer, I. C. M.; Silva, O. N.; Malik, U.; Ravipati, A. S.; Novaes, N. R. F.; Miranda, P. R. R.; Rodrigues, E. A.; Moreno, S. E.; Craik, D. J.; Franco, O. L. Effects of cyclotides against cutaneous infections caused by *Staphylococcus aureus*. *Peptides* **2015**, *63*, 38–42.
(303) Guzman-Rodriguez, J. J.; Ochoa-Zarzosa, A.; Lopez-Gomez, R.; Lopez-Meza, J. E. Plant antimicrobial peptides as potential anticancer agents. *BioMed Res. Int.* **2015**, *2015*, 735087.
(304) Harris, K. S.; Durek, T.; Kaas, Q.; Poth, A. G.; Gilding, E. K.; Conlan, B. F.; Saska, I.; Daly, N. L.; van der Weerden, N. L.; Craik, D. J.; et al. Efficient backbone cyclization of linear peptides by a recombinant asparaginyl endopeptidase. *Nat. Commun.* **2015**, *6*, 10199.
(305) Hellinger, R.; Koehbach, J.; Puigpinos, A.; Clark, R. J.; Tarrago, T.; Giralt, E.; Gruber, C. W. Inhibition of human prolyl oligopeptidase activity by the cyclotide psysol 2 isolated from *Psychotria solitudinum*. *J. Nat. Prod.* **2015**, *78*, 1073–1082.
(306) Hellinger, R.; Koehbach, J.; Soltis, D. E.; Carpenter, E. J.; Wong, G. K.-S.; Gruber, C. W. Peptidomics of circular cysteine-rich plant peptides: Analysis of the diversity of cyclotides from *Viola tricolor* by transcriptome and proteome mining. *J. Proteome Res.* **2015**, *14*, 4851–4862.
(307) Burman, R.; Yeshak, M. Y.; Larsson, S.; Craik, D. J.; Rosengren, K. J.; Göransson, U. Distribution of circular proteins in plants: Large-scale mapping of cyclotides in the Violaceae. *Front. Plant Sci.* **2015**, *6*, 855.
(308) Henriques, S. T.; Huang, Y.-H.; Chaousis, S.; Sani, M.-A.; Poth, A. G.; Separovic, F.; Craik, D. J. The prototypic cyclotide kalata B1 has a unique mechanism of entering cells. *Chem. Biol.* **2015**, *22*, 1087–1097.
(309) Phoenix, D. A.; Harris, F.; Mura, M.; Dennison, S. R. The increasing role of phosphatidylethanolamine as a lipid receptor in the action of host defence peptides. *Prog. Lipid Res.* **2015**, *59*, 26–37.
(310) Huang, Y. H.; Chaousis, S.; Cheneval, O.; Craik, D. J.; Henriques, S. T. Optimization of the cyclotide framework to improve cell penetration properties. *Front. Pharmacol.* **2015**, *6*, 17.
(311) Huang, Y.-H.; Henriques, S. T.; Wang, C. K.; Thorstholm, L.; Daly, N. L.; Kaas, Q.; Craik, D. J. Design of substrate-based BCR-ABL kinase inhibitors using the cyclotide scaffold. *Sci. Rep.* **2015**, *5*, 12974.
(312) Jagadish, K.; Gould, A.; Borra, R.; Majumder, S.; Mushtaq, Z.; Shekhtman, A.; Camarero, J. A. Recombinant expression and phenotypic screening of a bioactive cyclotide against α-synuclein-induced cytotoxicity in baker's yeast. *Angew. Chem. Int. Ed.* **2015**, *54*, 8390–8394.
(313) Maaß, F.; Wustehube-Lausch, J.; Dickgiessr, S.; Valldorf, B.; Reinwarth, M.; Schmoldt, H. U.; Daneschdar, M.; Avrutina, O.; Sahin, U.; Kolmar, H. Cystine-knot peptides targeting cancer-relevant human cytotoxic T lymphocyte-associated antigen 4 (CTLA-4). *J. Pept. Sci.* **2015**, *21*, 651–660.
(314) Kodari, N.; Bahramnejad, B.; Rostamzadeh, J.; Maroofi, H.; Torkaman, S. Molecular cloning and characterization of a cyclotide gene family in *Viola modesta* Fenzl. *J. Agric. Sci. Technol.* **2015**, *17*, 1637–1649.

(315) Mahatmanto, T.; Mylne, J. S.; Poth, A. G.; Swedberg, J. E.; Kaas, Q.; Schaefer, H.; Craik, D. J. The evolution of *Momordica* cyclic peptides. *Mol. Biol. Evol.* **2015**, *32*, 392–405.
(316) Hu, E.; Wang, D.; Chen, J.; Tao, X. Novel cyclotides from *Hedyotis diffusa* induce apoptosis and inhibit proliferation and migration of prostate cancer cells. *Int. J. Clin. Exp. Med.* **2015**, *8*, 4059–4065.
(317) Ravipati, A. S.; Henriques, S. T.; Poth, A. G.; Kaas, Q.; Wang, C. K.; Colgrave, M. L.; Craik, D. J. Lysine-rich cyclotides: A new subclass of circular knotted proteins from Violaceae. *ACS Chem. Biol.* **2015**, *10*, 2491–2500.
(318) Sangphukieo, A.; Nawae, W.; Laomettachit, T.; Supasitthimethee, U.; Ruengjitchatchawalya, M. Computational design of hypothetical new peptides based on a cyclotide scaffold as HIV gp120 inhibitor. *PLoS One* **2015**, *10*, e0139562.
(319) Slazak, B.; Jacobsson, E.; Kuta, E.; Göransson, U. Exogenous plant hormones and cyclotide expression in *Viola uliginosa* (Violaceae). *Phytochemistry* **2015**, *117*, 527–536.
(320) Slazak, B.; Sliwinska, E.; Saługa, M.; Ronikier, M.; Bujak, J.; Słomka, A.; Göransson, U.; Kuta, E. Micropropagation of *Viola uliginosa* (Violaceae) for endangered species conservation and for somaclonal variation-enhanced cyclotide biosynthesis. *Plant Cell Tissue Organ Cult.* **2015**, *120*, 179–190.
(321) Zhang, J.; Hua, Z. S.; Huang, Z. B.; Chen, Q. Z.; Long, Q. Y.; Craik, D. J.; Baker, A. J. M.; Shu, W. S.; Liao, B. Two Blast-independent tools, CyPerl and CyExcel, for harvesting hundreds of novel cyclotides and analogues from plant genomes and protein databases. *Planta* **2015**, *241*, 929–940.
(322) Zhang, J.; Li, J. T.; Huang, Z. B.; Yang, B.; Zhang, X. J.; Li, D. H.; Craik, D. J.; Baker, A. J. M.; Shu, W. S.; Liao, B. Transcriptomic screening for cyclotides and other cysteine-rich proteins in the metallophyte *Viola baoshanensis*. *J. Plant Physiol.* **2015**, *178*, 17–26.
(323) Attah, A. F.; Hellinger, R.; Sonibare, M. A.; Moody, J. O.; Arrowsmith, S.; Wray, S.; Gruber, C. W. Ethnobotanical survey of *Rinorea dentata* (Violaceae) used in South-Western Nigerian ethnomedicine and detection of cyclotides. *J. Ethnopharmacol.* **2016**, *179*, 83–91.
(324) Jones, P. M.; George, A. M. Computational analysis of the MCoTI-II plant defence knottin reveals a novel intermediate conformation that facilitates trypsin binding. *Sci. Rep.* **2016**, *6*, 23174.
(325) Aboye, T.; Meeks, C.; Majumder, S.; Shekhtman, A.; Rodgers, K.; Camarero, J. Design of a MCoTI-based cyclotide with angiotensin (1-7)-like activity. *Molecules* **2016**, *21*, 152.
(326) D'Souza, C.; Henriques, S. T.; Wang, C. K.; Cheneval, O.; Chan, L. Y.; Bokil, N. J.; Sweet, M. J.; Craik, D. J. Using the MCoTI-II cyclotide scaffold to design a stable cyclic peptide antagonist of SET, a protein overexpressed in human cancer. *Biochemistry* **2016**, *55*, 396–405.
(327) Chan, L. Y.; Craik, D. J.; Daly, N. L. Dual-targeting anti-angiogenic cyclic peptides as potential drug leads for cancer therapy. *Sci. Rep.* **2016**, *6*, 35347.
(328) Conibear, A. C.; Chaousis, S.; Durek, T.; Rosengren, K. J.; Craik, D. J.; Schroeder, C. I. Approaches to the stabilization of bioactive epitopes by grafting and peptide cyclization. *Biopolymers: Pept. Sci.* **2016**, *106*, 89–100.
(329) da Cunha, N. B.; Barbosa, A. E.; de Almeida, R. G.; Porto, W. F.; Maximiano, M. R.; Alvares, L. C.; Munhoz, C. B.; Eugenio, C. U.; Viana, A. A.; Franco, O. L.; et al. Cloning and characterization of novel cyclotides genes from South American plants. *Biopolymers: Pept. Sci.* **2016**, *106*, 784–795.
(330) Daly, N. L.; Gunasekera, S.; Clark, R. J.; Lin, F.; Wade, J. D.; Anderson, M. A.; Craik, D. J. The N-terminal pro-domain of the kalata B1 cyclotide precursor is intrinsically unstructured. *Biopolymers: Pept. Sci.* **2016**, *106*, 825–833.
(331) Esmaeili, M. A.; Abagheri-Mahabadi, N.; Hashempour, H.; Farhadpour, M.; Gruber, C. W.; Ghassempour, A. Viola plant cyclotide vigno 5 induces mitochondria-mediated apoptosis via cytochrome C release and caspases activation in cervical cancer cells. *Fitoterapia* **2016**, *109*, 162–168.
(332) Farhadpour, M.; Hashempour, H.; Talebpour, Z.; A-Bagheri, N.; Shushtarian, M. S.; Gruber, C. W.; Ghassempour, A. Microwave-assisted extraction of cyclotides from *Viola ignobilis*. *Anal. Biochem.* **2016**, *497*, 83–89.
(333) Gilding, E. K.; Jackson, M. A.; Poth, A. G.; Henriques, S. T.; Prentis, P. J.; Mahatmanto, T.; Craik, D. J. Gene coevolution and regulation lock cyclic plant defence peptides to their targets. *New Phytol.* **2016**, *210*, 717–730.
(334) Hemu, X.; Qiu, Y.; Nguyen, G. K. T.; Tam, J. P. Total synthesis of circular bacteriocins by butelase 1. *J. Am. Chem. Soc.* **2016**, *138*, 6968–6971.
(335) Porto, W. F.; Miranda, V. J.; Pinto, M. F. S.; Dohms, S. M.; Franco, O. L. High-performance computational analysis and peptide screening from databases of cyclotides from Poaceae. *Biopolymers: Pept. Sci.* **2016**, *106*, 109–118.

(336) Senthilkumar, B.; Kumar, P.; Rajasekaran, R. In-silico template selection of in-vitro evolved kalata B1 of *Oldenlandia affinis* for scaffolding peptide-based drug design. *J. Cell. Biochem.* **2016**, *117*, 66–73.
(337) Serra, A.; Hemu, X.; Nguyen, G. K. T.; Nguyen, N. T. K.; Sze, S. K.; Tam, J. P. A high-throughput peptidomic strategy to decipher the molecular diversity of cyclic cysteine-rich peptides. *Sci. Rep.* **2016**, *6*, 23005.
(338) Matsuura, H. N.; Poth, A. G.; Yendo, A. C. A.; Fett-Neto, A. G.; Craik, D. J. Isolation and characterization of cyclotides from Brazilian *Psychotria*: Significance in plant defense and co-occurrence with antioxidant alkaloids. *J. Nat. Prod.* **2016**, *79*, 3006–3013.
(339) Melander, E.; Eriksson, C.; Jansson, B.; Göransson, U.; Hammarlund-Udenaes, M. Improved method for quantitative analysis of the cyclotide kalata B1 in plasma and brain homogenate. *Biopolymers: Pept. Sci.* **2016**, *106*, 910–916.
(340) Wang, C. K.; Stalmans, S.; De Spiegeleer, B.; Craik, D. J. Biodistribution of the cyclotide MCoTI-II, a cyclic disulfide-rich peptide drug scaffold. *J. Pept. Sci.* **2016**, *22*, 305–310.
(341) Gao, X.; Stanger, K.; Kaluarachchi, H.; Maurer, T.; Ciepla, P.; Chalouni, C.; Franke, Y.; Hannoush, R. N. Cellular uptake of a cystine-knot peptide and modulation of its intracellular trafficking. *Sci. Rep.* **2016**, *6*, 35179.
(342) Slazak, B.; Kapusta, M.; Malik, S.; Bohdanowicz, J.; Kuta, E.; Malec, P.; Göransson, U. Immunolocalization of cyclotides in plant cells, tissues and organ supports their role in host defense. *Planta* **2016**, *244*, 1029–1040.
(343) Nguyen, K. N. T.; Nguyen, G. K. T.; Nguyen, P. Q. T.; Ang, K. H.; Dedon, P. C.; Tam, J. P. Immunostimulating and Gram-negative-specific antibacterial cyclotides from the butterfly pea (*Clitoria ternatea*). *FEBS J.* **2016**, *283*, 2067–2090.
(344) Niyomploy, P.; Chan, L. Y.; Poth, A. G.; Colgrave, M. L.; Sangvanich, P.; Craik, D. J. Discovery, isolation, and structural characterization of cyclotides from *Viola sumatrana* Miq. *Biopolymers: Pept. Sci.* **2016**, *106*, 796–805.
(345) Pinto, M. F.; Silva, O. N.; Viana, J. C.; Porto, W. F.; Migliolo, L.; da Cunha, N. B.; Gomes, N., Jr.; Fensterseifer, I. C.; Colgrave, M. L.; Craik, D. J.; et al. Characterization of a bioactive cyclotide from *Palicourea rigida*. *J. Nat. Prod.* **2016**, *79*, 2767–2773.
(346) Strömstedt, A. A.; Kristiansen, P. E.; Gunasekera, S.; Grob, N.; Skjeldal, L.; Göransson, U. Selective membrane disruption by the cyclotide kalata B7: Complex ions and essential functional groups in the phosphatidylethanolamine binding pocket. *Biochim. Biophys. Acta, Biomembr.* **2016**, *1858*, 1317–1327.
(347) Swedberg, J. E.; Mahatmanto, T.; Abdul Ghani, H.; de Veer, S. J.; Schroeder, C. I.; Harris, J. M.; Craik, D. J. Substrate-guided design of selective FXIIa inhibitors based on the plant-derived *Momordica cochinchinensis* trypsin inhibitor-II (MCoTI-II) scaffold. *J. Med. Chem.* **2016**, *59*, 7287–7292.
(348) Thell, K.; Hellinger, R.; Sahin, E.; Michenthaler, P.; Gold-Binder, M.; Haider, T.; Kuttke, M.; Liutkevičiūtė, Z.; Göransson, U.; Gründemann, C.; et al. Oral activity of a nature-derived cyclic peptide for the treatment of multiple sclerosis. *Proc. Natl. Acad. Sci. U. S. A.* **2016**, *113*, 3960–3965.
(349) Wang, C. K.; Northfield, S. E.; Huang, Y. H.; Ramos, M. C.; Craik, D. J. Inhibition of tau aggregation using a naturally-occurring cyclic peptide scaffold. *Eur. J. Med. Chem.* **2016**, *109*, 342–349.
(350) Wang, D. G.; Chen, J. Y.; Zhu, J. F.; Mou, Y. H. Novel cyclotides from Hedyotis biflora has potent bactericidal activity against Gram-negative bacteria and E. coli drug resistance. *Int. J. Clin. Exp. Med.* **2016**, *9*, 9521–9526.
(351) Craik, D. J.; Young Shim, Y.; Göransson, U.; Moss, G. P.; Tan, N.; Jadhav, P. D.; Shen, J.; Reaney, M. J. T. Nomenclature of homodetic cyclic peptides produced from ribosomal precursors: An IUPAC task group interim report. *Biopolymers: Pept. Sci.* **2016**, *106*, 917–924.
(352) Koehbach, J.; Clark, R. J. Unveiling the diversity of cyclotides by combining peptidome and transcriptome analysis. *Biopolymers: Pept. Sci.* **2016**, *106*, 774–783.
(353) White, A. M.; Craik, D. J. Discovery and optimization of peptide macrocycles. *Expert Opin. Drug Discov.* **2016**, *11*, 1151–1163.
(354) Weidmann, J.; Craik, D. J. Discovery, structure, function, and applications of cyclotides: Circular proteins from plants. *J. Exp. Bot.* **2016**, *67*, 4801–4812.
(355) de Veer, S. J.; Weidmann, J.; Craik, D. J. Cyclotides as tools in chemical biology. *Acc. Chem. Res.* **2017**, *50*, 1557–1565.
(356) Camarero, J. A. Cyclotides, a versatile ultrastable micro-protein scaffold for biotechnological applications. *Bioorg. Med. Chem. Lett.* **2017**, *27*, 5089–5099.

(357) Gould, A.; Camarero, J. A. Cyclotides: Overview and biotechnological applications. *ChemBioChem* **2017**, *18*, 1350–1363.
(358) Nielsen, D. S.; Shepherd, N. E.; Xu, W.; Lucke, A. J.; Stoermer, M. J.; Fairlie, D. P. Orally absorbed cyclic peptides. *Chem. Rev.* **2017**, *117*, 8094–8128.
(359) Qu, H.; Smithies, B. J.; Durek, T.; Craik, D. J. Synthesis and protein engineering applications of cyclotides. *Aust. J. Chem.* **2017**, *70*, 152–161.
(360) Uddin, S. J.; Muhammad, T.; Shafiullah, M.; Slazak, B.; Rouf, R.; Göransson, U. Single-step purification of cyclotides using affinity chromatography. *Biopolymers: Pept. Sci.* **2017**, *108*, e23010.
(361) Henriques, S. T.; Craik, D. J. Cyclotide structure and function: The role of membrane binding and permeation. *Biochemistry* **2017**, *56*, 669–682.
(362) Jagadish, K.; Camarero, J. A.: Recombinant expression of cyclotides using split inteins. In *Split Inteins: Methods and Protocols*; Mootz, H. D., Ed.; Springer New York: New York, NY, 2017; pp 41–55.
(363) Craik, D. J.; Du, J. Cyclotides as drug design scaffolds. *Curr. Opin. Chem. Biol.* **2017**, *38*, 8–16.
(364) Abdul Ghani, H.; Henriques, S. T.; Huang, Y. H.; Swedberg, J. E.; Schroeder, C. I.; Craik, D. J. Structural and functional characterisation of chimeric cyclotides from the Mobius and trypsin inhibitor subfamilies. *Biopolymers: Pept. Sci.* **2017**, *108*, e22927.
(365) Bernardino, K.; Pinto, M. E. F.; Bolzani, V. S.; de Moura, A. F.; Batista Junior, J. M. Pinpointing disulfide connectivities in cysteine-rich proteins. *Chem. Commun.* **2017**, *53*, 7337–7340.
(366) Bhima, B.; Al Saiqali, M.: Antimicrobial peptides from plants and their application. In *Microbial Biotechnology: Technological Challenges and Developmental Trends*; Bhukya, B. and Tangutur, A., Eds.; Apple Academic Press, 2017; pp 3–25.
(367) Fahradpour, M.; Keov, P.; Tognola, C.; Perez-Santamarina, E.; McCormick, P. J.; Ghassempour, A.; Gruber, C. W. Cyclotides isolated from an ipecac root extract antagonize the corticotropin releasing factor type 1 receptor. *Front. Pharmacol.* **2017**, *8*, 616.
(368) Feyzabadi, Z.; Ghorbani, F.; Vazani, Y.; Zarshenas, M. M. A critical review on phytochemistry, pharmacology of *Viola odorata* L. and related multipotential products in traditional Persian medicine. *Phytother. Res.* **2017**, *31*, 1669–1675.
(369) Cranfield, C. G.; Henriques, S. T.; Martinac, B.; Duckworth, P.; Craik, D. J.; Cornell, B. Kalata B1 and kalata B2 have a surfactant-like activity in phosphatidylethanolomine-containing lipid membranes. *Langmuir* **2017**, *33*, 6630–6637.
(370) Grage, S. L.; Sani, M. A.; Cheneval, O.; Henriques, S. T.; Schalck, C.; Heinzmann, R.; Mylne, J. S.; Mykhailiuk, P. K.; Afonin, S.; Komarov, I. V.; et al. Orientation and location of the cyclotide kalata B1 in lipid bilayers revealed by solid-state NMR. *Biophys. J.* **2017**, *112*, 630–642.
(371) Nawae, W.; Hannongbua, S.; Ruengjitchatchawalya, M. Molecular dynamics exploration of poration and leaking caused by kalata B1 in HIV-infected cell membrane compared to host and HIV membranes. *Sci. Rep.* **2017**, *7*, 3638.
(372) Hellinger, R.; Thell, K.; Vasileva, M.; Muhammad, T.; Gunasekera, S.; Kummel, D.; Göransson, U.; Becker, C. W.; Gruber, C. W. Chemical proteomics for target discovery of head-to-tail cyclized mini-proteins. *Front. Chem.* **2017**, *5*, 73.
(373) Kirkpatrick, C. L.; Broberg, C. A.; McCool, E. N.; Lee, W. J.; Chao, A.; McConnell, E. W.; Pritchard, D. A.; Hebert, M.; Fleeman, R.; Adams, J.; et al. The "PepSAVI-MS" pipeline for natural product bioactive peptide discovery. *Anal. Chem.* **2017**, *89*, 1194–1201.
(374) Lesniak, W. G.; Aboye, T.; Chatterjee, S.; Camarero, J. A.; Nimmagadda, S. In vivo evaluation of an engineered cyclotide as specific CXCR4 imaging reagent. *Chem. Eur. J.* **2017**, *23*, 14469–14475.
(375) Malik, S. Z.; Linkevicius, M.; Göransson, U.; Andersson, D. I. Resistance to the cyclotide cycloviolacin O2 in *Salmonella enterica* caused by different mutations that often confer cross-resistance or collateral sensitivity to other antimicrobial peptides. *Antimicrob. Agents Chemother.* **2017**, *61*, e00684–17.
(376) Mushtaq, Z.; Iqbal, T.; Ahmed, N.; Jamil, A. Antioxidants from selected indigenous plants possessing cyclotides. *Oxid. Commun.* **2017**, *1*, 102–119.
(377) Narayani, M.; Chadha, A.; Srivastava, S. Cyclotides from the Indian medicinal plant *Viola odorata* (Banafsha): Identification and characterization. *J. Nat. Prod.* **2017**, *80*, 1972–1980.
(378) Narayani, M.; Chadha, A.; Srivastava, S. Callus and cell suspension culture of *Viola odorata* as in vitro production platforms of known and novel cyclotides. *Plant Cell Tissue Organ Cult.* **2017**, *130*, 289–299.
(379) Lim, Y. Y.; Lai, K. S. Generation of transgenic rice expressing cyclotide precursor *Oldenlandia affinis* kalata B1 protein. *J. Anim. Plant Sci.* **2017**, *27*, 680–684.

(380) Nigro, E.; Colavita, I.; Sarnataro, D.; Scudiero, O.; Daniele, A.; Salvatore, F.; Pessi, A. Host defense peptide-derived privileged scaffolds for anti-infective drug discovery. *J. Pept. Sci.* **2017**, *23*, 303–310.
(381) Noonan, J.; Williams, W.; Shan, X. Investigation of antimicrobial peptide genes associated with fungus and insect resistance in maize. *Int. J. Mol. Sci.* **2017**, *18*, 1938.
(382) Nworu, C. S.; Ejikeme, T. I.; Ezike, A. C.; Ndu, O.; Akunne, T. C.; Onyeto, C. A.; Okpalanduka, P.; Akah, P. A. Anti-plasmodial and anti-inflammatory activities of cyclotide-rich extract and fraction of *Oldenlandia affinis* (R. & S.) DC (*Rubiaceae*). *Afr. Health Sci.* **2017**, *17*, 827–843.
(383) Oguis, G. K.; Kan, M.-W.; Craik, D. J.: Cyclotides: Plant defense toxins. In *Toxinology*; Gopalakrishnakone, P., Carlini, C. R. and Ligabue-Braun, R., Eds.; Springer Netherlands: Dordrecht, 2017; pp 221–242.
(384) Silva Lima, S. C. B.; Benko-Iseppon, A. M.; Bezerra-Neto, J. P.; Amorim, L. L.; Neto, J. R.; Crovella, S.; Pandolfi, V. Plants defense-related cyclic peptides: Diversity, structure and applications. *Curr. Protein Pept. Sci.* **2017**, *18*, 375–390.
(385) Zheng, Y. W.; Li, Z. R.; Ren, J.; Liu, W. D.; Wu, Y. Q.; Zhao, Y. B.; Wu, C. L. Artificial disulfide-rich peptide scaffolds with precisely defined disulfide patterns and a minimized number of isomers. *Chem. Sci.* **2017**, *8*, 2547–2552.
(386) Park, S.; Yoo, K. O.; Marcussen, T.; Backlund, A.; Jacobsson, E.; Rosengren, K. J.; Doo, I.; Göransson, U. Cyclotide evolution: Insights from the analyses of their precursor sequences, structures and distribution in violets (*Viola*). *Front. Plant Sci.* **2017**, *8*, 2058.
(387) Senthilkumar, B.; Rajasekaran, R. Analysis of the structural stability among cyclotide members through cystine knot fold that underpins its potential use as a drug scaffold. *Int. J. Pept. Res. Ther.* **2017**, *23*, 1–11.
(388) Zhou, Y.; Cai, M. Novel approaches to the design of bioavailable melanotropins. *Expert Opin. Drug Discov.* **2017**, *12*, 1023–1030.
(389) Ravipati, A. S.; Poth, A. G.; Henriques, S. T.; Bhandari, M.; Huang, Y. H.; Nino, J.; Colgrave, M. L.; Craik, D. J. Understanding the diversity and distribution of cyclotides from plants of varied genetic origin. *J. Nat. Prod.* **2017**, *80*, 1522–1530.
(390) Salehi, H.; Bahramnejad, B.; Majdi, M. Induction of two cyclotide-like genes Zmcyc1 and Zmcyc5 by abiotic and biotic stresses in Zea mays. *Acta Physiol. Plant.* **2017**, *39*, 131.
(391) Strömstedt, A. A.; Park, S.; Burman, R.; Göransson, U. Bactericidal activity of cyclotides where phosphatidylethanolamine-lipid selectivity determines antimicrobial spectra. *Biochim. Biophys. Acta, Biomembr.* **2017**, *1859*, 1986–2000.
(392) Valeur, E.; Guéret, S. M.; Adihou, H.; Gopalakrishnan, R.; Lemurell, M.; Waldmann, H.; Grossmann, T. N.; Plowright, A. T. New modalities for challenging targets in drug discovery. *Angew. Chem. Int. Ed.* **2017**, *56*, 10294–10323.
(393) Terrier, V. P.; Delmas, A. F.; Aucagne, V. Efficient synthesis of cysteine-rich cyclic peptides through intramolecular native chemical ligation of N-Hnb-Cys peptide crypto-thioesters. *Org. Biomol. Chem.* **2017**, *15*, 316–319.
(394) Yang, R. L.; Wong, Y. H.; Nguyen, G. K. T.; Tam, J. P.; Lescar, J.; Wu, B. Engineering a catalytically efficient recombinant protein ligase. *J. Am. Chem. Soc.* **2017**, *139*, 5351–5358.
(395) Schmidt, M.; Toplak, A.; Quaedflieg, P. J. L. M.; Ippel, H.; Richelle, G. J. J.; Hackeng, T. M.; van Maarseveen, J. H.; Nuijens, T. Omniligase-1: A powerful tool for peptide head-to-tail cyclization. *Adv. Synth. Catal.* **2017**, *359*, 2050–2055.
(396) Mikula, K. M.; Tascón, I.; Tommila, J. J.; Iwaï, H. Segmental isotopic labeling of a single-domain globular protein without any refolding step by an asparaginyl endopeptidase. *FEBS Lett.* **2017**, *591*, 1285–1294.
(397) Jackson, M. A.; Gilding, E. K.; Shafee, T.; Harris, K. S.; Kaas, Q.; Poon, S.; Yap, K.; Jia, H.; Guarino, R.; Chan, L. Y.; et al. Molecular basis for the production of cyclic peptides by plant asparaginyl endopeptidases. *Nat. Commun.* **2018**, *9*, 2411.
(398) James, A. M.; Haywood, J.; Mylne, J. S. Macrocyclization by asparaginyl endopeptidases. *New Phytol.* **2018**, *218*, 923–928.
(399) Poon, S.; Harris, K. S.; Jackson, M. A.; McCorkelle, O. C.; Gilding, E. K.; Durek, T.; van der Weerden, N. L.; Craik, D. J.; Anderson, M. A. Co-expression of a cyclizing asparaginyl endopeptidase enables efficient production of cyclic peptides in planta. *J. Exp. Bot.* **2018**, *69*, 633–641.

(400) Zauner, F. B.; Elsässer, B.; Dall, E.; Cabrele, C.; Brandstetter, H. Structural analyses of Arabidopsis thaliana legumain γ reveal differential recognition and processing of proteolysis and ligation substrates. *J. Biol. Chem.* **2018**, *293*, 8934–8946.
(401) Álvarez, C.; Barriga, A.; Albericio, F.; Romero, M.; Guzmán, F. Identification of peptides in flowers of *Sambucus nigra* with antimicrobial activity against aquaculture pathogens. *Molecules* **2018**, *23*, 1033.
(402) Álvarez, C.; Santana, P.; Luna, O.; Cárdenas, C.; Albericio, F.; Romero, M.; Guzmán, F. Chemical synthesis and functional analysis of VarvA cyclotide. *Molecules* **2018**, *23*, 952.
(403) Bobey, A. F.; Pinto, M. E. F.; Cilli, E. M.; Lopes, N. P.; Bolzani, V. d. S. A cyclotide isolated from *Noisettia orchidiflora* (Violaceae). *Planta Med.* **2018**, *84*, 947–952.
(404) Cao, P.; Yang, Y.; Uche, F.; Hart, S.; Li, W.-W.; Yuan, C. Coupling plant-derived cyclotides to metal surfaces: An antibacterial and antibiofilm study. *Int. J. Mol. Sci.* **2018**, *19*, 793.
(405) Dabrowski-Tumanski, P.; Rubach, P.; Goundaroulis, D.; Dorier, J.; Sułkowski, P.; Millett, K. C.; Rawdon, E. J.; Stasiak, A.; Sulkowska, J. I. KnotProt 2.0: a database of proteins with knots and other entangled structures. *Nucleic Acids Res.* **2018**, *47*, D367–D375.
(406) Balaraman, S.; Ramalingam, R. The structural and functional reliability of circulins of *Chassalia parvifolia* for peptide therapeutic scaffolding. *J. Cell. Biochem.* **2018**, *119*, 3999–4008.
(407) Kwon, S.; Duarte, J. N.; Li, Z.; Ling, J. J.; Cheneval, O.; Durek, T.; Schroeder, C. I.; Craik, D. J.; Ploegh, H. L. Targeted delivery of cyclotides via conjugation to a nanobody. *ACS Chem. Biol.* **2018**, *13*, 2973–2980.
(408) Swedberg, J. E.; Ghani, H. A.; Harris, J. M.; de Veer, S. J.; Craik, D. J. Potent, selective, and cell-penetrating inhibitors of kallikrein-related peptidase 4 based on the cyclic peptide MCoTI-II. *ACS Med. Chem. Lett.* **2018**, *9*, 1258–1262.
(409) Niyomploy, P.; Chan, L. Y.; Harvey, P. J.; Poth, A. G.; Colgrave, M. L.; Craik, D. J. Discovery and characterization of cyclotides from *Rinorea* species. *J. Nat. Prod.* **2018**, *81*, 2512–2520.
(410) Parsley, N. C.; Kirkpatrick, C. L.; Crittenden, C. M.; Rad, J. G.; Hoskin, D. W.; Brodbelt, J. S.; Hicks, L. M. PepSAVI-MS reveals anticancer and antifungal cycloviolacins in *Viola odorata*. *Phytochemistry* **2018**, *152*, 61–70.
(411) Pinto, M. E. F.; Najas, J. Z. G.; Magalhães, L. G.; Bobey, A. F.; Mendonça, J. N.; Lopes, N. P.; Leme, F. M.; Teixeira, S. P.; Trovó, M.; Andricopulo, A. D.; et al. Inhibition of breast cancer cell migration by cyclotides isolated from *Pombalia calceolaria*. *J. Nat. Prod.* **2018**, *81*, 1203–1208.
(412) Slazak, B.; Kapusta, M.; Strömstedt, A. A.; Słomka, A.; Krychowiak, M.; Shariatgorji, M.; Andrén, P. E.; Bohdanowicz, J.; Kuta, E.; Göransson, U. How does the sweet violet (*Viola odorata* L.) fight pathogens and pests – Cyclotides as a comprehensive plant host defense system. *Front. Plant Sci.* **2018**, *9*, 1296.
(413) Narayani, M.; Sai Varsha, M. K. N.; Potunuru, U. R.; Sofi Beaula, W.; Rayala, S. K.; Dixit, M.; Chadha, A.; Srivastava, S. Production of bioactive cyclotides in somatic embryos of *Viola odorata*. *Phytochemistry* **2018**, *156*, 135–141.
(414) Keov, P.; Liutkevičiūtė, Z.; Hellinger, R.; Clark, R. J.; Gruber, C. W. Discovery of peptide probes to modulate oxytocin-type receptors of insects. *Sci. Rep.* **2018**, *8*, 10020.
(415) Craik, D. J.; Lee, M.-H.; Rehm, F. B. H.; Tombling, B.; Doffek, B.; Peacock, H. Ribosomally-synthesised cyclic peptides from plants as drug leads and pharmaceutical scaffolds. *Bioorg. Med. Chem.* **2018**, *26*, 2727–2737.
(416) Hemu, X.; Serra, A.; Darwis, D. A.; Cornvik, T.; Sze, S. K.; Tam, J. P.: Peptidomic identification of cysteine-rich peptides from plants. In *Peptidomics: Methods and Strategies*; Schrader, M. and Fricker, L., Eds.; Springer New York: New York, NY, 2018; pp 379–393.
(417) Kan, M.-W.; Craik, D. J.: Trends in cyclotide research. In *Cyclic Peptides: From Bioorganic Synthesis to Applications*; The Royal Society of Chemistry, 2018; Chapter 14; pp 302–339.
(418) Wang, C. K.; Craik, D. J. Designing macrocyclic disulfide-rich peptides for biotechnological applications. *Nat. Chem. Biol.* **2018**, *14*, 417–427.
(419) Camarero, J. A.; Campbell, M. J. The potential of the cyclotide scaffold for drug development. *Biomedicines* **2019**, *7*, 31.
(420) Chaudhuri, D.; Aboye, T.; Camarero, J. A. Using backbone-cyclized Cys-rich polypeptides as molecular scaffolds to target protein–protein interactions. *Biochem. J.* **2019**, *476*, 67–83.
(421) Chervin, J.; Talou, T.; Audonnet, M.; Dumas, B.; Camborde, L.; Esquerré-Tugayé, M.-T.; Roux, C.; Cabanac, G.; Marti, G. Deciphering the phylogeny of violets based on multiplexed genetic and metabolomic approaches. *Phytochemistry* **2019**, *163*, 99–110.

(422) Sternberger, A. L.; Bowman, M. J.; Kruse, C. P. S.; Childs, K. L.; Ballard, H. E.; Wyatt, S. E. Transcriptomics identifies modules of differentially expressed genes and novel cyclotides in *Viola pubescens*. *Front. Plant Sci.* **2019**, *10*, 156.
(423) Hashemi, M.; Gharaylou, Z.; Sepand, M. R.; Hamedi, S.; Raminfard, S.; Alimohamadi, M.; Sherkatkhamene, N.; Zarepour, L.; Hadjighassem, M. Apoptosis induced by *Viola odorata* extract in human glioblastoma multiforme. *Arch. Neurosci.* **2019**, *6*, e81233.
(424) Du, J.; Chan, L. Y.; Poth, A. G.; Craik, D. J. Discovery and characterization of cyclic and acyclic trypsin inhibitors from *Momordica dioica*. *J. Nat. Prod.* **2019**, *82*, 293–300.
(425) Gerlach, S. L.; Chandra, P. K.; Roy, U.; Gunasekera, S.; Göransson, U.; Wimley, W. C.; Braun, S. E.; Mondal, D. The membrane-active phytopeptide cycloviolacin O2 simultaneously targets HIV-1-infected cells and infectious viral particles to potentiate the efficacy of antiretroviral drugs. *Medicines* **2019**, *6*, 33.
(426) Gründemann, C.; Stenberg, K. G.; Gruber, C. W. T20K: An immunomodulatory cyclotide on its way to the clinic. *Int. J. Pept. Res. Ther.* **2019**, *25*, 9–13.
(427) Schmidt, M.; Nuijens, T.: Chemoenzymatic synthesis of linear- and head-to-tail cyclic peptides using omniligase-1. In *Enzyme-Mediated Ligation Methods*; Nuijens, T. and Schmidt, M., Eds.; Springer New York: New York, NY, 2019; pp 43–61.
(428) Agwa, A. J.; Craik, D. J.; Schroeder, C. I.: Cyclizing disulfide-rich peptides using sortase A. In *Enzyme-Mediated Ligation Methods*; Nuijens, T. and Schmidt, M., Eds.; Springer New York: New York, NY, 2019; pp 29–41.
(429) Harris, K. S.; Poon, S.; Quimbar, P.; Anderson, M. A.: In vitro and *in planta* cyclization of target peptides using an asparaginyl endopeptidase from *Oldenlandia affinis*. In *Enzyme-Mediated Ligation Methods*; Nuijens, T. and Schmidt, M., Eds.; Springer New York: New York, NY, 2019; pp 211–235.
(430) Hemu, X.; Zhang, X.; Bi, X.; Liu, C.-F.; Tam, J. P.: Butelase 1-mediated ligation of peptides and proteins. In *Enzyme-Mediated Ligation Methods*; Nuijens, T. and Schmidt, M., Eds.; Springer New York: New York, NY, 2019; pp 83–109.
(431) Hemu, X.; El Sahili, A.; Hu, S.; Wong, K.; Chen, Y.; Wong, Y. H.; Zhang, X.; Serra, A.; Goh, B. C.; Darwis, D. A.; et al. Structural determinants for peptide-bond formation by asparaginyl ligases. *Proc. Natl. Acad. Sci. U. S. A.* **2019**, *116*, 11737–11746.
(432) Hemu, X.; Zhang, X.; Tam, J. P. Ligase-controlled cyclo-oligomerization of peptides. *Org. Lett.* **2019**, *21*, 2029–2032.
(433) Schmidt, M.; Huang, Y.-H.; Texeira de Oliveira, E. F.; Toplak, A.; Wijma, H. J.; Janssen, D. B.; van Maarseveen, J. H.; Craik, D. J.; Nuijens, T. Efficient enzymatic cyclization of disulfide-rich peptides by using peptide ligases. *ChemBioChem* **2019**, *20*, 1524–1529.
(434) Rehm, F. B. H.; Jackson, M. A.; De Geyter, E.; Yap, K.; Gilding, E. K.; Durek, T.; Craik, D. J. Papain-like cysteine proteases prepare plant cyclic peptide precursors for cyclization. *Proc. Natl. Acad. Sci. U. S. A.* **2019**, *116*, 7831–7836.
(435) Pathan, E. K.; Deshpande, M. V. The puzzle of highly virulent Metarhizium anisopliae strains from Annona squamosa fields against Helicoverpa armigera. *J. Basic Microbiol.* **2019**, *59*, 392–401.
(436) Poth, A. G.; Huang, Y.-H.; Le, T. T.; Kan, M.-W.; Craik, D. J. Pharmacokinetic characterization of kalata B1 and related therapeutics built on the cyclotide scaffold. *Int. J. Pharm.* **2019**, *565*, 437–446.
(437) Rubio-Cervilla, J.; Frisch, H.; Barner-Kowollik, C.; Pomposo, J. A. Synthesis of single-ring nanoparticles mimicking natural cyclotides by a stepwise folding-activation-collapse process. *Macromol. Rapid Commun.* **2019**, *40*, 1800491.
(438) Silva, O. N.; Pinto, M. F. S.; Vianna, J. F. C.; Freitas, C. G.; Fensterseifer, I. C. M.; Craik, D. J.; Franco, O. L. Evaluation of the *in vitro* antitumor activity of nanostructured cyclotides in polymers of Eudragit® L 100-55 and RS 30 D. *Lett. Drug Des. Discov.* **2019**, *16*, 437–445.
(439) Wang, C. K.; Craik, D. J. Toward structure determination of disulfide-rich peptides using chemical shift-based methods. *J. Phys. Chem. B* **2019**, *123*, 1903–1912.
(440) Oguis, G. K.; Gilding, E. K.; Jackson, M. A.; Craik, D. J. Butterfly pea (*Clitoria ternatea*), a cyclotide-bearing plant with applications in agriculture and medicine. *Front. Plant Sci.* **2019**, *10*, 645.
(441) Jackson, M. A.; Yap, K.; Poth, A. G.; Gilding, E. K.; Swedberg, J. E.; Poon, S.; Qu, H.; Durek, T.; Harris, K.; Anderson, M. A.; et al. Rapid and scalable plant-based production of a potent plasmin inhibitor peptide. *Front. Plant Sci.* **2019**, *10*, 602.
(442) Dawson, P. E.; Muir, T. W.; Clark-Lewis, I.; Kent, S. B. Synthesis of proteins by native chemical ligation. *Science* **1994**, *266*, 776–779.

(443) Camarero, J. A.; Muir, T. W. Chemoselective backbone cyclization of unprotected peptides. *Chem. Commun.* **1997**, 1369–1370.
(444) Hojo, H.; Aimoto, S. Polypeptide synthesis using the *S*-alkyl thioester of a partially protected peptide segment. Synthesis of the DNA-binding domain of *c*-Myb protein (142–193)–NH_2. *Bull. Chem. Soc. Jpn.* **1991**, *64*, 111–117.
(445) Camarero, J. A.; Cotton, G. J.; Adeva, A.; Muir, T. W. Chemical ligation of unprotected peptides directly from a solid support. *J. Pept. Res.* **1998**, *51*, 303–316.
(446) Hackeng, T. M.; Griffin, J. H.; Dawson, P. E. Protein synthesis by native chemical ligation: Expanded scope by using straightforward methodology. *Proc. Natl. Acad. Sci. U. S. A.* **1999**, *96*, 10068–10073.
(447) Backes, B. J.; Virgilio, A. A.; Ellman, J. A. Activation method to prepare a highly reactive acylsulfonamide "safety-catch" linker for solid-phase synthesis. *J. Am. Chem. Soc.* **1996**, *118*, 3055–3056.
(448) Backes, B. J.; Ellman, J. A. An alkanesulfonamide "safety-catch" linker for solid-phase synthesis. *J. Org. Chem.* **1999**, *64*, 2322–2330.
(449) Blanco-Canosa, J. B.; Dawson, P. E. An efficient Fmoc-SPPS approach for the generation of thioester peptide precursors for use in native chemical ligation. *Angew. Chem. Int. Ed.* **2008**, *47*, 6851–6855.
(450) Blanco-Canosa, J. B.; Nardone, B.; Albericio, F.; Dawson, P. E. Chemical protein synthesis using a second-generation *N*-acylurea linker for the preparation of peptide-thioester precursors. *J. Am. Chem. Soc.* **2015**, *137*, 7197–7209.
(451) Fang, G. M.; Li, Y. M.; Shen, F.; Huang, Y. C.; Li, J. B.; Lin, Y.; Cui, H. K.; Liu, L. Protein chemical synthesis by ligation of peptide hydrazides. *Angew. Chem. Int. Ed.* **2011**, *50*, 7645–7649.
(452) Taichi, M.; Hemu, X.; Qiu, Y.; Tam, J. P. A thioethylalkylamido (TEA) thioester surrogate in the synthesis of a cyclic peptide via a tandem acyl shift. *Org. Lett.* **2013**, *15*, 2620–2623.

Table of Contents graphic